



U.S. DEPARTMENT OF COMMERCE

Rogers C. B. Morton, Secretary

NATIONAL OCEANIC AND ATMOSPHERIC ADMINISTRATION

Robert M. White, Administrator

ENVIRONMENTAL DATA SERVICE

Thomas S. Austin, Director

Solar - Geophysical Data

NO. 378 FEBRUARY 1976

Supplement

**NATIONAL GEOPHYSICAL AND SOLAR - TERRESTRIAL DATA CENTER
BOULDER, COLORADO**

For obtaining bulletins on a data exchange basis, send request to: World Data Center A for Solar-Terrestrial Physics, NOAA, Boulder, Colorado 80302.

For sale through the National Climatic Center, Federal Building, Asheville, NC 28801, Attn: Publications. Subscription Price: \$34.00 annually for both Part I (Prompt Reports) and Part II (Comprehensive Reports) or \$18.00 annually for either part. Annual supplement containing explanation is included. For foreign mailing add \$32.00 for both parts or \$16.00 for either part. Single issue price \$1.50 for either part and \$1.40 for the extra issue. Make checks and money orders payable to: Department of Commerce, NOAA.

To standardize referencing these reports in the open literature, the following format is recommended:

Solar-Geophysical Data, 366 Part I (or Part II), pages, February 1975, U.S. Department of Commerce, (Boulder, Colorado, U.S.A. 80302)

SOLAR-GEOPHYSICAL DATA

EXPLANATION OF DATA REPORTS

I N T R O D U C T I O N

This pamphlet contains the description and explanation of the data in the monthly publication, *Solar-Geophysical Data*, compiled by the National Geophysical and Solar-Terrestrial Data Center (NGSDC) in Boulder, Colorado, U.S.A. NGSDC is one of the several components of the Environmental Data Service in the National Oceanic and Atmospheric Administration. The monthly bulletins are available on a data exchange basis through the World Data Center A for Solar-Terrestrial Physics, which is operated by NGSDC, or at a nominal cost through the National Climatic Center.* These data reports continue a series which was issued by the Central Radio Propagation Laboratory of the National Bureau of Standards, known beginning 1956 and for many years as the CRPL-F Series Part B. The title *Solar-Geophysical Data* was first used in 1955. The name of the organization compiling the data reports has changed many times but the personnel involved have stayed pretty much the same. Since June 1965, the compilations and editing have been done by Miss Hope I. Leighton under the supervision of Mr. Dale B. Bucknam and Miss J. Virginia Lincoln. Mr. A. H. Shapley is Director of NGSDC.

Solar-Geophysical Data is intended to keep research workers abreast on a timely schedule of the major particulars of solar activity and the associated interplanetary, ionospheric, radio propagation and other geophysical effects. This report series is made possible through the cooperation of many observatories, laboratories and agencies as recorded in the detailed descriptions which follow.

For many data types, the material published in *Solar-Geophysical Data* is only a fraction of what is available from the NGSDC archives. The published data is considered to be that in greatest demand and thus the dissemination in this form is efficient and economical for both the user and the data center. Users are invited to avail themselves of the data services of NGSDC and the collocated World Data Center A for STP.

Beginning with the July 1969 issue the publication was divided into two Parts (I and II). Part I (Prompt Reports) contains data for 1 and 2 months prior to the month of publication. Part II (Comprehensive Reports) contains data for 6 and 7 months prior to the month of publication plus, from time to time, data from miscellaneous earlier months. These reports may be referenced in the open literature.** It must be understood, however, that because of the rapid publication schedule, some data categories are not considered to be definitive. This applies particularly to the Prompt Reports where such data sets are marked as provisional. Errata or revisions are included from time to time. Additions to the descriptive text will appear with the data when new material is added, or revision is made.

The first page of each issue of Part I and II gives the general contents and is backed by a running index to locate data for a specific month for the past year. A complete index for data since July 1957 is given in the blue section of this pamphlet.

*For sale through the National Climatic Center, Federal Building, Asheville, NC 28801, Attn: Publications, Subscription Price: \$34.00 annually for both Part I (Prompt Reports) and Part II (Comprehensive Reports) or \$18.00 annually for either part. This supplement is included. For foreign mailing add \$32.00 for both parts or \$16.00 for either part. Single issue price \$1.50 for either part and \$1.40 for this extra issue. Make checks and money orders payable to: Department of Commerce, NOAA/NCC.

**To standardize referencing these reports in the open literature, the following format is recommended (with this issue as the example):

Solar-Geophysical Data, 378 Part I (or Part II), pages, February 1976, U.S. Department of Commerce (Boulder, Colorado, U.S.A. 80302).

In various places in this text, data types are identified both by name and an alphanumeric designation (A.2, C.3, etc.). The latter come from the data categories given in *Guide to International Data Exchange*, issued in 1973 by the ICSU Panel on World Data Centres.

A useful reference containing descriptions of many solar and geophysical phenomena as well as directing the reader to more detailed discussions is the *Handbook of Correlative Data*, issued February 1971 by the National Space Science Data Center, NASA, Goddard Space Flight Center, Greenbelt, Md. 20771. (The Handbook is also available through World Data Center A for Solar-Terrestrial Physics.)

TABLE OF CONTENTS

	<u>Page</u>
<u>Data for One Month Before Month of Publication</u>	
Alerts	5
Daily Solar Indices	7
Solar Flares	9
Solar Radio Waves	10
Solar X-ray Radiation	11
Coronal Holes	11
Solar Wind Measurements	12
Solar Proton Monitoring	15
Interplanetary Magnetic and Electric Fields	17
Solar Proton Events (Provisional)	19
<u>Data for Two Months Before Month of Publication</u>	
Solar Activity Centers	21
Sudden Ionospheric Disturbances	29
Solar Radio Waves	32
Cosmic Rays	36
Geomagnetic Activity	37
Radio Propagation Indices	40
<u>Data for Six Months Before Month of Publication</u>	
Solar Flares	43
Solar Radio Waves	46
Energetic Solar Particles and Plasma	52
Reduced Magnetograms	56
<u>Data for Seven Months Before Month of Publication</u>	
Abbreviated Calendar Record	59
Flare Index by Region	60
<u>Data for Miscellaneous Time Periods</u>	
Retrospective World Intervals	61
<u>Partial List of Contributors of Data</u>	62
<u>Index to Volumes for 1957-1974</u>	
Key to Index for <i>Solar-Geophysical Data</i>	67
Index Tables	71
<u>Stonyhurst Disks</u>	

DATA FOR ONE MONTH BEFORE MONTH OF PUBLICATION

TABLE OF CONTENTS

	<u>Page</u>
<u>Alert Periods</u>	
H.60 IUWDS Alert Periods (Advance and Worldwide)	5
<u>Daily Solar Indices</u>	
A.2,A.8 Relative Sunspot Numbers and Adjusted 2800 MHz Solar Flux	7
A.2,A.8 Combined Sunspot Numbers and Solar Flux Values	7
A.2 Graph of Sunspot Cycle	7
A.2 Predicted and Observed Relative Sunspot Numbers	7
<u>Solar Flares</u>	
C.1 H α Solar Flares	9
C.1d No-Flare-Patrol Chart	10
<u>Solar Radio Waves</u>	
A.10 Solar Interferometric Charts	10
A.10 East-West Solar Scans	10
C.3 Outstanding Occurrences at Fixed Frequencies (SELECTED)	11
<u>Solar X-Ray Radiation</u>	
A.11g, C.5e SMS/GOES	11
<u>Coronal Holes</u>	
A.7f Helium D3 Chromosphere	11
<u>Solar Wind Measurements</u>	
A.13a Measurements of Pioneers 6, 7, 8 and 9	12
A.13d IPS Measurements	13
<u>Solar Proton Monitoring</u>	
A.12ba Pioneer 6	15
A.12bb Pioneers 8 and 9	17
<u>Interplanetary Magnetic and Electric Fields</u>	
A.17 Interplanetary Magnetic Field - Pioneers 8 and 9	17
A.18 Interplanetary Electric Field - Pioneers 8 and 9	18
A.17c Inferred Interplanetary Magnetic Field	19
<u>Solar Proton Events</u>	
Provisional Data	19

ALERT PERIODS (H.60)

The table gives the Advance Geophysical Alerts (PRESTO) as initiated by (or received by) the Western Hemisphere Regional Warning Center of the International Ursigram and World Days Service (IUWDS) at Boulder, Colorado, and also the Worldwide Geophysical Alerts (GEOALERTS) as designated by the IUWDS World Warning Agency, Boulder, Colorado.

These alerts are of the types recommended by the International Ursigram and World Days Service. A description of the IUWDS program can be found in *Synoptic Codes for Solar and Geophysical Data*, Third Revised Edition 1973, revised by RWC Circular Letters. This code book and its revisions are available from the IUWDS Secretary for Ursigrams, Mr. R. B. Doeker, NOAA, Boulder, Colorado, U.S.A., 80302.

The PRESTO messages are originated by the reporting observatory or at the Regional Warning Centers. They are for advance reporting of major events. The format of these messages follows (extracted from *Synoptic Codes for Solar and Geophysical Data*):

PRESTO

1. Content.

- Report of major events to the other RWC and to the local or regional customers.

2. General form.

PRESTO observatory JJHHmm report

3. Definition of symbols.

PRESTO = key word for RAPID reporting of major events

observatory = name of reporting observatory in clear text

JJHHmm = Greenwich date and time of issue of message in hours and minutes UT

report = one or more of statements as below

For GEOMAGNETIC ACTIVITY

MAGSTORM BEGINS JJHHmm

STRONG MAGSTORM IN PROGRESS JJHHmm (A≥50)

WEAK MAGSTORM IN PROGRESS JJHHmm (30≤A<50)

Note: One may add plain language comments related to auroral reports or Forbush effect expected

For MAJOR FLARES

SOFLARE - importance class - coordinates (i.e. N20 E78)
 - JJHHmm
(date and time) - "duration in minutes given" or statement "in progress"

Note: One may add plain language comments like "Y-shaped" or "covering spots" or "suspected proton flare"

For TENFLARE (solar radio emission outburst at 10 cm > 100% over background)

TENFLARE - XX units - JJHHmm for onset - duration in minutes, or statement "in progress" at the time of PRESTO, or statement "observed until hours and minutes UT"

Note: Units give the increase of the flux density over the pre-burst level in conventional units ($10^{-22} \text{W m}^{-2} \text{Hz}^{-1}$) by significant digits and words such as "1700 units over background"

For PROTON EVENT

COSMIC RAY INCREASE - JJHHmm - percent increase above normal based on neutron monitor

POLCAP ABSORPTION - JJHHmm - dB of absorption by riometer or ionospheric forward scatter technique

PROTON EVENT - JJHHmm - specify energy range from a spacecraft report

Notes: 1. PRESTO should be circulated as soon as the event has been recognized.

2. The PRESTO will only report events and no forecasts. Any change of a forecast would be sent to the interested customers as a GEOSOL, GEOALERT or in plain language.

3. If the observatories follow this scheme, it is not necessary to report the kind of experiment

SOFLARE signifies a chromospheric report
TENFLARE signifies a centimetric outburst
COSMIC RAY INCREASE signifies a neutron monitor count increase
POLCAP ABSORPTION signifies a ground based polar cap report
PROTON EVENT signifies spacecraft reports only

The GEOSOL or GEOALERT messages are originated by the Regional Warning Center or by the World Warning Agency in Boulder, Colorado, U.S.A. They are for the purposes of reporting the current level of solar activity and for forecasting solar-geophysical events. The format of these messages follows:

GEOSOL
or
GEOALERT

1. Content.

- For sending combined data and forecasts to other RWCs and for general data users

- For sending ADVICE information to other RWCs

2. General form.

GEOALERT or GEOSOL	<u>IIINN</u> [warning center of origin, serial number of message]	<u>DDHHmm</u> [date time group of message in UT]
--------------------------	--	---

key word - [use GEOALERT when ADVICE included in message]

<u>9HHJJ</u> [signifies indices for preceding 24 hours follow]	<u>laaab</u> [relative sunspot number, and number of new spot groups]	<u>2cccd</u> [10 cm flux and number of bursts]	<u>3eeef</u> [geomagnetic A index and events]	<u>4gggh</u> [cosmic ray intensity and events]
---	--	---	--	---

[repeat for each region]
 QXXYY nniijk ...FLARE JJHHmm QXXYY
 heliographic coordinates of flare
 date and UT of Outstanding flare
 key word
 total number of flares, number > Imp I, number of M and X flares in active region

heliographic coordinates of active region,

MAGSTORM JJHHmm BHHJJ 7777C
 key numbers and observations used for forecast
 key numbers signify solar forecast to follow for day
 date and UT of beginning of magnetic storm
 key word

[may be repeated or omitted]
 QXXYY ZZZZZZ...ZZZZ ---ALERT FIN
 end of message
 type of alert
 active region description
 heliographic coordinates of active region

3. Definition of symbols.

GEOSOL = key word for sending combined data and forecasts
 GEOLERT = key word for sending combined data and forecasts including ADVICE information

- III = warning center of origin
 - MEU - Meudon
 - WVA - Boulder (SOLTERWARN)
 - MOS - Moscow
 - NN = originating center's serial number
 - DDHHmm = date (DD) hour (HH) and minutes (mm) in UT of issue of message
- 9 = key number to indicate indices follow
- BHHJJ = the middle of the 24-hour period for which the indices apply in UT; HH - hour; JJ - date
- 1 = key number to indicate sunspot data follows
- aaa = relative sunspot number (Wolf number)
- b = number of new sunspot groups that have appeared (by rotation or birth) during this period
- 2 = key number to indicate 10 cm solar flux data follows
- ccc = value of 10 cm solar flux in $10^{-22} \text{Wm}^{-2} \text{Hz}^{-1}$ units
- d = number of known IMPORTANT 10 cm bursts during this period
- 3 = key number to indicate magnetic activity follows
- eee = Ak index for Greenwich date
- f = important event, if any, where
 - 0 - no event
 - 1 = end of magnetic storm
 - 2 = storm in progress
 - 6 = gradual storm commencement
 - 7 = sudden storm commencement(sc)
 - 8 = very pronounced sudden storm commencement
- 4 = key number to indicate cosmic radiation data observed by neutron monitor follows
- ggg = median level in thousandths of an arbitrary normal level
- h = important event, if any, where
 - 0 - no event
 - 1 = pre-decrease
 - 2 = beginning of a Forbush decrease
 - 3 = Forbush decrease in progress
 - 4 = end of Forbush decrease
 - 5 = arrival of solar particles (GLE)
- Q = quadrant (heliographic coordinates) of the active region where
 - 1 = NE (north-east)
 - 2 = SE (south-east)
 - 3 = SW (south-west)
 - 4 = NW (north-west)
- [XX = distance to central meridian in degrees (longitude)
- [YY = heliographic latitude in degrees
- [heliographic location of active region
- nn = total number of flares
- i = number of flares greater than Importance I
- j = number of M flares
- k = number of class X flares
- [in this region during this period

Note: Definitions of class C, M or X flares follow:

- CLASS C: A solar flare which is not associated with significant X-ray production.
- CLASS M: Solar flares which are accompanied by significant X-ray production, greater than $10^{-2} \text{ergs cm}^{-2} \text{sec}^{-1}$ in 0-8Å band, or $10^{-2} \text{ergs cm}^{-2} \text{sec}^{-1}$ in 0.5-5Å band, comparable SID (SWF or SPA).
- CLASS X: Solar flares which are accompanied by great X-ray production, greater than $10^{-1} \text{ergs cm}^{-2} \text{sec}^{-1}$ in 0-8Å band, or $10^{-2} \text{ergs cm}^{-2} \text{sec}^{-1}$ in 0.5-5Å band, comparably great SID, or by a 10 cm radio noise outburst of more than 1000 flux units over background and duration greater than 10 minutes.

This classification is designed to give an indication of the geophysical effect which is likely to be associated with a solar event. Class C events will usually be accompanied by only minor sudden ionospheric disturbances (SID), class M by significant SID, and class X by major SID.

OUTSTANDING EVENTS

- ...FLARE = key word to indicate OUTSTANDING event data follows, where
 - PROTONFLARE - protons from this flare have been observed in the earth's vicinity
 - MAGFLARE - a geomagnetic and/or cosmic storm has been associated with this flare
 - MAJORFLARE - this flare is the basis for the forecast of geomagnetic storm, cosmic storm and/or protons in the earth's vicinity

JJHHmm = UT of beginning of OUTSTANDING flare

Q = quadrant of the OUTSTANDING flare location, where
 1 = NE (north-east) 3 = SW (south-west)
 2 = SE (south-east) 4 = NW (north-west)

[XX = distance to central meridian in degrees
 [YY = heliographic latitude in degrees
 [heliographic location of OUTSTANDING FLARE

MAGSTORM = key to indicate magnetic storm data follows
 JJHHmm = UT of beginning of magnetic storm

Notes: Omit these groups if no events to be reported.
 Use clear text if event does not correspond to conventional classification.
 Include data from earlier PRESTO messages for this period.

DETAILED FORECASTS

- 8 = key number to indicate 24-hour forecast information follows
- BHHJJ = the UT hour (HH) and date (JJ) of the beginning of the 24-hour forecast period
- 7777 = key numbers to indicate available local observatories follow
- C = definitions of available local observatories, where
 - 0 = none
 - 1 = solar radio observations
 - 2 = partial solar optical observations
 - 3 = all (optical and radio)
 - 4 = all including solar magnetic field measurements
- Q = quadrant of PREDICTED ACTIVE REGION, where
 - 1 = NE (north-east)
 - 2 = SE (south-east)
 - 3 = SW (south-west)
 - 4 = NW (north-west)
- [XX = distance to central meridian in degrees
- [YY = heliographic latitude in degrees
- [heliographic location of ACTIVE REGION at BHHJJ
- ZZZ...ZZZ = key word to describe the PREDICTED ACTIVE REGION, where
 - SPOTNIL - indicates spotless disc
 - PLAGENIL - indicates spotless disc free of calcium plage
- [when these are used, QXXYY omitted

QUIET = less than one chromospheric event per day
 ERUPTIVE = at least one radio event (10cm) and several chromospheric events per day (Class C Flare)
 ACTIVE = at least one geophysical event or several larger radio events (10cm) per day (Class M Flare)
 PROTON = at least one high energy event (Class X Flare)

Notes: 1. Events are classified as below:

- a) Chromospheric Events: some flares are just Chromospheric Events without Centimetric Bursts or Ionospheric Effects. (SID). (Class C flare)
- b) Radio Event: flares with Centimetric Bursts and/or definite Ionospheric Event. (SID).
- c) Geophysical Event: flare (Importance two or larger) with Centimetric Outbursts (maximum of the flux higher than the Quiet Sun flux, duration longer than 10 minutes) and/or strong SID. Sometimes these flares are followed by Geomagnetic Storms or small PCA. (Class M flare)
- d) High Energy Event: flare (class two or more) with outstanding Centimetric Bursts and SID. High Energy Protons are reported at the Earth in case of most of these events occurring on the western part of the solar disk. (Class X flare)

2. Some quiet groups being of very little importance, these can be reported only by their number.

3. If the word CAUTION is inserted between QXXYY group and the description word, it signifies one cannot forecast real evolution of the group at time of the message.

4. If the word DOUBTFUL is inserted between QXXYY group and description word, it signifies it is impossible to determine definitely the true class of activity expected.

ADVICES AND ALERTS

---ALERT--- key word(s) to describe one or more of the following situations during the next 24 hours or longer:

- SOLNIL } End of active period
- MAGNIL } or
- PROTONNIL } Beginning of period of very low activity

SOLQUIET - No active regions on the solar disk
MAGQUIET - Only sporadic weak geomagnetic activity

SOLALERT JJ/KK - increased solar activity expected between days JJ and KK
MAGALERT JJ/KK - increased geomagnetic activity expected between days JJ and KK

MAJOR FLARE ALERT JJ/KK QXXYY - large bright flare (Class X) expected between days JJ and KK in region QXXYY

PROTON FLARE ALERT JJ/KK QXXYY - protons expected in earth's vicinity as a result of proton flare predicted to occur between days JJ and KK in region QXXYY

PRESTO PROTON ARRIVAL ALERT KK/JJHm - forecast of arrival of protons in earth's vicinity on day KK from flare which occurred on day JJ at Hm (UT)

STRATWARM STARTS ---- } includes day of week and
STRATWARM EXISTS ---- } geographical area
STRATWARM ENDS

- Notes:
- 1) The Alert section is always included in the GEO-ALERT code format as it is used as ADVICE by RWCs & WWA.
 - 2) More than one type of Alert may be included in a message
 - 3) Previous transmission of ALERT (SOL, MAG, MAJOR FLARE, PROTON FLARE, PRESTO PROTON ARRIVAL) requires the eventual transmission of appropriate NIL (SOL, MAG, PROTON)
 - 4) Transmission of STRATWARM STARTS or EXISTS requires the eventual transmission of STRATWARM ENDS
 - 5) GEOALERTS are converted by WWA to plain language and broadcast on WWV and WWVH as described in Circular letter RWC-123.

DAILY SOLAR INDICES (A.2, A.8)

Relative Sunspot Numbers and Adjusted 2800 MHz Solar Flux -- The first table presents Zürich relative sunspot numbers, R_z , for the month. The corresponding data for eleven earlier months are reprinted to permit the trend of solar activity to be followed. On the same page is presented a similar table of twelve months of daily solar flux values at 2800 MHz adjusted to one Astronomical Unit, S_a , as reported by the Algonquin Radio Observatory (ARO) of the National Research Council near Ottawa.

Combined Sunspot Numbers and Solar Flux Values -- The next table gives several available daily indices for the month preceding that of publication. In addition to the calendar date, the table gives the day-number of the year and the day-number of the standard 27-day (solar rotation) cycles. The data presented are Zürich relative sunspot numbers, (R_z), American relative sunspot numbers, (R_A), daily solar flux values at 2800 MHz, (S), and daily solar flux values, (S_a), adjusted to 1 A.U. for 15400, 8800, 4995, 2800, 2695, 1415, 606, 410 and 245 MHz.

Graph of Sunspot Cycle and Table of Predicted and Observed Relative Sunspot Numbers -- As of this publication date the end of Cycle 20 and, thus, the beginning of Cycle 21 has still not been ascertained. However, the first new cycle spot was observed in November 1974 and a determination of sunspot minimum may be made at almost any time as other indications present themselves.

Whenever a good estimate of sunspot minimum can be made a new graph and table will be prepared. Smoothed sunspot numbers are used for these purposes and are defined by:

$$R_{12} = 1/12 \left\{ \sum_{n-5}^{n+5} (R_k) + 1/2 (R_{n+6} + R_{n-6}) \right\} \quad \text{in which } R_k \text{ is the mean value of } R \text{ for a single}$$

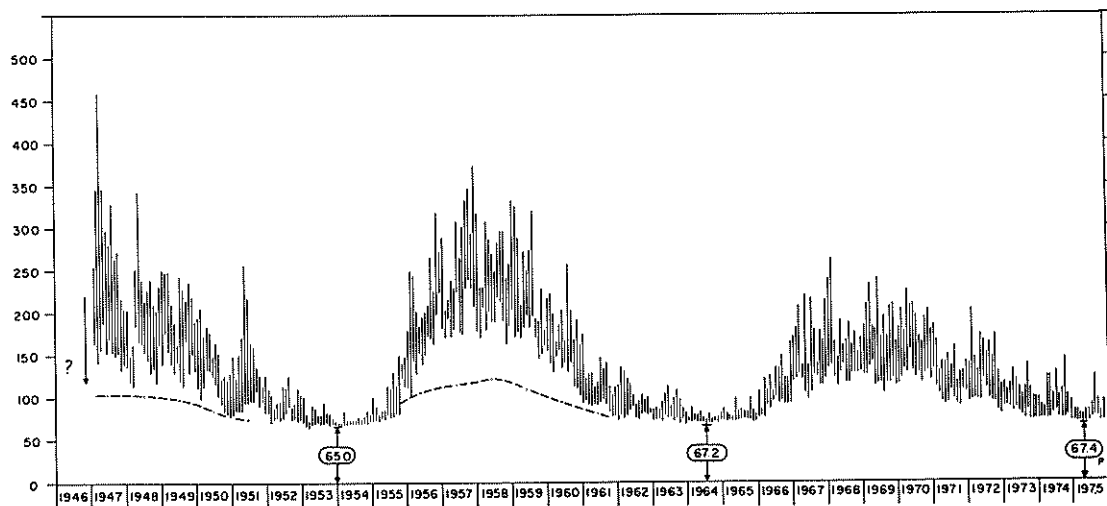
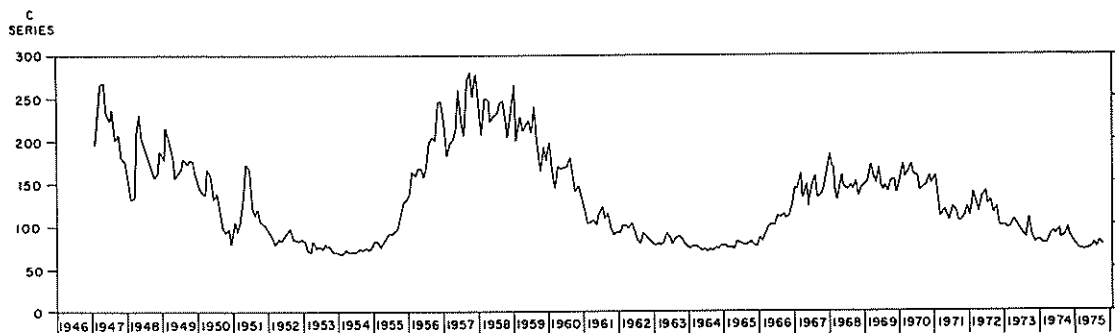
month k and R_{12} is the smoothed index for the month represented by $k = n$. Predictions shown are those made for one year after the latest available datum by the method of A. G. McNish and J. V. Lincoln [Trans. Am. Geophys. Union, 30, 673-685, 1949] modified by the use of regression coefficients and mean cycle values to be recomputed for Cycles 8 through 20. The last prediction made will also show again the 90% prediction interval, an indication of the uncertainty above and below the predicted number. The values of observed and predicted Zürich smoothed relative sunspot numbers are given in the table. The predicted values are based on observed data available and will change as calculated each month and new observations are included. The 90% prediction interval is shown in parentheses for each month.


Relative Sunspot Numbers -- The relative sunspot number is an index of the activity of the entire visible disk of the sun. It is determined each day without reference to preceding days. Each isolated cluster of sunspots is termed a sunspot group and it may consist of one or a large number of distinct spots whose size can range from 10 or more square degrees of the solar surface down to the limit of resolution (e.g. 1/25 square degree). The relative sunspot number is defined as $R = K(10g + s)$, where g is the number of sunspot groups and s is the total number of distinct spots. The scale factor K (usually less than unity) depends on the observer and is intended to effect the conversion to the scale originated by Wolf. The provisional daily Zürich relative sunspot numbers, R_Z , based upon observations made at Zürich and its two branch stations in Arosa and Locarno are communicated by M. Waldmeier of the Swiss Federal Observatory. The daily American relative sunspot numbers, R_A' , are compiled by Casper Hossfield, for the Solar Division of the American Association of Variable Star Observers. The R_A' observations for sunspot numbers are made by a rather small group of extraordinarily faithful observers, many of them amateurs, each with many years of experience. The counts are made visually with small, suitably protected telescopes.

Final values of R_Z appear in the *IAU Quarterly Bulletin on Solar Activity*, these reports, and elsewhere. They usually differ slightly from the provisional values. The American numbers, R_A' , being computed solely from observations made under favorable conditions selected from the reports of numerous observers, are final numbers and do not require revision.

Daily Solar Flux Values - Ottawa-ARO -- Daily observations of the 2800 MHz radio emissions which originate from the solar disk and from any active regions are made at the Algonquin Radio Observatory (ARO) of the National Research Council of Canada with a reflector of 1.8 meters diameter. These are a continuation of observations which commenced in Ottawa in 1947. Numerical values of flux in the tables

SOLAR RADIO FLUX, 10.7 CM
ADJUSTED TO I.A.U.



UPPER CURVE — MONTHLY MEANS OF RADIO FLUX
 LOWER CURVE — MONTHLY HIGH & LOW VALUES OF RADIO FLUX
 APPROXIMATE THE SLOWLY VARYING COMPONENT.
 CURVE (---) — APPROXIMATELY SEPARATES SUNSPOT COMPONENT FROM
 BASIC COMPONENT.
 MAGNITUDE OF THE RADIO QUIET SUN AT SUNSPOT MINIMA.

are in units of $10^{-22}\text{Wm}^{-2}\text{Hz}^{-1}$ and refer to a single calibration made near local noon at 1700 UT. When the flux changes rapidly, or there is a burst in progress at that time, the reported value is the best estimate of the undisturbed level and provides the reference level for measuring the burst intensity. The various types of outstanding events are listed separately in another table. The observed flux values have variations resulting from the eccentric orbit of the earth in its annual path around the sun. Although these radio values are suitable to use with observed ionospheric and other data, an adjustment must be introduced when the observations are used in studies of the absolute or intrinsic variation of the solar radio flux. Thus the tables show both the observed flux, S , and the flux adjusted to 1 A.U., S_a . The observations are made for a single North-South polarization but reduced for the assumption of two equal orthogonal polarizations. Graphs showing the monthly mean adjusted flux and the monthly high and low values since 1947 are shown in this text. Relative errors over long periods of time are believed to be $\pm 2\%$, over a few days may be $\pm 0.5\%$. The characteristics of the observations are surveyed in "Solar Radio Emission at 10.7 cm" by A. E. Covington [*J. Royal Astron. Soc., Canada*, 63, 125, 1969]. Values of the quiet sun for the minima of January 1954, and July 1964 have been derived as 65.0 and 67.2 s.f.u. using the solar flux adjusted to 1 A.U. [Covington, *J. Royal Astro. Soc., Canada*, 68, 31, 1974]. When the same method is applied to the daily values for 1975, it would appear that April may be provisionally regarded as the radio minimum with a quiet solar flux value of 67.4 s.f.u. This month is also characterized as having no bursts. Though experiments have indicated that a multiplying factor of 0.90 should be applied to the reported flux values in order to derive the absolute flux values, the published flux values have not been corrected by this factor because of the number of data series which have been computerized listing these values. Maintaining homogeneity of the published series is considered of greater value than having the absolute flux values published. A review of the history of the absolute calibration of the Ottawa series as well as a number of other series of observations made within the microwave region has been prepared by H. Tanaka of the Research Institute of Atmospheric, Nagoya University, as convener of a Working Group of Commission 5 of URSI [H. Tanaka et al., "Absolute calibration of solar radio flux density in the microwave region," *Solar Physics*, 29, 243, 1973].

The factor of 0.90 stated above applies directly only to "Series C" data beginning in 1966. The reported correction factor includes a correction of 0.01 for the atmospheric attenuation referred to the zenith as well as the appropriate modification for the zenith angle of the sun at the times of calibrations. In data taken previously to 1966, this correction was neglected. A provisional summary of corrected daily flux values prior to 1966 has been made so that the early values may be compared on the same basis as later values and is available in World Data Center A. It has also been found necessary to incorporate a correction of -4% for the period July 1967 to May 1968. [ERB 790 Radio and Electrical Engineering Division, NRC.]

These solar radar noise indices are being published in accordance with a CCIR Recommendation originally from the the Xth Plenary Assembly, Geneva, 1963 (maintained at XIth, XIIth, and XIIIth Plenaries), which states "that the monthly-mean value of solar radio-noise flux at wavelengths near 10 cm should be adopted as the index to be used for predicting monthly median values of foE and foF1, for dates certainly up to 6, and perhaps up to 12 months ahead of the date of the last observed values of solar radio-noise flux".

Daily Solar Flux Values - Sagamore Hill -- the Sagamore Hill Solar Radio Observatory of the Air Force Geophysics Laboratories (located at $42^{\circ}37'54.36''\text{N}$, $70^{\circ}49'15.15''\text{W}$) in 1966 began operating solar patrols at 8800, 4995, 2695, 1415, and 606 MHz. The patrol was extended to 15400 MHz in 1967, to 245 MHz in early 1969 and 410 MHz was added in early 1971. Flux calibrations in units of $10^{-22}\text{Wm}^{-2}\text{Hz}^{-1}$ are made at about meridian transit each day. All flux data are corrected to sun-earth distance of 1 A.U. Corrections are also made for atmospheric attenuation based on the following average vertical attenuations:

15400 MHz	0.085 dB	4995 MHz	0.055 dB	1415 MHz	0.05 dB
8800	0.070	2695	0.051	606	0.045

A very small error has been discovered in the computer program which generates the observed daily solar flux values. The error exists in all reported values through June 1974 and may be corrected by multiplying the values reported by 0.9975. Starting with July 1974, this correction factor was included in the computation of the observed daily solar fluxes.

S O L A R F L A R E S (C.1)

The $H\alpha$ solar flare data in Part I (Prompt Reports) are presented as a preliminary record of those flares received on a rapid schedule. Definitive data are published later in Part II (Comprehensive Reports). After six months the flares have been grouped and an attempt made to verify that errors in reporting have been eliminated. The explanation of these definitive flare data begins on page 43 of

this text. It includes an explanation of the column headings together with definition of the letters used in the Remarks Column. A table of solar flare patrol observatories is on page 45.

The solar flare reports are received from throughout the world at World Data Center A for Solar-Terrestrial Physics, NOAA, Boulder, Colorado 80302. Observations are made in the light of the center of $H\alpha$ line unless noted otherwise. NOAA operates the flare patrol at Boulder, and NOAA provides support and jointly operates with the Ionospheric Prediction Service of Australia the flare patrol at Culgoora. Tehran is operated by the USAF using NOAA equipment. The USAF operates Ramey, Palehua and Athens.

The no-flare patrol observations matching the solar flare table are given in graphical form. The observatories reporting the patrols are indicated. The dark areas at the bottom half of each day are times of no cinematographic patrol. The dark areas at the top half of the day are times of neither visual nor cinematographic patrol.

S O L A R R A D I O W A V E S (A.10, C.3)

Interferometric Observations -- The chart presents solar interferometric observations at 169 MHz as recorded around local noon at Nancay, France (47°23'N, 8°47'E) the field station of the Meudon Observatory.

The main lobes are parallel to the meridian plane: the half-power width is 3.8 minutes of arc in the East-West direction. The main lobes are about 1° apart [*Am. Astroph.*, 20, 155, 1957]. The records give the strip intensity distribution from the center of the disk to 30' to the West and East.

These daily distributions are plotted on the same chart giving diagrams of evolution. Points of equal intensity given in relative units are joined day after day in the form of isophotes. Four equal intensity levels have been chosen to draw the isophotes. These intensities are proportional to 0.6, 1, 1.5 and 2. The first level corresponds to the sun without any radio storm center.

In each noisy radio region the smoothed intensity around noon is given in $10^{-22} \text{Wm}^{-2} \text{Hz}^{-1}$.

East-West Solar Scans - Algonquin 10.7 cm -- East-West solar scans at 10.7 cm are taken daily at the Algonquin Radio Observatory of the National Research Council of Canada (N 45°56'43", W 78°3'33").

The antenna consists of an array of 32 3-meter paraboloids having interference fringes separated by approximately 1°. The zero order fringe on the meridian (where most of the published curves are taken) has an east-west width of 1.5', but the width increases to 1.7' for fringes 30° from the meridian. The antennas are kept fixed during each drift curve to avoid changes in sensitivity due to scanning and an effort is made to maintain a constant sensitivity from one day to another. When necessary, however, the receiver gain is adjusted to accommodate large fluxes. (Antenna specification can be found in *Solar Phys.*, 1, 465-473, 1967 and details of the antennas performance appear in *Astron. J.*, 73, 749-755, 1968.)

The position of the limbs of the photosphere are indicated on each curve by the vertical bars at the ends of the horizontal line, which itself represents the cold-sky level. The estimated level of the quiet sun, shown at the center of the photosphere, is based on an assumed quiet sun of 60 solar flux units (one solar flux unit = $10^{-22} \text{Wm}^{-2} \text{Hz}^{-1}$). This level is determined for each curve by comparing the area under the curve with the total solar flux at 10.7 cm. (Prior to December 1968 the quiet-sun level was estimated each day from a calibrating noise signal inserted between the antenna and receiver. The present method was begun in December 1968 when it was discovered that the quiet-sun levels shown for September and October 1968 were approximately 8% too low.)

East-West scans with 30 seconds of arc resolution (recorded simultaneously with the 1.5 minutes scans) have been taken at selected intervals between 1969 and November 1971. Commencing November 1, 1971 they have been obtained on a routine basis along with circular polarization data. These data have not been included in the monthly summaries but can be made available on request.

East-West Solar Scans - Fleurs 21 cm and 43 cm -- East-West strip scans of the sun at 21 cm and 43 cm are made possible by the "Fleurs" Radio Astronomy Station of the University of Sydney, Sydney, Australia.

For the East-West solar scans from the 21 cm solar radio array the fan-beam has 2' of arc resolution. The two short horizontal lines drawn crossing the center line indicate the cold-sky level and the estimated quiet-sun level. The gain may differ from day to day. The curves have not been normalized to account for these gain variations other than by the indication of the estimated quiet-sun level.

For the East-West solar scans from the 43 cm solar radio array the fan beam has a resolution of 4' of arc. The estimated quiet sun is indicated on the published profiles in the same manner as for the 21 cm scans. The curves have not been normalized for variations in gain.

Outstanding Occurrences (SELECTED) -- A list of SELECTED centimeter and millimeter wavelength events at fixed frequencies is published one month following observations. Selections are made to provide 24-hour coverage as nearly as possible. See page 46, Outstanding Occurrences, for descriptions of the types of events and observatory characteristics.

S O L A R X - R A Y R A D I A T I O N (A.11, C.5)

The Space Environment Monitor (SEM) aboard the Synchronous Meteorological Satellites (SMS) and the Geostationary Operational Environmental Satellites (GOES) include a $\frac{1}{2}$ to 4Å x-ray ion chamber and a 1-8Å chamber. SMS-1 was launched in June 1974; SMS-2 was launched in February 1975; and GOES-1 in October 1975. These geostationary satellites are located over the western hemisphere and provide nearly continuous solar x-ray data. The SEM's data from two satellites are recorded, processed and disseminated in real time by the Space Environment Services Center of the NOAA Space Environment Laboratory in Boulder, Colorado. Further details of the SEM system are given in *The SMS/GOES Space Environment Monitor Subsystem* by R. N. Grubb [NOAA SEL, Boulder, Colorado 80302]. The x-ray ion chambers are described in *Calibration of X-ray Ion Chambers for the Space Environment Monitoring System* by A. Unzicker and R. F. Donnelly, NOAA Tech. Rept. ERL 310-SEL 31, 1974 [U.S. Government Printing Office, Washington, DC 20402].

The 1-8Å ion chamber has 300 mm Hg of Argon as a filler gas and a beryllium window that is 5×10^{-5} m thick with an x-ray viewing area of 1.9×10^{-4} m². The listed 1-8Å flux is based on a gray-body spectrum of 3×10^6 °K, which gives an average transfer function in good agreement with gray-body or free-free thermal spectra with temperatures in the range 3 to 100×10^6 °K. The $\frac{1}{2}$ - 4Å ion chamber has 180 mm Hg of Xenon as a filler gas, with a beryllium window that is 5×10^{-4} m thick with an area of 5.8×10^{-4} m². The listed $\frac{1}{2}$ - 4Å flux is based on a 10^7 °K gray-body spectrum.

The average x-ray flux values include data obtained during solar flares. Low values of the x-ray flux are contaminated by a photoelectric effect on SMS-1, radio frequency interference within GOES-1, and by particle interference during solar proton events. Therefore, no flux values below 10^{-7} Wm⁻² for the 1-8Å detector or 10^{-8} Wm⁻² for the $\frac{1}{2}$ - 4Å detector are reported. A "B" in the hourly average table indicates the flux was below these cut-off levels. An "M" in these tables denotes periods of missing data. The hourly average flux values are averages of 5-minute averaged data. The daily average values are averages of the 1-hour averaged data. The list of events does not include events with a maximum flux less than 3×10^{-6} Wm⁻² in the 1-8Å channel. The end of a flare is taken as that time when the 1-8Å flux enhancement above the preflare level has decreased to half its maximum value. Often an active region will remain bright after a flare or the x-ray flux will remain above the preflare value long after the half peak-enhancement end time.

C O R O N A L H O L E S (A.7f)

The helium D3 chromosphere is observed at the solar limb using the 10-inch vacuum telescope of Big Bear Solar Observatory with a Lyot filter of 0.3 Å bandpass. The observations are made visually by scanning the limb and recording the regions in which the double limb characteristic of the helium chromosphere are visible. This technique enables the positions of coronal holes to be determined at the limb to an accuracy of typically $\pm 3^\circ$ in position angle, and is carried out on a routine daily basis at Big Bear when seeing conditions permit.

Observational and theoretical evidence that the gaps in the D3 chromosphere correspond to coronal holes has been presented by H. Zirin, [*Ap. J.*, 199, L63, 1975] who showed that the properties of the helium lines can be explained by a model in which the helium is photoionized by coronal back-radiation. The weakening of chromospheric D3 in coronal holes is then a consequence of the reduced back-radiation in these regions.

The angular extent of the double limb is plotted versus time, where the position angle is measured from the sun's north pole (0°) to south pole (180°), with a positive sign for east limb and a negative sign for west. Days for which data are missing correspond to poor seeing conditions and/or equipment maintenance periods, and do not imply that the D3 double-limb was absent. A dashed line in the figure indicates that the hole boundary was indefinite.

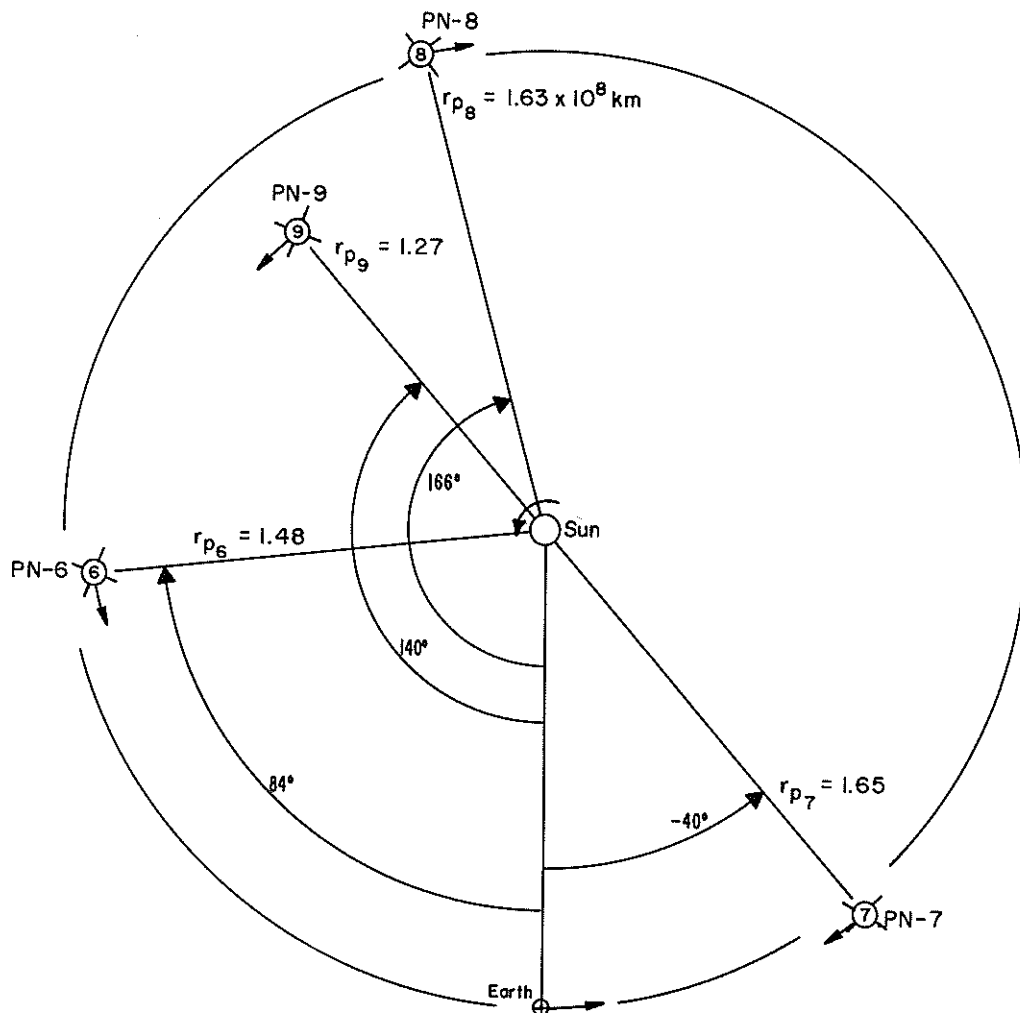
These observations are furnished by H. Zirin and K. A. Marsh of Big Bear Solar Observatory, California Institute of Technology.

S O L A R W I N D M E A S U R E M E N T S (A.13)

Pioneers 6, 7, 8 and 9 -- The NASA Ames Research Center plasma probe solar wind velocity data from Pioneers 6 through 9 are supplied by John H. Wolfe. These data include the date, the Deep Space Network (DSN) coverage period, the observation time in UT, the solar wind bulk velocity, U_{H+} , in kilometers/second, the density N_{H+} , in particles/cubic centimeter, the temperature, T_{H+} , in millions of degrees Kelvin, the Earth-Sun-Probe (ESP) angle in degrees and the co-rotation delay time in days.

On Pioneers 8/9, the U_{H+} , the N_{H+} and the T_{H+} are derived by a least squares computer fit of the solar wind energy distribution to a Maxwell-Boltzmann distribution in a moving frame of reference. The velocity represents the bulk of convective velocity of the solar wind. On Pioneers 6/7, the peak velocities are reported because a least squares program is not developed for these data.

The co-rotation delay, τ , defined as the time in days required for a steady state solar corotating plasma beam to rotate from the spacecraft to earth. A diagram showing the angular positions of Pioneers 6 through 9 with respect to the earth is on page 12. Viewing from the North Ecliptic Pole onto the Ecliptic plane, note that Pioneers 6, 8, and 9 are lagging the earth and therefore the τ is positive. Pioneer 7 is leading the earth and therefore its τ is negative. The co-rotation delay depends on the heliocentric radial distance of the earth and the spacecraft, the angular separation between the earth



Locations of Pioneers 6 through 9 on 1 Jan 76 in the Ecliptic Plane relative to the Earth (in a fixed Sun-Earth line plot) as viewed from the North Ecliptic Pole.

and the spacecraft, the solar angular velocity and the solar wind bulk velocity which defines the degree of the hose angle of the co-rotating Interplanetary Magnetic Field.

The equation used to compute the co-rotation delay, τ , follows:

$$\tau(\text{in seconds}) = \phi/\omega - (r_D - r_e)/U_{H+}$$

where ω is the angular velocity of the sun (in radians/second) corresponding to a 27-day solar synodical rotation period, and ϕ is the Earth-Sun-Probe angle (in radians).

Instead of using the solar equatorial projection of the Earth-Sun-Probe (ESP) angle ϕ' , the ESP angle itself, ϕ , is used. The error caused by this substitution can be no more than approximately 0.008 radians (0.5°), as explained in the following paragraph.

Because the solar equatorial plane is inclined approximately 7.25° to the ecliptic plane, and also the ESP angles for the Pioneers are all very nearly in the ecliptic plane, the projection of the ESP angles in the solar equatorial plane, ϕ' , can be related to the ESP angle, ϕ , as follows: Define ϕ as $\alpha_2 - \alpha_1$. α_2 is the angle in the ecliptic plane of the Earth from the "northern crossing" side of the line defined by the intersection of the ecliptic plane and the solar equatorial plane. The "northern crossing" side of this line is the side where the Earth crosses into the space to the north of the equatorial plane from the space to the south as it circles the Sun. α_1 is similarly defined for the Pioneer spacecraft. Then ϕ' (the projection of the ESP angle, ϕ , in the solar equatorial plane) can be expressed:

$$\phi' = \tan^{-1}(\cos 7.25^\circ \tan \alpha_2) - \tan^{-1}(\cos 7.25^\circ \tan \alpha_1)$$

A difference of approximately 0.008 radians (0.5°) between ϕ' and ϕ occurs when $\alpha_2 = 45^\circ$ and $\alpha_1 = 135^\circ$ (or vice versa). The difference is less than 0.5° for other combinations of α_2 and α_1 . Hence using ϕ rather than ϕ' is sufficiently accurate for the purposes of these calculations.

Solar Wind Speed from IPS Measurements at UC San Diego -- The solar wind speed is measured regularly with the three-station scintillation observatory at UCSD [Armstrong and Coles, *J. Geophys. Res.*, 77, 4602, 1972]. The data are supplied by W. A. Coles and B. J. Rickett. The interplanetary scintillation (IPS) technique, pioneered by Dennison and Hewish [*Nature*, 213, 343, 1967] yields an average velocity transverse to the line-of-sight to a distant radio source. Listed each month will be the solar wind speed and an error from observations of eight radio sources each day (however, in a typical month only five or six sources will be useful).

Each velocity is a weighted average from along the line-of-sight to the radio source, where the weighting factor decreases rapidly with distance from the sun. This spatial average is centered on an effective position (P), which is nominally at the point of closest approach of the line-of-sight to the sun, unless this point is closer to the earth than 0.3 A.U. In the latter case, P is taken to be at the point 0.3 A.U. from the earth along the line-of-sight. The heliographic coordinates of P vary slowly over the year as shown in Figure 1. Each month the solar distance (in A.U.), heliographic latitude and the difference in longitude between the point P and the earth are tabulated at 10-day intervals. Each source is observed for 1-2 hours per day and the observation time (in UT) is also tabulated. Details of the spatial weighting function can be computed and examples are shown in Figure 2 on the assumption of a power law shape for the density spectrum. The results are not very sensitive to the assumed density spectrum as can be seen by comparison with Readhead's [*MNRAS*, 155, 185, 1971] calculations for a Gaussian spectrum, but they assume spherical symmetry. Close agreement is found between ecliptic IPS observations and IMP 7 observations of the solar wind speed, when the spacecraft data are smoothed by a weighting factor proportional to the expected turbulence level [Coles, Harmon, and Lazarus, *EOS*, 56, 440, 1975].

Coles and Kaufman [*EOS*, 55, 556, 1974] carefully analyzed the flow angle, as well as the speed, and found it to be very close to radial. Thus we analyze the regular data under the assumption that the flow is indeed radial. This allows a least-square estimate of the radial component of velocity and also an associated error estimate. When the solar elongation is greater than about 73°, the pattern velocity (at P) is less than the radial velocity (because the angle Earth-P-Sun is less than 90°); the tabulated velocities have been corrected for this projection effect. A further assumption is that the scintillation pattern is spatially isotropic; this introduces a second order error [Coles et al., *EOS*, 56, 1180, 1974] and in these preliminary data it has not been corrected. We also estimate the flow angle but only use it in editing data with poor signal-to-noise ratio. The data are not included in

LAG 2 days per division ; DISTANCE .25 A.U. per division ; LATITUDE 15 degrees per division

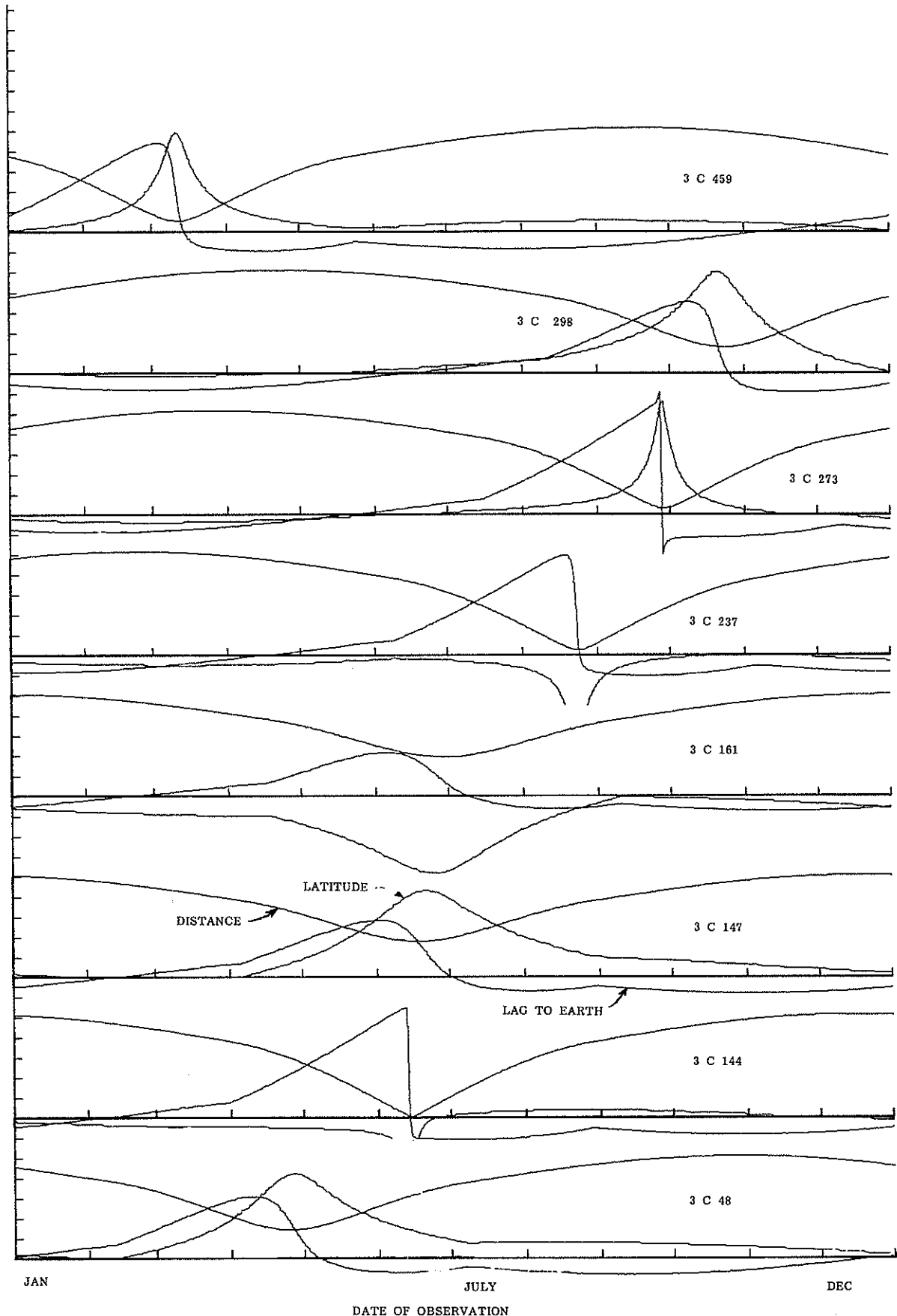


Figure 1

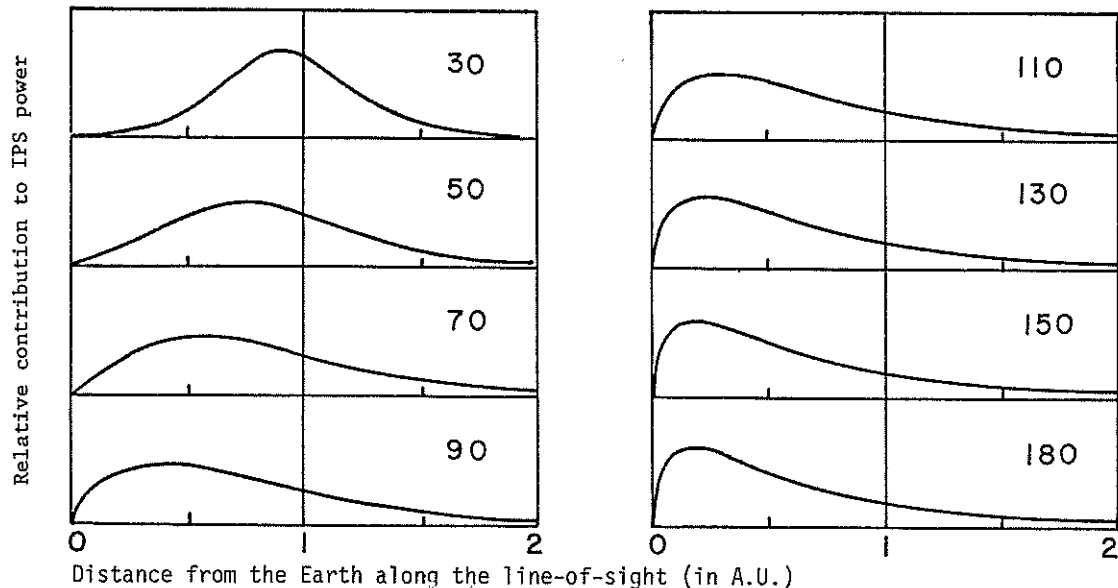


Figure 2. Computed IPS weighting functions along the line-of-sight, at the solar elongation angles indicated. The density spectrum was assumed to be power law $\propto q^{-3.3}r^{-4}$ (where q is wave number and r is solar distance); a source diameter of 0.25 sec of arc was also assumed.

this table if the apparent flow angle is greater than 30° from the radial or if the speed error is greater than 33 percent of the speed estimate itself. Further analysis may yield speeds from data rejected by these criteria; those interested in particular periods should contact the authors directly.

The speed estimate is derived from the "mid-point" of the correlation functions. This is found to be a reliable estimator for the solar wind speed. [See Coles and Maagoe, *J. Geophys. Res.*, 77, 5622, 1972; Coles, Rickett and Rumsey, a review of IPS in "*Solar Wind Three*", published by UCLA, 1974]. The solar wind speeds derived from elongated radio sources [e.g., 3C273 and 3C298] are preliminary in that a bias of less than about 10% is sometimes present; corrected data will be available to anyone interested. The "peak" velocity and other parameters of the scintillations are also computed, but will not be included in the monthly reports.

The use of scintillation observations to obtain solar wind velocities represents part of the activity conducted by the SCOSTEP project, Study of Travelling Interplanetary Phenomena (STIP).

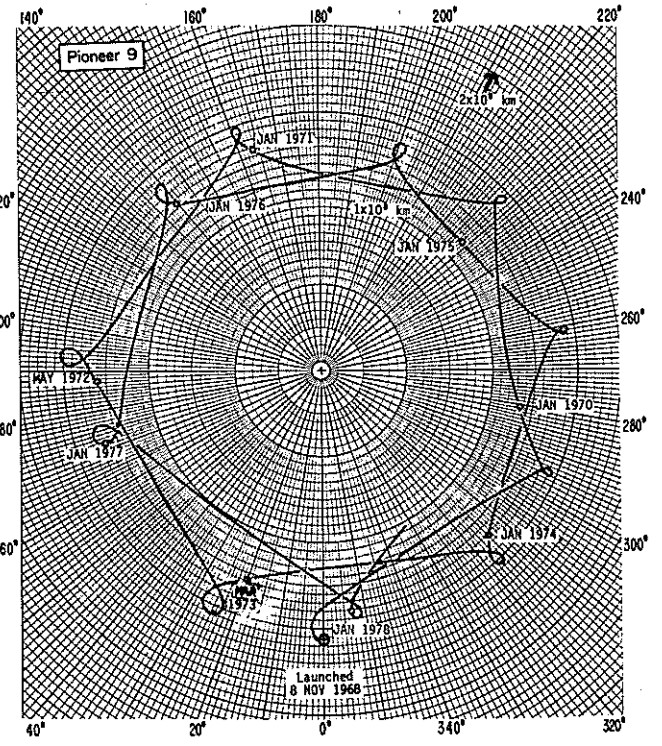
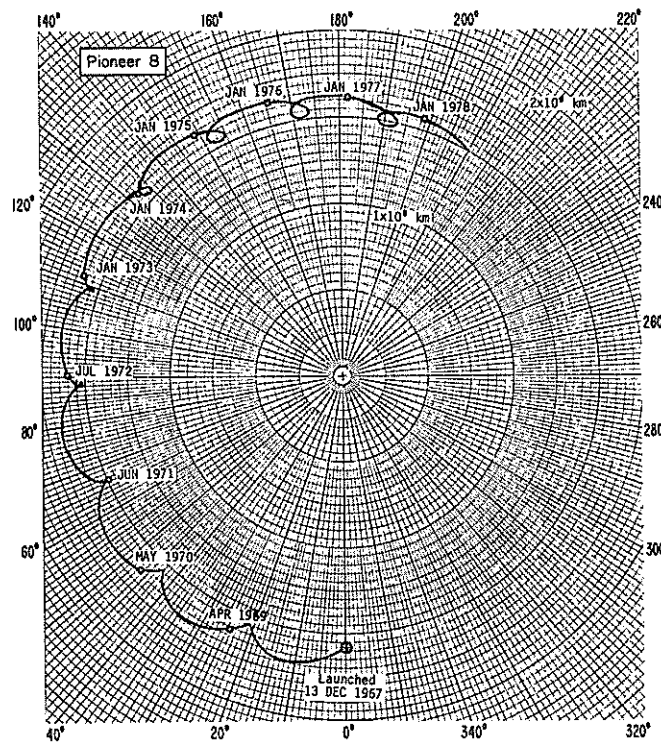
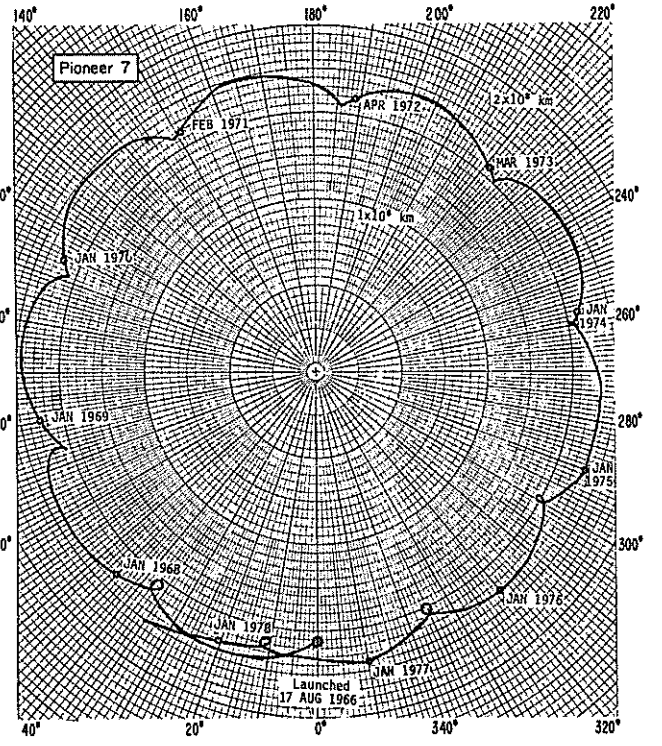
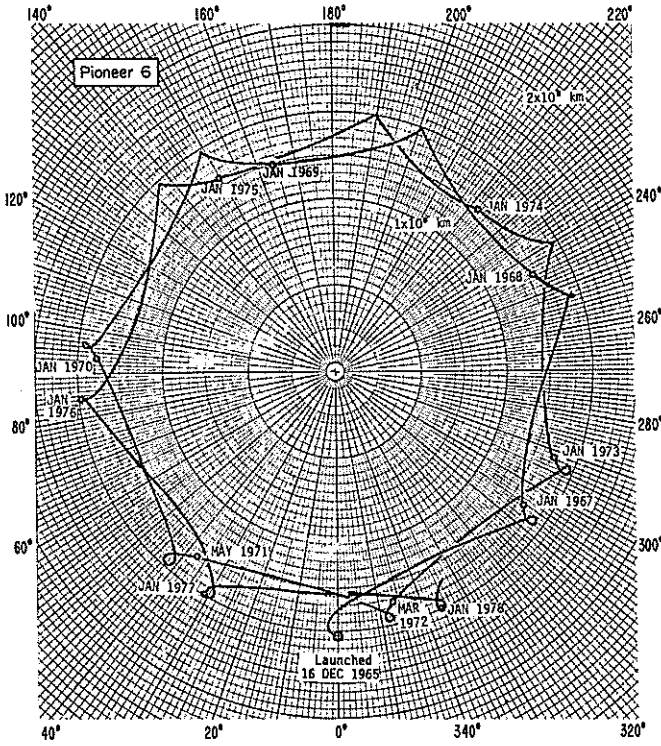
S O L A R P R O T O N M O N I T O R I N G (A.12)

Pioneer 6 -- These data are provided by Professor J. A. Simpson and his co-workers at the University of Chicago. Cosmic-ray particle counting rates are provided for three ascending energy ranges, from 0.6 to >175 Mev/nucleon. Counting rate measurements are made by the University of Chicago cosmic-ray telescopes aboard Pioneer 6. These are supplied, when possible, hourly throughout the pass.

Both instruments consist of a stack of three solid-state detectors separated by absorbers, surrounded by an anti-coincidence cylinder. The figure shows a cross-section view of the particle telescope.

Counting rates are provided for the coincidence modes $D_1 \bar{D}_2 \bar{D}_4$ (protons and helium nuclei 0.6-13 Mev/nucleon, electrons 400-700 kev), $D_1 D_2 \bar{D}_4$ (protons 13-175 Mev helium nuclei >13 Mev/nucleon and $\bar{D}_1 \bar{D}_2 D_3 \bar{D}_4$ (proton >175 Mev). The geometrical factors for the three coincidence modes are 5.4, 0.92, and 0.5-1.65 (see below) $\text{cm}^2\text{-ster}$, respectively. At energies above ~ 200 Mev, the last two coincidence modes become bidirectional. A detailed description of the telescope and the related electronics may be

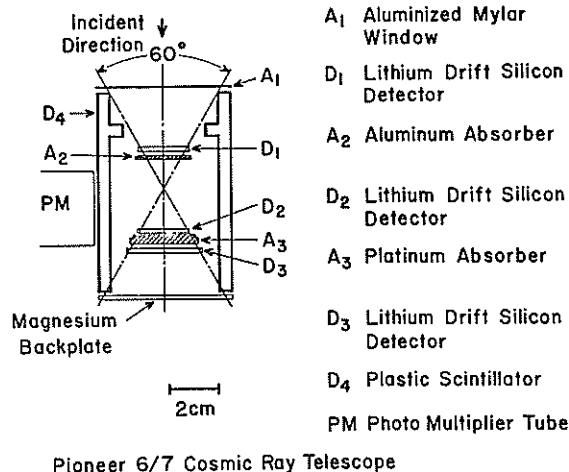
LOCATION OF PIONEER SPACECRAFTS



The above diagrams illustrate the position of Pioneers 6, 7, 8 and 9. Several types of observations are reported from these spacecraft as discussed in the accompanying descriptions.

found in Fan et al. [*J. Geophys. Res.*, 73, 1552-1582, 1968] and Retzler and Simpson [*J. Geophys. Res.*, 74, 2149-2160, 1969].

The counting rates are prepared from quick-look data, and are subject to future revision when the final data tapes reach the University of Chicago. Times given are only approximate (time accurate to ± 15 minutes), and the counting rates are accurate to $\sim 10\%$. When one of the two high-energy counting rates is at the quiescent level, a symbol Q is used instead of the actual rate. For the 0.6-13 Mev proton counting rate, the quiescent level is approximately 0.08-0.15 c/s. The two highest ranges exhibit a pronounced variation of the quiescent level with the solar cycle.



Pioneers 8 and 9 -- The cosmic-ray proton count rates as observed on Pioneers 8 and 9 are provided through the cooperation of Dr. W. R. Webber and Dr. J. Lezniak of the University of New Hampshire.

Quick look data from telescopes "5" and "1+2" are supplied.

Telescope 5 is a wide angle, two-element solid-state telescope with an energy threshold of 14 Mev for protons and 0.6 Mev for electrons. The geometric factor is approximately 8.3 cm²-sterad during quiet times and 4.2 cm²-sterad during solar flare times.

Telescope 1+2 is a narrow-angle, five-element, solid-state telescope with a proton energy threshold of 64 Mev on Pioneer 8 and 42 Mev on Pioneer 9. The geometric factor of this telescope is 2.35 cm²-sterad.

INTERPLANETARY MAGNETIC AND ELECTRIC FIELDS (A.17, A.17a, A.18)

Pioneer 8 -- The Interplanetary (IP) Magnetic Field data from the NASA-Goddard Space Flight Center magnetometer on Pioneer 8 are being supplied by Franco Mariani of the University of Roma and N. F. Ness of Goddard. The data supplied are the absolute magnitude, $|B|$, (in gammas, one gamma equals one nano-tesla) and the solar ecliptic longitude, ϕ , (in degrees) of the field measured counterclockwise from the spacecraft-sun line, as viewed from the North Ecliptic Pole.

The instrument is a mono-axial fluxgate magnetometer. The sensor is mounted on one of three transverse booms 2.1 meters from the spin axis and at an angle of 54°45' to the spin axis.

Three samples are taken at equal intervals during one spacecraft rotation yielding three independent mutually orthogonal measurements defining the total vector magnetic field. The magnetometer incorporates an automatic inflight range switch between two dynamic range scales of ± 32 and ± 96 gammas for a resolution of ± 0.125 and ± 0.375 gammas. The accuracy of the instrument is limited by spacecraft-associated magnetic fields and the sensor zero drift. A non-magnetic explosive-actuated indexing device is used to reorient the fluxgate by 180° to establish its zero level.

Five bit rates are possible: 512, 256, 64, 16 and 8 bits/second. At the three higher rates, the average time interval between successive determinations of the field vector is 1.3, 1.4 and 1.75 seconds, respectively. A special purpose digital computer is included in the instrument to compute time averages of the field components when the spacecraft is operating at the low bit rates of 16 and 8.

The data supplied include the date, the Deep Space Network (DSN) coverage period, the observation time in UT, the magnitude and solar ecliptic longitude of the field, as described above.

The magnetic field data are sampled approximately every hour. Each hourly sample is an average over three consecutive vectors which are separated by 14 seconds or less, depending on the spacecraft bit rate.

The IP sector structure at the Pioneer 8 position can be inferred from the longitudinal angle: angles between 45 and 225 degrees are associated with outward sectors, and the remaining angles with inward sectors. It is recognized, however, that the field direction, at the time of observation, may not adequately represent the direction over a period of hours.

Pioneer 9 -- The Interplanetary (IP) Magnetic Field data from the NASA Ames Research Center magnetometer on Pioneer 9 are being supplied by Chas. P. Sonett and David S. Colburn. The data supplied are in magnitude, B , of the field in gammas and the solar ecliptic longitude, ϕ , of the field in degrees, measured from the spacecraft-sun line in a counterclockwise direction, as viewed from the North Ecliptic Pole. The instrument is a triaxial fluxgate magnetometer with onboard spin demodulation and use of appropriate filters to avoid aliasing errors. The filter time constant is adjusted to be proportional to the sampling interval. The sampling interval is 0.292, 0.583, 2.33, 9.33 and 18.7 seconds for 512, 256, 64, 16 and 8 bps, respectively. The digitization uncertainty in each component of the field is ± 0.2 gammas. The quicklook data are not corrected for sensor offset in the component along the spin axis of the spacecraft. This, in general, gives an uncertainty in the field magnitude of less than one gamma and does not affect the determination of the longitude, ϕ .

The data supplied include the date, the Deep Space Network (DSN) coverage period, the observation time in UT, the field magnitude and its solar ecliptic longitude, as described above.

The magnetic field data are sampled approximately every hour. Each hourly sample is an average over three consecutive vectors which are separated by 18.7 seconds or less, depending on the spacecraft bit rate.

The IP sector structure at the Pioneer 9 spacecraft can be inferred from the longitudinal angle: angles between 45 and 225 degrees are associated with outward sectors, and the remaining angles with inward sectors. It is recognized, however, that the field direction at the time of observation may not adequately represent the direction over a period of hours.

Pioneers 8 and 9 -- The Interplanetary (IP) Electric Field data, as observed on Pioneers 8 and 9 on a real-time basis, are provided through the cooperation of Dr. F. L. Scarf from the Space Sciences Department of the TRW Group. These IP Very Low Frequency (VLF) wave data consist of a sequence of narrowband (400 Hz) signal amplitudes.

The table presents the date and Universal Time (UT) when the Electric Field Potential amplitudes (in millivolts) were read.

The real time 400 Hz data are selected to illustrate or characterize the activity during each pass and are being presented so that interested scientists can:

1. Attempt to correlate terrestrially-observed phenomena with variations noted in the IP Electric Field intensities at the spacecraft position.
2. Have access to simultaneous measurements of Plasma and E-field data on each spacecraft.
3. Study Solar Wind fluctuations and magnetic sectoring with the E- and B-field data on Pioneer 9.

Instrumental details of the Electric Field experiments are available in the following references: Pioneer 8: [*J. Geophys. Res.*, 73, 6655, 1968] and Pioneer 9: [*Cosmic Electrodynamics*, 1, 496, 1970].

INFERRED INTERPLANETARY MAGNETIC FIELD (A.17c)

The table shows daily inferences of the polarity of the interplanetary magnetic field. The first half of the day is based principally on magnetograms produced by the magnetometer at the Vostok Antarctic Station of the USSR. The magnetometer of the U.S. Air Weather Service operated by the Air Force Geophysics Laboratories (formerly Air Force Cambridge Research Laboratories) at the Thule Geopole Station is used for the second half of the day. The inference relies on the studies of Mansurov [*Geomag. Aeron.*, 9, 622-623, 1969] and Svalgaard [*Geophys. Pap. R-6*, 11 pp. Dan. Meteorol. Inst., Copenhagen, 1968] relating the variation of the polar cap magnetic field to the polarity of the interplanetary magnetic field. During 1972, the inferred polarity agreed with spacecraft observations on 83% of the days for which a definitive polarity was inferred. The rate of successful inferences for "toward" (interplanetary field directed toward the sun) days was somewhat greater than "away" days, 85% and 80%, respectively [Russell et al., *J. Geophys. Res.*, 80, 4747, 1975]. Forming a combined index from the two individual station inferences yields an overall success rate of 87% [Wilcox et al., *J. Geophys. Res.*, 80, 3685, 1975].

It appears that the sign of the east-west component of the interplanetary field is actually being inferred [Friis-Christensen et al., *J. Geophys. Res.*, 77, 371, 1972], rather than the polarity toward or away from the sun. Russell and Rosenberg [*Solar Phys.*, 37, 251, 1974] show that the east-west component is an accurate predictor of the magnetic polarity approximately 90% of the time. On "toward" days incorrectly inferred to have "away" polarity in 1972, the average Ap index was 20% less than the average Ap index on "toward" days. "Away" days incorrectly inferred to be "toward" days had no significant geomagnetic bias [Russell et al., 1975]. This effect when combined with the success rate results in a slight (2.5%) bias of the average Ap index for all inferred "toward" days over inferred "away" days. The subject of inferring the polarity of the interplanetary magnetic field has been reviewed by Svalgaard [*Correlated Interplanetary and Magnetospheric Observations*, D. Reidel, 1974].

The effect is visible at Vostok in the first half of the Greenwich Universal Day and at Thule in the second half of the day. The inferences from Vostok and sometimes from Thule are made at the Institute for Terrestrial Magnetism, Ionosphere and Radiowave Propagation (IZMIRAN), Moscow, and are shown in the table as the first value (or set of values) each day. The inferences from Thule are made at the Space Environment Services Center, Boulder, Colorado, and are shown as the second value (or set of values) each day. If two values are shown for a half-day period, an apparent change of polarity occurred within that half day.

The notation adopted for the table is that T represents days of negative Y-solar magnetospheric interplanetary magnetic field which would be characteristic of a "toward" sector and A represents days of positive Y-solar magnetospheric field, i.e., "away" polarity. An asterisk along with an A or T indicates half days when the effect was somewhat doubtful, but one polarity seemed predominant. An asterisk alone indicates half days when no clear polarity effect could be discerned. A dash indicates half days when missing data prevented inference of the polarity.

SOLAR PROTON EVENTS

An unnumbered page with a diagonal slash across it will be included whenever *provisional* outstanding solar proton events have been reported during the month before month of publication. This will be prepared by the Space Environment Services Center of the Space Environment Laboratory. These sheets will be self-explanatory and *are not to be used for research reference purposes*. They will merely provide some of the immediately available evidence when significant solar proton events have occurred in the previous month.

DATA FOR TWO MONTHS BEFORE MONTH OF PUBLICATION

TABLE OF CONTENTS

	<u>Page</u>
<u>Daily Solar Activity Centers</u>	
A.6 H α Synoptic Charts	21
Daily Charts Including:	
A.11e X-ray Spectroheliograms	22
A.9d 8.6 mm and 2.0 cm Spectroheliograms	22
A.3a,c Solar Magnetograms	23
A.5 Calcium Plages	24
A.4 Daily H α Spectroheliograms	24
A.1 Daily Sunspot Drawings	24
A.6 H α Prominences	24
A.7b λ 5303Å Coronal Intensities	24
A.5a Individual Regions of Solar Activity Combining Calcium Plages and Sunspots	24
A.5b Daily Calcium Indices	28
<u>Sudden Ionospheric Disturbances</u>	
C.6 SID Events	29
<u>Solar Radio Waves</u>	
C.4 Spectral Observations	32
C.3t 43.25, 80 and 160 MHz Selected Bursts	35
<u>Cosmic Rays</u>	
F.1 Table of Daily Average Neutron Counting Rates per Hour	36
F.1 Chart of Variations	37
<u>Geomagnetic Activity</u>	
D.1a Table of Indices Kp, Kn, Ks, Km, Cp, Ap, aa	37
D.1ba Musical-note 27-day Recurrence Diagram	39
D.1g Table and Graph of Hourly Equatorial Dst Index	39
D.1d Principal Magnetic Storms	39
D.1f Sudden Commencements and Solar Flare Effects	40
<u>Radio Propagation Indices</u>	
B.51ca North Atlantic Quality Figures and Forecasts	40
B.52 Transmission Frequency Ranges - North Atlantic Path	41
B.53 Quality Indices on Transmissions to Lüchow, (GFR)	41

S O L A R A C T I V I T Y C E N T E R S

(A.1, A.3a, A.3c, A.4, A.5, A.5a, A.5b, A.6, A.7b, A.9cb, A.9d, A.11h)

H-alpha Synoptic Charts -- These charts of the entire solar surface show solar activity in terms of polarity of magnetic fields, filaments (cross-hatched), major sunspots (large dots), H-alpha plage (stipple), distinct neutral lines (solid lines), and estimated neutral lines (dashed lines).

Longitude is in terms of the mean rotation rate for sunspots as determined by Carrington. This is the heliographic longitude tabulated in the American Ephemeris and Nautical Almanac. The value for 0^h UT each day appears at the top of the pages of photographs and charts. The dates at the top of the synoptic chart correspond to these values, showing the time of central meridian passage for the corresponding heliographic longitudes.

The charts are labeled with the serial number of the solar rotation as counted by Carrington, with the first rotation commencing November 9, 1853.

The positions of magnetic polarity reversal are inferred according to the techniques described by McIntosh [*Rev. Geophys. and Space Phys.*, 11, 837-846, 1972; also *Solar Activity Observations and Predictions*, McIntosh and Dryer, ed., MIT Press, 1972]. The H-alpha structures that reveal these "neutral" lines are: filaments, filament channels, plage corridors, "iron-filing" pattern of fibrils adjacent to active centers, and arch-filament systems. The patterns are mapped by accumulating the positions of features on H-alpha filtergrams from several consecutive days. Seldom does a single photograph show the patterns in their complete form, owing to the transient nature of the filaments and the variable observing conditions.

Magnetic polarities are inferred from Hale's law: leader sunspots in opposite solar hemispheres have opposite polarities. Northern leaders possess negative polarity during even-numbered solar cycles, while southern leaders are positive. We are now seeing some solar cycle #21 sunspot groups with polarities reversed from the cycle #20 sunspots. The polarities of all areas on the sun are inferred by beginning with a leader sunspot, or the leading portion of a bipolar plage, and alternating polarities with each successive neutral line.

The H-alpha patterns mapped are the forms seen when the particular features were near W40 on the visible solar hemisphere. This bias toward the west enables a more realistic comparison with solar wind, particle, and magnetic-field data measured near the earth. Whenever a pattern undergoes a conspicuous change from the time of first visibility to the time when at W40, the former neutral-line position is depicted as a line with dots superimposed.

The charts published here are preliminary versions constructed as part of the real-time solar monitoring at NOAA's Space Environment Services Center in Boulder. In most cases, there has been corroboration with solar magnetograms made with photospheric spectral lines (Kitt Peak, Mt. Wilson, and Sacramento Peak). Some changes and additions will be necessary when more careful study of the filtergrams and magnetic-field data can be made. The date in the lower right corner is the date of the last revision before the publication.

The mapping techniques include comparison with previous synoptic charts for maintenance of consistency and continuity. Daily use of inferred solar magnetic field data has demonstrated a 90% reliability within active regions and at least 75% reliability in the large-scale patterns in quiet regions. The reliability is degraded in regions where estimated neutral lines (dashed lines) are used extensively. Large portions of the charts for the period near solar minimum are so delineated.

The preliminary charts are produced by Ms. Janice Leighton with support from AFCRL Contract F19628-73-0070 to the University of New Hampshire and with a subcontract to NOAA Space Environment Laboratory (Letter Agreement No. 600405) from the Applied Physics Laboratory, The Johns Hopkins University. Support by Air Force Geophysics Laboratory (formerly AFCRL) does not necessarily imply endorsement.

Photographs or Charts -- On two pages per day are presented several photographs or charts of active solar centers recorded at optical and radio wavelengths. For each day the ephemeris heliographic longitude, L_0 , at 0000 UT, position angle, P , and center of sun, B_0 , are given. Transparent Stonyhurst disks (regular or modified) are provided with this text to fit the size of the charts. Regular Stonyhurst disks have the longitude lines spaced in intervals of 10° east and west of central meridian. Modified Stonyhurst disks have the longitude lines spaced at days east and west of central meridian. With the 1975 Descriptive Text the large size transparencies were regular and the small size were modified. In this issue the large ones are modified and the small regular. Though a magnifying glass is needed to read detail, it is felt that the significant regions stand out on the scale used. *For those interested, larger sizes of these photographs or charts can be made available at cost through the World Data Center A for Solar-Terrestrial Physics.*

These data for each day are x-ray spectroheliograms, 8.6 mm and 2 cm spectroheliograms, solar magnetograms, calcium plage and sunspot tracings, and H α filtergrams. The sunspot drawing also shows prominences and green line corona.

Details of these individual observations follows:

X-ray Maps from OSO-8 -- The Lockheed Palo Alto Research Laboratory Mapping X-Ray Heliumeter (MXRH) instrument on OSO-8 has been in operation since launch in June of 1975. The MXRH, which is in the wheel looking radially outward, consists of three one-dimensionally collimated (FWHM = 2.0 arcmin) systems, each tilted 120° from the other. Three one-dimensional distributions are obtained approximately every 20 seconds and can be unfolded to locate and isolate the emitting x-ray regions on the solar disk. The detection elements are proportional counters with three different detector types being employed in order to obtain a detectable, yet unsaturated, response over a dynamic range of 10⁵. Fourteen channel pulse height analyzers provide the energy information. The MXRH spectral response is approximately 1.5-30 keV where the lower value is set by the 75 μ m thick Be window of the most sensitive detectors. The actual upper value is spectrum and intensity dependent and for most cases will be substantially below 30 keV.

The maps presented here are prepared from quick-look data which are received daily over a phone line from GSFC to Lockheed. As such, they are based on a daily data sample which on average includes 200 minutes of solar coverage. A typical (neither the quietest nor the most active) thirty minute period is selected from these data to construct a map. The relative intensity of a region is indicated by differing dot sizes where "detectable" varies from system to system but nominally corresponds to a counting rate which is about 5 times the average background. The three dot sizes represent detectable (D) to 20D, 20D to 500D, and >500D. If a source has been highly variable in intensity (varying by more than an order-of-magnitude over a time period of less than two hours) no typical intensity is assigned, but rather a highly-variable indicator is used. The temperature assigned to each source is determined by fitting the observed data to that predicted by convolving the instrument response function with the spectra of an isothermal low density plasma as obtained from an updated Tucker Koren formulation [Ap. J., 168, 283, 1971]. The temperatures assigned should be considered preliminary pending final in-orbit instrument calibration. When this calibration is complete, the MXRH maps will include emission measure and absolute flux information.

Additional explanation or data may be obtained from L. W. Acton or C. J. Wolfson of Lockheed Palo Alto Research Laboratory, Dept. 52-12, Bldg. 202, Palo Alto, California 94304 (Telephone: (415) 493-4411, Ext. 45261). Workers needing historical or near-real-time solar X-ray information are invited to contact the Lockheed investigators.

2.0 cm and 8.6 mm Spectroheliograms -- The 2.0 cm wavelength (15.3 GHz) and 8.6 mm wavelength (35.0 GHz) solar radio maps are made at the La Posta Astrogeophysical Observatory of the Naval Electronics Laboratory Center, San Diego, Calif. (NELC La Posta). The program is funded in part by the Air Force Geophysics Laboratory. The geographic coordinates of the observatory are: Long. 116°26'6.43"W, Lat. 32°40'39.33"N; elevation 1188 m above mean sea level.

The antenna used for the observations is a 18.3 m (60 ft) diameter circular paraboloid with a Cassegrain feed system, on a computer controlled altitude-azimuth mount. The half power beam width of the antenna is approximately 4.0' at 2.0 cm and 2.8' at 8.6 mm. The observations are made with Dicke switch radiometers, the antenna being switched against a noise tube. The central disk quiet area solar antenna temperature is ~ 7000°K at 2.0 cm and ~ 3800°K at 8.6 mm. The measured rms noise of both radiometer systems when looking at the sun is ~ 2°K for a 1.0 second time constant.

The data for the maps are collected by automatically directing the telescope to perform a square boustrophendonic raster with lines perpendicular to heliographic north-south, filling a 19 by 19 grid of points spaced 2.0' apart at 2.0 cm wavelength, and a 35 by 35 grid of points spaced 1.0' apart at 8.6 mm wavelength. The corners of the resulting grid are indicated on the maps. Note that at 2.0 cm the grid is 36' square while at 8.6 mm the grid is 34' square. The scale of the map is shown at the lower left corner of the grid by short axes with 1.0' tic marks. The Universal Time at which the map was begun is shown below the map. Approximately 25 minutes are required to fill the 2.0 cm wavelength grid, while approximately 65 minutes are required at 8.6 mm wavelength. The quantity being contoured is antenna temperature; all contours are labeled in units of 100°K. The contour interval is not necessarily constant on a map, and may be changed from map to map in order to provide a clearer picture of the radio emission.

On days for which no map is presented the words NO DATA appear near the center of the grid. Below this appears a one word indicator of why no map has been provided. These words have the following specific meanings:

- CLOUDY ----- A map was made for the day beginning at the time shown; however, the data were so seriously affected by clouds that it was deemed unwise to publish it. Such maps will be provided to individual researchers upon request.
- WEATHER ----- The weather at the observatory was so inclement that no observations were made. No time is given in the format.
- CALIBRATION -- A map was made for the day beginning at the time shown; however, the operation of the equipment was such that the reliability of the antenna temperature is in doubt. Such maps will be provided to individual researchers upon request.
- EQUIPMENT ---- The situation and condition of the equipment were such that no map was made. This includes such causes as receiver malfunction, mechanical and computer problems, and preventative maintenance. No start time is given in the format.

Further information and requests for extra data as stated above should be addressed to: Max P. Bleiweiss, NELC La Posta, Rt. 1 Box 591, Campo, California 92006, Attention: Fred L. Wefer.

Mount Wilson Observatory Solar Magnetograms -- The Mount Wilson Observatory solar magnetograms are computer-plotter iso-gauss drawings made with the magnetograph at the 150-foot tower telescope on Mount Wilson. The program is supported in part by the Office of Naval Research and the National Aeronautics and Space Administration. The polarities are indicated with "Plus" signifying the magnetic vector pointed toward the observer. The gauss levels are also indicated. This instrument measures the longitudinal component of the magnetic field using the line $\lambda 5250.216$ Fe I. A solar magnetograph is basically a flux measuring instrument. It measures the total flux over the aperture which is being used. The magnetograph apertures are square (image slicer is used) and the raster scan lines are separated by the dimension of the aperture. This separation of the scan lines is given by the ΔY (DELTAY) printed on the magnetogram. The units of ΔY are arc seconds. The DELTAX represents in the same units the distance along the scan line between points at which the data were digitized.

The scan is a boustrophedonic raster scan which extends for all scan lines beyond the disk. The data within about 12 arc seconds of the solar limb are not plotted. The scanning system is always oriented so that the scan lines are perpendicular to the central meridian of the sun. The cardinal points on the magnetogram refer to heliocentric coordinates so that the "N" and "S" define the rotation axis of the sun.

Because the magnetic field strength measured by the magnetograph is the product of the true field strength and the brightness of the image, the fields used to make the contours have been corrected for the brightness at each point. So effects of limb darkening and variable sky transparency have been corrected.

Effects due to weakening of the line profile in magnetic field regions have not been accounted for. In general the magnetic field strengths on the map are low by about a factor of two because of these effects, but this varies somewhat with distances from the disk's center. For more details c.f. *Solar Physics*, 22, 402-417, 1972.

It is difficult to estimate precisely the errors in the magnetic data which goes into these magnetograms, and in any case, the errors vary from day-to-day. The zero level is probably accurate to a few tenths of a gauss or better, on almost all magnetograms. The gauss scale is probably almost always accurate to 15% or better. The noise level is almost always well below the first isogauss level (5 gauss).

Sometimes, because of the small scale of the reproductions, it is difficult to make out the details of the field distribution in some regions. *Large scale copies of the particular magnetograms may be obtained by writing to:*

*World Data Center A for
Solar-Terrestrial Physics
NOAA
Boulder, Colorado, U.S.A. 80302*

Kitt Peak Observatory Solar Magnetograms -- Full disk magnetograms are now made daily, weather permitting, at the vacuum telescope on Kitt Peak in Arizona. At the exit focus of the spectrograph is a Babcock type magnetograph which utilizes as detectors a pair of 512-element silicon-diode arrays. The diode spacing, referred to the entrance slit, is one arc-second. Resolution achieved depends in practice mainly on "seeing", but in any case falls to zero at this one arc-second limit. At present the magnetograms are taken in the wings of Fe I 8688.6 Å, a line selected to faithfully record network, plage and penumbral magnetic flux but which underestimates umbral flux by a factor of about two. A full disk recording is made up of four swaths and requires 37 minutes of scan time.

The display of magnetograph data is by a CRT generated picture where bright represents positive flux and dark negative flux. The display intensity is non-linear in an effort to compress the dynamic range so that weak fields can be seen along with the strong sunspot fields. The noise is about 10^{17} maxwells (i.e., 15 gauss over one arc-second). Blank areas indicate interfering clouds. These high resolution maps complement the Mt. Wilson iso-gauss charts. Detailed numeric listings exist and can be retrieved from the observatory archives. For further information contact: J. Harvey or W. Livingston, Kitt Peak National Observatory, P.O. Box 26732, Tucson, Arizona 85727.

Calcium Plage Reports -- The contours are based on estimates made and reported on the day of observation. These data on calcium plage regions are as reported by the McMath-Hulbert Observatory of The University of Michigan supported by NOAA contract. They are the same regions which are summarized in the following section. Listed beside the drawings in each case are the quality of the day's observations and the initials of the observer for the day followed by a table of the plages by region number, then area in millionths of the solar hemisphere and intensity, if area ≥ 3000 millionths or intensity ≥ 2.5 . When McMath-Hulbert Observatory has been unable to observe, available drawings supplied by the Solar Observatory at Catania, Italy are used. The areas will differ from the McMath-Hulbert areas since there is considerable subjectivity in the grouping of the bright calcium areas into regions. Each series should be homogeneous in itself.

H-alpha Spectroheliograms -- The H-alpha spectroheliograms are furnished by the solar observatory at Ramey Air Force Base, Puerto Rico, operated by the U. S. Air Force 12th Weather Squadron of the 3rd Weather Wing. The telescope is a 25 cm (10 inch) refractor of approximately 160 cm (63-inch) effective focal length, equipped with a half-Angstrom bandpass Halle birefringent filter. These photographs are supplemented by photographs provided by the NOAA Space Environment Services Center Observatory at Boulder, Colorado, using a 11 cm (4.5 inch) refractor.

Sunspot Drawings -- These drawings are simplified copies of originals made at the Boulder solar observatory operated by the NOAA Space Environment Services Center. Sunspot groups are boxed according to a judgment of bipolar pairs based on spot group evolution and the structure of associated H-alpha plage, following guidelines developed by P. S. McIntosh of the NOAA Space Environment Laboratory. Serial numbers appearing adjacent to some of the sunspot groups are the last three digits in the McMath-Hulbert plage number. It is not uncommon for more than one bipolar group to occur within the same large calcium plage. Drawings from the Sacramento Peak Observatory or photographs from the Culgoora Solar Observatory (C.S.I.R.O., Narrabri, N.S.W., Australia) may be used when Boulder data are missing.

H-alpha Prominences -- Drawings of prominences are added to the limb of the sunspot drawings by tracing detail from photographic prints made from the NOAA Boulder H α patrol films.

Coronal Emission -- Emission intensity values for each 5° interval together with peak values greater than 250 are presented adjacent to the sunspot drawing disks for each day that data are available for the $\lambda 5303 \text{ \AA}$ (FeXIV) coronal line. The measurements are expressed in millionths of an angstrom (10^{-6} \AA) of the continuum of the center of the solar disk (at the same wavelength as the line) that would contain the same energy as the observed coronal lines [Billings, D. E., *A Guide to the Solar Corona*, Academic Press, p. 104, 1966]. The date of data presentation corresponds to the date of observation. The data are from a single station selected in the following priority: Kislovodsk, Pic-du-Midi, Wendelstein, Norikura and Lomnický Štít.

The data are presented for three intensity levels: 80-119, 120-199, and 200-249. Any values equal to or greater than 250 will be shown as a peak and its actual value given. The values will be centered on the appropriate 5° interval, overlapping on both sides by $2\frac{1}{2}^\circ$. The three levels of intensity are indicated by arcs: the one nearest the disk represents the lowest level, the next arc the intermediate level, and the highest arc the highest level.

Individual Regions of Solar Activity -- The table provides a history of each active center visible on the solar disk using data from McMath-Hulbert Observatory (calcium plages under NOAA contract) supplemented by data from Catania for days of no data at McMath-Hulbert; Mt. Wilson Observatory (magnetic classification of sunspots) and NOAA, Boulder (area, count and Brunner classification of sunspots). The Greenwich date of central meridian passage of each region is given in the lead line for each region as well as prior rotation number.

After the year, month, and day the McMath-Hulbert calcium plage region number is repeated followed by the latitude, central meridian distance, and heliographic longitude of the center of the region on that day. The next two columns give the corrected area in millionths of a solar hemisphere, and the intensity of the region at time of measurement on that day, on a scale of 1 = faint to 5 = very bright, referring to the brightest part of the plage.

These data are based upon estimates made and reported on the day of observation. However, they have been compared with the re-evaluated data and all significant discrepancies have been corrected, either directly in the data or by means of footnotes. These data are from observations obtained and reduced by different observers on days of widely different observing quality. For the quality of the observation on each day and the identification of the observer see daily calcium maps. The McMath-Hulbert Observatory requests that special attention be paid to the quality of observation for the days in question and to the possible personal equation of the respective observers.

The sunspot data lists the Mt. Wilson* group number, the latitude, central meridian distance and heliographic longitude of each spot group and the magnetic classification and largest magnetic field strength measured in each group. The magnetic classifications are defined as follows:

- AP = αp All the magnetic measures in the group are of the same polarity which is that corresponding to the preceding spots in that hemisphere for that cycle.
- AF = αf All the magnetic measures in the group are of the same polarity which is that corresponding to the following spots in that hemisphere for that cycle.
- BP = βp A bipolar group in which the magnetic measures indicate that the preceding spots are dominant.
- B = β A bipolar group in which the magnetic measures indicate a balance between the preceding and following spots.
- BF = βf A bipolar group in which the magnetic measures indicate that the following spots are dominant.
- BY = $\beta \gamma$ A group which has general β characteristics but in which one or more spots are out of place as far as the polarities are concerned.
- Y = γ A group in which the polarities are completely mixed.

Statements will be added to the above classifications if the group is also of the "D = δ -configuration": spots of opposite polarity within 2° of one another and in the same penumbra.

The Mt. Wilson magnetic sunspot classifications are given for spot groups observed at Mt. Wilson. If a magnetic classification is based on magnetic measurements, that classification is enclosed in parentheses. When only half of the sunspot group is measured, a half parenthesis indicates which half was measured — either the leader or the follower. A magnetic classification not enclosed in parentheses is determined from the appearance of the spot groups and the plage. A blank in the classification column indicates sufficient information was not available to make an intelligent determination of the magnetic classification. Prior to July 1966 the only magnetic classifications included in the lists were those for which there were magnetic measurements.

The largest magnetic field strength measured in each group is given. The number which appears under the column headed "H" is a coded representation of the largest magnetic field strength measured in the group. The field strength is only given to the nearest 500 gauss because it is felt that the uncertainties of measurement do not permit greater accuracy. These measurements are made with the line $\lambda 5250.216 \text{ \AA} (\text{Fe I})$. No correction is made for blending the Zeeman components. The code is as follows:

Code	Maximum Field Strength in Gauss	Code	Maximum Field Strength in Gauss
1	100- 500	6	2600-3000
2	600-1000	7	3100-3500
3	1100-1500	8	3600-4000
4	1600-2000	9	4100-4500
5	2100-2500	10	>4500

The area in millionths of a solar hemisphere, sunspot count and classification as observed at NOAA-Boulder are used to complete the sunspot information. Telegraphic Ramey or Manila sunspot data are substituted when available to fill gaps in Boulder data. The initial letter is used in the table to indicate the source of sunspot information.

*The Mt. Wilson daily observations in monthly summary form may be obtained upon request from World Data Center A for Solar-Terrestrial Physics.

The sunspot classification in column "C" is represented by three consecutive upper-case letters. It is the revised classification devised by P. S. McIntosh of NOAA. It consists of a modified Zürich Brunner class, the type of largest spot within the group, and the relative spot distribution or compactness of the group. This classification is included in the USSPS code, *I.U.W.D.S. "Synoptic Codes for Solar and Geophysical Data, Third Revised Edition 1973"*, p. 108. The definitions of the classification and an illustration of the types of sunspots follow.

When possible separate bipolar sets of spots are identified by measured magnetic polarities, by the positions of spots relative to lines of polarity reversal inferred from structures on H-alpha filtergrams, and by the record of birth and evolution of spots. If these observations are not available, the following definitions identify most unipolar and bipolar spot groups: (see Figure and definitions to follow).

Unipolar Group: A single spot or a single compact cluster of spots with the greatest distance between two spots of the cluster not exceeding three heliographic degrees. In modified Zürich H-class groups, this distance is measured from the outer penumbral border of the largest spot to the center of the most distant spot in the group. Strong new spots which are clearly younger than a nearby h-type spot (see Penumbra: Largest Spot) are usually members of a new emerging bipolar group and should be called a separate group.

Bipolar (Elongated) Group: Two spots of a cluster of many spots extending roughly east-west with the major axis exceeding a length of three heliographic degrees. An h-type major spot can have a diameter of three degrees, so a bipolar group with an h-type spot must exceed five degrees in length.

Modified Zürich Class (first upper case letter in column "C")

- A A unipolar group with no penumbra.
- B A bipolar group with no penumbra.
- C A bipolar group with penumbra on spots of one polarity, usually on spots at only one end of an elongated group. Class C groups become compact class D when the penumbra exceeds five degrees in longitudinal extent.
- D A bipolar group with penumbra on spots of both polarities, usually on spots at both ends of an elongated group. The length does not exceed 10 degrees of heliographic longitude.
- E A bipolar group with penumbra on spots of both polarities and with a length between 10 and 15 heliographic degrees.
- F A bipolar group with penumbra on spots of both polarities and with a length exceeding 15 heliographic degrees.
- H A unipolar group with penumbra. The principal spots are nearly always the leader spots remaining from an old bipolar group. Class H groups become compact class D when the penumbra exceeds five degrees in longitudinal extent.

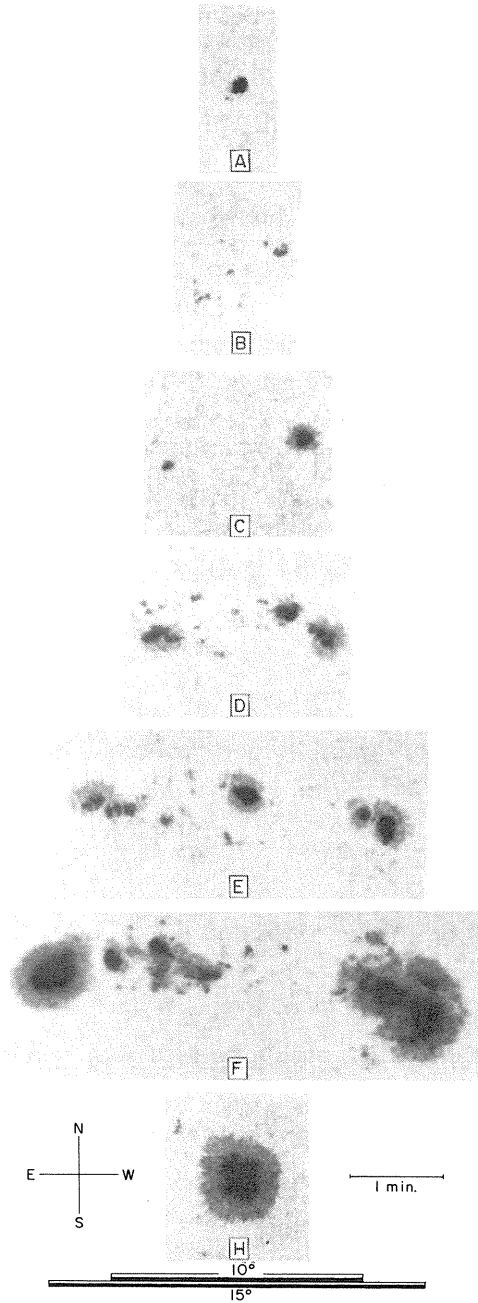
Note that Zürich classes G and J are missing in this revision. Class G groups are included in the definition of classes E and F, and class J groups are included in class H.

Penumbra: Largest Spot (second upper case letter in column "C")

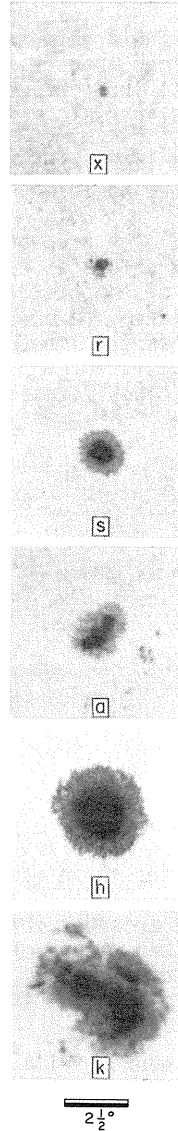
- "x" No penumbra. The width of the gray area bordering spots must exceed three arc seconds in order to classify as penumbra.
- "r" The penumbra is rudimentary. It is usually incomplete, irregular in outline, as narrow as three arc seconds, brighter intensity than normal penumbra and has a mottled, or granular, fine structure. Rudimentary penumbra represents the transition between photospheric granulation and filamentary penumbra. Recognition of rudimentary penumbra will ordinarily require photographs or direct observation at the telescope.
- "s" Symmetric, nearly circular penumbra with filamentary fine structure and a spot diameter not exceeding $2\frac{1}{2}$ heliographic degrees. The umbrae form a compact cluster near the center of the penumbra. Also, elliptical penumbra are symmetric about a single umbra. Spots with symmetric penumbra change very slowly.

McINTOSH
SUNSPOT GROUP CLASSIFICATION

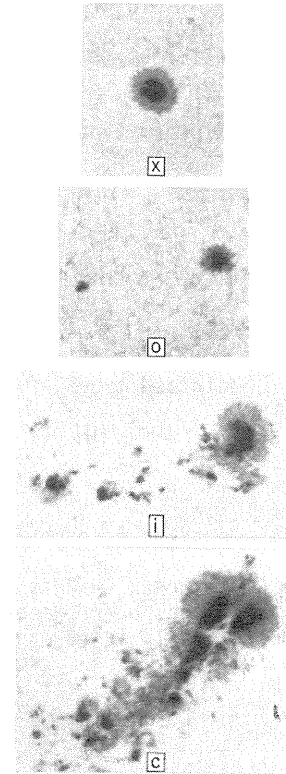
Modified Zurich Class



Penumbra: Largest Spot



Sunspot Distribution



- "a" Asymmetric, or complex penumbra with filamentary fine structure and a spot diameter along a solar meridian not exceeding $2\frac{1}{2}$ heliographic degrees. Asymmetric penumbra is irregular in outline or clearly elongated (not circular) with two or more umbrae scattered within it. The example in the figure is transitional between "s" and "a". Asymmetric spots typically change form from day-to-day.
- "h" A large symmetric penumbra with diameter greater than $2\frac{1}{2}$ heliographic degrees. Other than size, it has characteristics the same as "s" penumbra.

"k" A large asymmetric penumbra with diameter along a solar meridian greater than $2\frac{1}{2}$ heliographic degrees. Other than size, its characteristics are the same as "a" penumbra. When the longitudinal extent of the penumbra exceeds five heliographic degrees, it is almost certain that both magnetic polarities are present within the penumbra and the classification of the group becomes Dkc or Ekc or Fkc.

Sunspot Distribution (third upper case letter in column "C")

"x" Single spot.

"o" An open spot distribution. The area between leading and following ends of the group is free of spots so that the group appears to divide clearly into two areas of opposite magnetic polarity. An open distribution implies a relatively low magnetic field gradient across the line of polarity reversal.

"i" An intermediate spot distribution. Some spots lie between the leading and following ends of the group, but none of them possesses penumbra.

"c" A compact spot distribution. The area between the leading and following ends of the spot group is populated with many strong spots, with at least one interior spot possessing penumbra. The extreme case of compact distribution has the entire spot group enveloped in one continuous penumbral area. A compact spot distribution implies a relatively steep magnetic field gradient across the line of polarity reversal.

The first letter of the McIntosh classification is essentially the Brunner classification with the following exceptions:

McIntosh types:	Ero	and	Fro	=	Brunner class G
	Eso		Fso		
	Eao		Fao		
	Eho		Fho		
	Eko		Fko		
McIntosh types:	Hrx			=	Brunner class J
	Hsx				
	Hax				

N.B. For detailed research analyses these region tabulations should be used with caution.

Calcium Plage Index -- This table provides the daily calcium plage index based on the formula by Wesley R. Swartz, Ionosphere Research Laboratory, Pennsylvania State University as published in February 1971 text. The formula is re-expressed below:

$$Ca II_{index} = \left[\sum_i I_i A_i \cos \theta_i \cos \phi_i \right] / 1000$$

where the summation includes all the plages visible on the day.

I_i = intensity of plage i

A_i = corrected area of plage i in millionths of a solar hemisphere (McMath-Hulbert Observatory data)

θ_i = central meridian distance of plage i in degrees

ϕ_i = latitude of plage i.

Values of this index for the period January 1, 1958 through January 31, 1971 appear in the Pennsylvania State University Ionosphere Research Laboratory Report 373(E), *The Solar Ca II Plage Index*, Wesley E. Swartz and Regan Overbeck, October 8, 1971.

S U D D E N I O N O S P H E R I C D I S T U R B A N C E S (C.6)

Sudden ionospheric disturbances (SID) are presented in a table as one line per SID event. This table gives the date, beginning, ending and maximum time in UT of each event; an importance rating; types of SID observations; and flare, if known. The selected times of beginning, ending and maximum are usually those of a sudden phase anomaly (SPA). The time that is chosen from the SPA reporting stations is selected by taking into consideration the amplitude of the event and the time of the associated flare, if known. In the table D = greater than, E = less than and U = approximate time indicated. The importance rating is obtained by subjective averaging of the importances reported by all stations for all the different types of SID. The importance rating is based on a scale of 1, the least, to 3+, the most important. If SPA events are not available, shortwave fade out (SWF) events are used to determine the times. The degree of confidence of identifying the event is reported by the stations as a subjective estimate. This is then evaluated to decide whether the reported event is an SID or not. From the reports believed to be SID, a wide spread index is prepared signifying that the SID is geographically widespread. The index ranges from 1 (possible-single station) to 5 (definite-many stations). Some phenomena are listed if noted at only one location, if there has been a flare or other type of flare-associated effect reported for that time. In the flare column an * represents no flare patrol as yet available for time of event, and NF means no flare observed though there was a flare patrol at that time. Consideration is also given as to whether other reports are available from that longitude on that date. Below the table are listed the stations together with the type of SID reported which were analyzed to prepare the SID event table. A second table lists the number of SID for each day by the McMath region of the associated flare, if known.

The table on page 30 of this text gives the two-letter station code, the geographic location of the station and the type or types of SID information submitted. These data are made possible through the auspices of the International Ursigram and World Days Service, the U.S. Coast Guard, and private interested individual observers (AAVSO). Greater detail concerning the reporting stations can be found in "The Listing of Sudden Ionospheric Disturbances" by J. Virginia Lincoln [*Plant. Space Sci.*, 12, 419-434, 1964] and in earlier versions of this text.

The SID stations presently active are shown on the chart on page 31 by their longitude and by the type of SID recorded. The numbers across the top at 30° intervals indicate the earliest sunrise (top) and latest sunset (bottom) times in UT for the stations within ± 15° longitude. The times are based on the summer solstice (June 22). The small triangles throughout the chart indicate the midpoint of transmitting paths for SWF, SPA, SES, and SFD for only those stations that are underlined. (Many of the non-underlined SWF stations are commercial terminals, and the locations of the transmitters being recorded are not always known.) The world-wide coverage of SID effects is indicated by the density of the triangles, and will show in which parts of the world the ionosphere is studied for SID effects. The boxes around the three SCNA stations note that those stations record cosmic noise absorption with the same equipment; i.e., recorders designed by Robert Lee of the High Altitude Observatory, Boulder, Colorado.

N.B. The detailed data as formerly published are available at cost of reproduction from World Data Center A for Solar-Terrestrial Physics, NOAA, Boulder, Colorado 80302.

SID, sudden ionospheric disturbances (and GID, gradual ionospheric disturbances) may be detected in a number of ways: shortwave fadeouts (SWF), increases in cosmic noise absorption (SCNA), enhancement or decrease of low frequency atmospherics (SEA or SDA), sudden phase anomalies at VLF (SPA), sudden enhancements at VLF (SES), sudden phase anomalies at LF (SPA and SFA), and sudden frequency deviations (SFD).

SWF -- SWF events are recognized on field-strength recordings of distant high-frequency radio transmissions.

In the coordinated program, the abnormal fades of field strength not obviously ascribable to other causes are described as shortwave fadeouts with the following further classification:

- S-SWF (S) : sudden drop-out and gradual recovery
- Slow S-SWF (SL) : drop-out taking 5 to 15 minutes and gradual recovery
- G-SEF (G) : gradual disturbance: fade irregular in either drop-out or recovery or both.

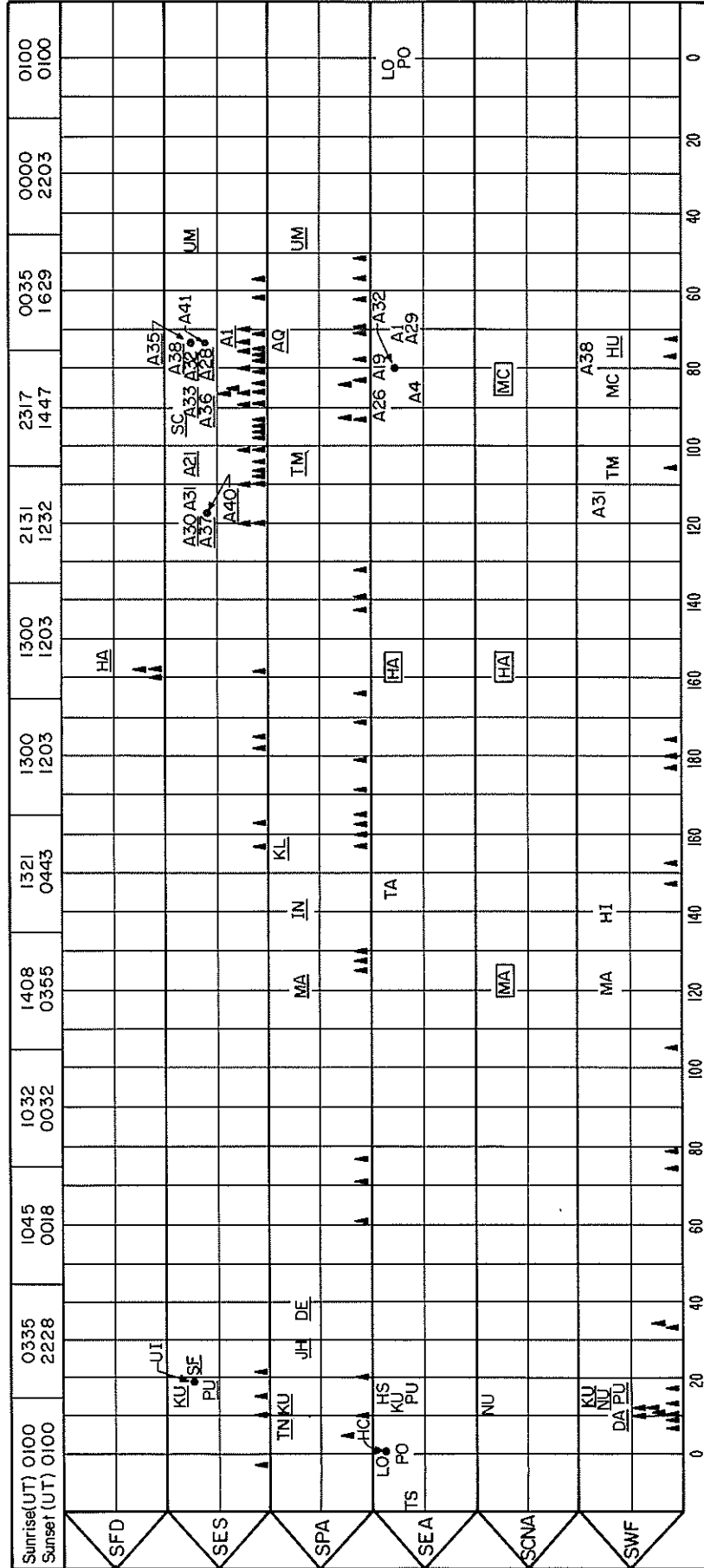
SCNA-SEA -- Sudden ionospheric disturbances recognized on recorders for detecting cosmic noise absorption at about 18 or 25 MHz are known as SCNA, or recognized on records for detecting enhancements of low frequency atmospherics at about 27 kHz are known as SEA.

SPA and SES -- Sudden phase anomalies (SPA) are observed as a phase shift of the downcoming sky-wave on VLF recordings or on pulse measurements on LF recordings. An estimate of the intensity can be obtained in terms of the degree of phase shift [see Chilton, C. J., et al., *J. Geophys. Res.*, 68, 5421-5435, 1963]. The length of path and amount of sunlight on the path must of course be considered.

STATION LIST FOR SUDDEN IONOSPHERIC DISTURBANCES TABLE

CODE	STATION LOCATION	SWF	SCNA	SEA	SES	SFO	SPA
AQ	AREQUIPA, PERU						X
DA	DARMSTADT, GFR	X					
DE	DEBRE ZEIT, ETHIOPIA						X
HA	HAWAII, USA		X	X		X	
HC	HERSTMONCEAUX, ENGLAND			X			
HI	HIRAISO, JAPAN	X					
HS	HERMANUS, SOUTH AFRICA			X			
HU	HUANCAYO, PERU	X					
IN	INUBO, JAPAN						X
JH	JOHANNESBURG, SO AFERICA						X
KL	KULA, MAUI, HAWAII, USA						X
KU	KUHLUNGSBORN, GDR			X			X
LO	PRESTON, ENGLAND			X			
MA	MANILA, PHILIPPINE ISLANDS	X	X				X
MC	MCMATH-HULBERT OBS., MICHIGAN, USA	X	X				
NU	NEUSTRELITZ, GDR	X	X				
PO	POITIERS, FRANCE			X			
PU	PRAGUE, CZECHOSLOVAKIA	X		X	X		
SC	ST. CLOUD, MINNESOTA, USA				X		
SF	SOFIA, BULGARIA				X		
TA	HOBART, TASMANIA			X			
TM	TABLE MOUNTAIN (BOULDER, COLO, USA)	X					X
TN	TORINO, ITALY						X
TS	TORTOSA, SPAIN			X			
UI	UPICE, CZECHOSLOVAKIA			X			
UM	SAO PAULO, BRAZIL				X		X
AMERICAN ASSOCIATION OF VARIABLE STAR OBSERVERS (AAVSO)							
A1	VALLEY COTTAGE, NEW YORK, USA			X	X		
A4	COLUMBUS, OHIO, USA			X			
A19	LATROBE, PENNSYLVANIA, USA			X			
A21	LITTLETON, COLORADO, USA				X		
A26	LOUISVILLE, KENTUCKY, USA			X			
A28	MAYFIELD VILLAGE, OHIO, USA				X		
A29	LEXINGTON, MASSACHUSETTS, USA			X			
A30	SUNNYVALE, CALIFORNIA, USA				X		
A31	MISSOULA, MONTANA, USA	X			X		
A32	POMPTON PLAINS, NEW JERSEY, USA			X			
A35	BROOKLYN PARK, MINNESOTA, USA				X		
A36	WORTHINGTON, OHIO, USA				X		
A37	YAKIMA, WASHINGTON, USA				X		
A38	ORMOND BEACH, FLORIDA, USA	X			X		
A40	LA CRESCENTA, CALIFORNIA, USA				X		
A41	HAMILTON, NEW YORK, USA				X		

MERIDIONAL POSITION OF SID STATIONS, BY TYPE



West

International Date Line

East

— LONGITUDE —

Presently active SID stations are shown above. The numbers across the top at 30° intervals indicate the earliest sunrise (top) and latest sunset (bottom) times in UT for the stations within ± 15° longitude. The times are based on the summer solstice (June 22). The small triangles throughout the chart indicate the midpoint of transmitting paths for SWF, SPA, SES, and SFD for only those stations that are underlined. The boxes around the 4 SCNA-SEA stations indicate similar equipment.

Sudden enhancements of signal strength (SES) are observed on field-strength recordings of extremely stable VLF transmissions.

SPA recorded by LF pulse observations over a one-hop propagation path yield information more indicative of the ionospheric changes occurring at the mid-point of the path, rather than over the entire path. LF phase observations, reported in degrees, represent an increase in sensitivity over VLF observations. The phase sensitivity is directly proportional to the ratio of the frequencies for identical paths. However, since the height of energy deposition is related to the type of flare x-rays emitted, the LF measurements in conjunction with the VLF measurements will tend to indicate the x-ray intensity range. Since the LF signal can apparently be reflected from either of two layers within the D-region [Doherty, R. H., *Radio Science*, 2, 645-651, 1967]. phase retardations as well as phase advances may occur during an SID at LF.

The amplitude of the low frequency pulse observations made at Loran stations normally changes during an SID. This change is usually, but not always, in the direction of a signal enhancement (SES). The height of signal absorption is below the height of signal reflection. LF amplitude observations along with the LF and VLF phase observations for any one event tend to indicate the x-ray intensities associated with that event. Amplitude changes are reported in dB to the nearest dB of voltage change. Since 6 dB represents doubling of the received signal and 20 dB represents a ten fold change in amplitude, it is obvious that many SIDs produce large effects in LF propagation.

SFA -- On LF amplitude recordings on paths about 1000 km long, sudden phase anomalies of the type known as SFA can be detected. These are events recognized by indirect phase measurements made evident by the one-hop sky wave interfering with the ground wave.

SFD -- A sudden frequency deviation (SFD) is an event where the received frequency of an HF radio wave reflected from the ionosphere increases suddenly, peaks, and then decays back to the transmitted frequency. Sometimes several peaks occur and usually the frequency deviation takes on negative values during the decaying portion of an SFD. The peak frequency deviation for most SFDs is less than 0.5 Hz. The start-to-maximum time is typically about 1 minute. SFDs are caused by sudden enhancements of ionization at E and F1 region heights produced by impulsive flare radiation at wavelengths from 10 - 1030Å. A more complete discussion of SFDs can be found in Report UAG-36, *An Atlas of Extreme Ultraviolet Flashes of Solar Flares Observed via Sudden Frequency Deviations During the ATM-SKYLAB Missions*, 1974.

S O L A R R A D I O W A V E S S P E C T R A L O B S E R V A T I O N S (C.4)

Solar spectral events from Fort Davis (Texas), Culgoora (Australia), Boulder (Colorado), Sagamore Hill (Massachusetts), Manila Observatory (Philippines), Weissenau (GFR), Dürnten (Switzerland) and Dwingeloo (Netherlands) are presented in a combined table. The contents of the table are described below:

Universal (Greenwich) date

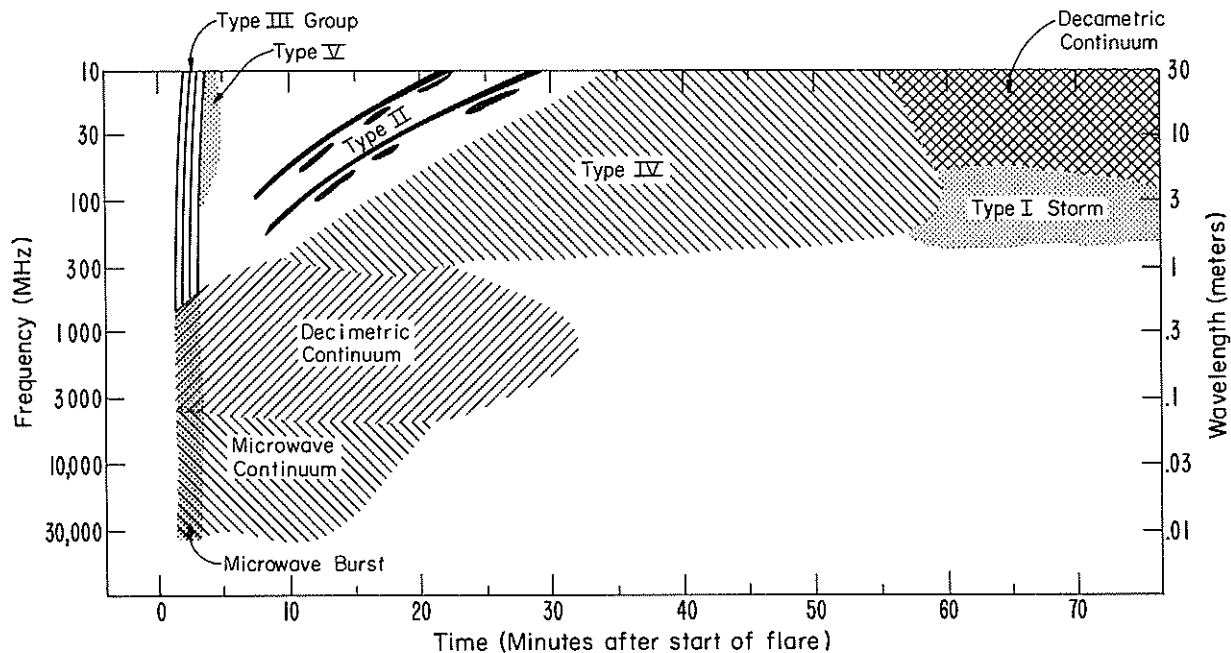
Observing periods during day (UT) -- aligned with first burst from observatory

Station -- HARV = Fort Davis, CULG = Culgoora, BOUL = Boulder, MANI = Manila, SGMR = Sagamore Hill, WEIS = Weissenau, DURN = Dürnten and DWIN = Dwingeloo.

Burst indicated in wavelength band by beginning and ending times in UT together with an indication of intensity on a 1 to 3 scale, 3 the most important. Symbol "E" is used for an event in progress before the time given and "D" for one that ends after the given time.

Spectral type -- I = storm bursts
 II = slow drift bursts
 III = fast drift bursts
 IV = prolonged continuum
 V = brief continuum (normally following type III bursts)
CONT = continuum in close association with type III burst storms, often with reverse drift bursts and often, but not always, associated with noise storms on metric wavelengths (used by BOUL and SGMR)
DCIM = decimetric burst defined by very fast drift spike or group of spikes with very high degree of polarization extending usually less than one octave in or close to decimeter range
UNCLF = unclassified activity

See J. P. Wild, S. F. Smerd and A. A. Weiss, *Annual Review of Astronomy and Astrophysics*, 1, 291, 1963 for description of types I through V.



The schematic diagram above illustrates a typical dynamic spectrum which might be produced by a large flare (Importance 2B and larger). Various flares produce many variations to this "typical spectrum". Microwave continuum will no longer be listed here except as special comments in the Remarks column.

Symbols appended to spectral type:

- | | |
|--|--|
| B = Single burst | DC = Drifting chains |
| G = Small group (<10) of bursts | H = Herringbone |
| GG = Large group (>10) of bursts | W = Weak activity |
| C = Underlying continuum (particularly with type I) | P = Pulsations |
| S = Storm in the sense of intermittent but apparently connected activity | MOV = Moving (Type IV) |
| N = Intermittent activity in this period | STA = Stationary (Type IV) |
| U = U-shaped burst of Type III | Z = Zebra patterns (parallel drifting bands) |
| RS = Reverse slope burst | F = Fiber bursts (intermediate drift bursts) |
| DP = Drifting pairs | |

The bursts are divided into dekameter, meter, and decimeter wavelength ranges. For the reporting stations listed below, these ranges cover approximately the frequency bands 10-30, 30-300, and 300-3000 MHz. There has been little uniformity among observatories in interpreting the intensity levels. The reason for this stems from the fact that equipment and antenna systems at different stations are different, having different gains, different dynamic ranges and saturate at different levels.

The Instruction Manual for reporting solar radio emission prepared by World Data Center-C2, Toyokawa Observatory, 1975, recommends that spectral observations be given a uniform intensity classification by all observatories. These are:

Intensity Classes	Flux Density in $10^{-22} \text{Wm}^{-2} \text{Hz}^{-1}$
1	<50
2	50-500
3	>500

Because of equipment and antenna differences this recommendation has not been followed at most observatories as is seen in the following observatory discussions:

Weissenau Radio Astronomy Observatory, Astronomical Institute of Tübingen University -- This research work is supported by the University of Tübingen, Baden-Württemberg, GFR. Instrumental descriptions are given by Urbarz, *Solar Phys.*, 7, 147-152, 1969; Urbarz, *Information Bulletin of Solar Radio Observations*, No. 25, 8-10, 1969; Kraemer, *Kleinheubacher Berichte*, 13, FTZ Darmstadt, 165-168; Urbarz, *Z. Astrophys.*, 67, 321-338, 1967.

A 35 mm film is used with a 0.2 mm/s feed, the sweep rate is 4 per sec. The number of resolution elements of recorded events is about 100 per octave on film.

Since May 27, 1970, the attenuation on channels 3, 4, and 5 is considerably lower than before, due to feeder replacement. The minimum detectable flux has decreased on channels 1, 3, 4, 5, and 6 from about 100 to 50 flux units ($10^{-22}\text{Wm}^{-2}\text{Hz}^{-1}$) and on channel 2 from 600 to 200 flux units. The saturation flux is also greater on channel 2 than on the other channels.

In 1971 the ratios of the numbers of type III bursts reported at Weissenau to those reported at Ft. Davis and Culgoora, respectively, was 1:2.5 and 1:3.5. It was concluded that the same ratios hold for the average minimum detectable flux on the film recordings.

Harvard Radio Astronomy Station, Fort Davis, Texas -- Summaries are presented of solar radio bursts recorded in the frequency range 25-320 MHz. (During periods of considerable solar activity the range is increased to 25-2000 MHz.) The equipment used at the Station has been described by Thompson [*Astrophys. J.*, 133, 643, 1961] and by Maxwell [*Solar Physics*, 16, 224, 1971]. At 100 MHz the intensity ranges listed as 1, 2, and 3 correspond approximately to 5-50, 50-500, and $>500 \times 10^{-22}\text{Wm}^{-2}\text{Hz}^{-1}$.

Culgoora Solar Observatory, Australia -- The observations at C.S.I.R.O. Solar Observatory, Culgoora, N.S.W., Australia are made by the C.S.I.R.O. Division of Radiophysics, Epping, N.S.W. Summaries are presented of solar radio bursts in the frequency range 8-8000 MHz. For a description of the equipment see K. V. Sheridan, *Proc. Astron. Soc. Australia*, 1, 58, 1967. The intensity scale is qualitative.

Astro-geophysics Department, University of Colorado -- Data are presented on solar radio emission recorded at Nederland near Boulder, Colorado in the spectral range 7.6 to 80 MHz. This range is broken into three subranges; each is swept in 0.5 seconds. The collecting area of the antennas is approximately 1000 square meters, in two corner reflectors forming an interferometer pair. Observations are taken routinely throughout the Boulder observing day from about 1400 UT to 2400 UT. On the low-frequency side, strong bursts are frequently limited by external reflection of the wave above the ionosphere; weaker bursts are obscured by ionospherically reflected telecommunications stations at frequencies lower than about 20 or 25 MHz, and by television stations near 54 MHz and near 68 MHz. The equipment is described by R. H. Lee and J. W. Warwick, *Radio Science*, 68D, 807, 1964.

Examples taken with this equipment are published in J. W. Warwick, *Solar System Radio Astronomy*, (J. Aarons, ed.), Plenum Press 1967. Intensities are on a rough scale from 1 to 3+, crudely convertible to flux densities as follows:

1- to 1+;	$5 \times 10^{-22} < S < 2 \times 10^{-21}$
2- to 2+;	$2 \times 10^{-21} < S < 8 \times 10^{-21}$
3- to 3+;	$8 \times 10^{-21} < S \leq 3 \times 10^{-20}$

Above about $3 \times 10^{-20}\text{Wm}^{-2}\text{Hz}^{-1}$, the equipment saturates and does not indicate relative intensities satisfactorily.

Bursts lying exclusively above 40 MHz are reported as metric band events and those lying exclusively below 40 MHz are reported as dekametric band events. Most bursts are observable in both bands and are so reported.

Sagamore Hill Radio Observatory -- Spectral measurements of dekameter wavelength Type II, III, IV and V radio emission are made at Sagamore Hill on a patrol basis. A special purpose radiometer sweeps the 25-75 MHz frequency range at a rate of 1 sweep per second. Two semi-bicone stationary antennas, spaced 300 meters apart on an E-W line to form the interferometer, are used with the spectral receiver.

With this array, positive identification of any solar event is enhanced by the resultant fringe pattern on the spectrogram. (The bicone antennas are a D. Gaunt design.)

All raw data are recorded on a Varian Statos-V x, y, z Electrostatic Recorder (Model 500) for real time readout. An improved solid state sweep frequency radiometer whose basic component is a H.P. Spectrum Analyzer provides up to 10 dB greater sensitivity than the original instrument and is now in routine operation at Sagamore Hill. On 12 July 1970 the frequency interval of the dekameter spectral observations was changed from 19-41 MHz to 24-48 MHz. This observed frequency interval was changed to 25-75 MHz on 12 August 1975 to provide a better representation of the burst phenomena observed at these wavelengths. With the 25-75 MHz equipment at Sagamore Hill:

Intensity 1 = 8 to 80 flux units
Intensity 2 = 80 to 1600 flux units
Intensity 3 = >1600 flux units

where 1 flux unit = $10^{-22}\text{Wm}^{-2}\text{Hz}^{-1}$.

Manila Observatory -- The Manila Observatory observes in the spectral range 24-48 MHz and coordinates its observations with the observers at Sagamore Hill.

Dürnten Spectrograph, Switzerland -- The Dürnten spectrograph was constructed under support of the Swiss National Science Foundation. It is located at Dürnten near Zürich, Switzerland. The film registration now covers a frequency range from 100-1000 MHz in one continuous sweep. The sweep rate is normally set at 4 Hz. The threshold intensity I_{th} amounts to about 110 ± 30 flux units between 140 and 200 MHz. Between 500 and 1000 MHz the threshold intensity is related to the frequency by the expression $I_{th} = (f-500)^2/100 \pm 20\%$ (where f is in MHz). Saturation occurs roughly at $I = 3 I_{th}$. Intensities are indicated according to the following intensity levels:

- Intensity 1 = not saturated
- Intensity 2 = nearly saturated
- Intensity 3 = clearly saturated

For more detailed description of the instrument see: Tarnstrom, G. L., *Astr. Mitt. Eidg. Sternwarte Zürich, No. 317*, 1973.

Dwingeloo Radio Spectrograph, Netherlands -- The radiospectrograph at Dwingeloo is operated by the Netherlands Foundation for Radio Astronomy, which is financed by the Netherlands Organization for the Advancement of Pure Research (Z.W.O.). It is a 60-channel receiver measuring intensity and circular polarization. The intensity is displayed in two ways: one sensitive for fluctuations, which has a dynamical range of ± 1.7 dB, and one with a logarithmic measuring range of about 15 dB over quiet sun level (q.s.l.). Saturation occurs about 20 dB over q.s.l. The threshold sensitivity is 0.2 dB. The time resolution is 0.01 sec. The bandwidth of the channels is 0.9 MHz. The outputs are routinely recorded on 35 mm cinefilm. In addition, for particularly interesting events, they are recorded on digital magnetic tape. The receiver is regularly calibrated against Cassiopeia-A.

Intensities of bursts are reported as estimated from the film in ranges approximately as:

- 1: 1 - 50 flux units ($10^{-22} \text{Wm}^{-2} \text{Hz}^{-1}$)
- 2: 50 - 200 flux units.
- 3: > 200 flux units.

Since September 1975 the spectrograph has been tuned between 260-227 MHz and 177-160 MHz. Bursts observed between 160 and 177 MHz are reported as metric, those between 227 and 260 MHz as decimetric.

A number of single frequency recordings are derived from the spectrograph channels. These recordings are reported as "Distinctive Events".

For detailed descriptions of the spectrograph see: [De Groot, T. and J. Van Nieuwkoop, *Solar Phys.*, 4, 332, 1968] and [Van Nieuwkoop, J., A Multi-channel Solar Radio-Spectrograph, *Thesis, Utrecht*, 1971].

Culgoora Radioheliograph at 43.25, 80 or 160 MHz -- The radioheliograph at the CSIRO Solar Observatory, Culgoora (Australia) is a circular array of 96 paraboloid reflector antennas equally spaced around a circle of 3 km diameter. It records 2 two-dimensional pictures of the Sun each second: one in the left-handed, the other in the right-handed sense of circular polarization [J. P. Wild, editor, *Proc. IEEE (Aust.)*, 28, 277, 1967]. Originally the heliograph operated at 80 MHz; it has been converted to time-sharing operation at 43.25, 80 and 160 MHz covering fields of view of $2^\circ \times 1.6^\circ$, $2^\circ \times 1.6^\circ$ and $1^\circ \times 0.8^\circ$ with half-power beamwidths at zenith of 7.4', 3.7' and 1.9', respectively [K. V. Sheridan, N. R. Labrum and W. J. Payten, *Proc. IEEE*, 61, 1312, 1973]. For the 43.25 MHz frequency an array of 48 corner reflector antennas set on a circle of 2.77 km diameter has been built just inside the main radioheliograph array. At this frequency only one sense of linear polarization is received.

The heliograph pencil beam can track the Sun for 6 hours and 40 minutes centered on local noon. The mechanical movement of the antennas is limited to 4 hours and 48 minutes (slightly less near the summer and winter solstices) so that the Sun drifts into and out of the broad antenna beams during the first and the last hour of observation. The normal observing hours are approximately 2300 to 0500 UT. The necessity to provide time for maintenance and development has limited observations to about 2/3 of all days since the end of 1967.

The events selected for listing in the Table may be: small, isolated events during periods of little activity; daily samples during prolonged storms; or outstanding events during active periods. Source positions are given by their central distance in units of the Sun's optical radius, R_0 and their position angle; the latter is the angle of 0° to 360° measured eastward from the north point of the solar disk (i.e., from celestial north). The apparent projected positions and the polarization listed here are taken from the visual analogue display of the taped, digital heliograph data; the expected

relative accuracy is about $0.1 R_0$ in distance and 10° in PA. The polarization is described qualitatively as weak [l or r] or strong [L or R] circular polarization. The intensity is given on a scale 1 to 3, with the corresponding flux densities, S, very approximately in the range:

- 1 : $S < 2 \times 10^{-21} \text{Wm}^{-2}\text{Hz}^{-1}$
 2 : $2 \times 10^{-21} < S < 2 \times 10^{-20} \text{Wm}^{-2}\text{Hz}^{-1}$
 3 : $S > 2 \times 10^{-20} \text{Wm}^{-2}\text{Hz}^{-1}$

Storms which are mostly of intensity 1 will not normally be listed. The positions may be affected by unknown amounts of ionospheric refraction; this effect is more pronounced the lower the frequency. If refraction errors are suspected this will be noted in the "remarks" column of the Table.

C O S M I C R A Y S (F.1)

Tabulated Observations -- The table presents the daily (UT) average counting rates per hour (scaled) for eight high counting rate neutron monitors: Thule, Alert, Deep River, Calgary, Sulphur Mountain, Kiel, Climax, and Tokyo. These monitors have different values of magnetic cutoff rigidity, while their asymptotic cones of acceptance "look" approximately in the equatorial plane in essentially the same direction in space. The eight sets of data can therefore be used to estimate the rigidity dependence of fluctuations which occur in the primary cosmic radiation.

The characteristics of the eight stations are given below; the data have been corrected applying the barometric coefficients to the listed mean station pressures.

<u>Station</u>	<u>Thule</u>	<u>Alert</u>	<u>Deep River</u>	<u>Calgary</u>	<u>Sulphur Mt.</u>	<u>Kiel</u>	<u>Climax</u>	<u>Tokyo</u>
Geog. Lat., N.	76°35'	82°31'	46°06'	51°05'	51°12'	54°18'	39°22'	35°45'
Geog. Long., E.	291°35'	297°40'	282°30'	245°52'	244°24'	10°06'	253°49'	139°43'
Cutoff, GV	0.00	0.00	1.02	1.09	1.14	2.29	3.03	11.61
Altitude, m	260	66	145	1128	2283	54	3400	20
Detector type	NM 64	NM 64	NM 64	NM 64	NM 64	NM 64	IGY	NM 64
Scaling factor	100	100	300	100	100	100	100*	128
Baro. coeff., % mm Hg	1.00	.987	.987	1.0155	1.0085	.961	.943	.844
Mean press. mm Hg	730	752	747	671	582	755	504	760.5

* From January 1, 1966.

The Climax, Colorado, U.S.A., neutron monitor, station B305, data are communicated by J. A. Simpson and G. Lentz of the Enrico Fermi Institute for Nuclear Studies, University of Chicago. The instrument is a standard Chicago type neutron monitor, utilizing 12 BF₃ counter tubes. The station has a mean barometric pressure of 504.0 mm Hg. For a more detailed description of the neutron intensity monitor and its associated electronics see J. A. Simpson, *Annals of the IGY, Vol. IV, Part VII, 351-373, 1957*. The publication of these data in this monthly series began September 1960. *Earlier data, beginning January 1953, are available in hourly form at the World Data Center A for Solar-Terrestrial Physics.*

The Deep River, Ontario, Canada, neutron monitor, Station B211, follows the IQSY design [*IQSY Instruction Manual No. 7*]. Publication of the daily rates in this series began in January 1966 but a chart of hourly values from Deep River, described below has been published herein since January 1959. Until December 31, 1972 the station was operated and maintained by Atomic Energy of Canada Ltd., but on January 1, 1973 the National Research Council of Canada took over the responsibility for maintenance of the station. The data are now provided by Margaret D. Wilson of the National Research Council of Canada. *The original data can be obtained from National Research Council of Canada, Ontario, Canada, KIA OR6, or from any of the World Data Centers.*

The 18-NM-64 neutron monitor located at Alert, North West Territories, Canada, is unique because its asymptotic cone of acceptance in space is less than 10° wide and is aligned within 7° of the spin axis of the earth. Hence, unlike the stations whose cones of acceptance rotate with the earth approximately in the plane of the ecliptic, Alert always "looks" into a fixed cone directed northwards. It experiences negligible periodic diurnal intensity variation.

The monitor at Alert was provided by Atomic Energy of Canada, Ltd., and housed in a building provided by National Research Council of Canada. It is the responsibility of the National Research Council, and day-to-day operation is by courtesy of the Canadian Meteorological Service.

The two high counting rate neutron monitors at Sulphur Mountain and Calgary have values for magnetic cutoff rigidity comparable to the Deep River monitor. Their asymptotic cones of acceptance "look" approximately in the equatorial plane in essentially the same direction in space.

The data, beginning January 1971, from Sulphur Mountain and Calgary Super neutron monitors are communicated by D. Venkatesan and T. Mathews of the Department of Physics, University of Calgary, Calgary 44, Alberta, Canada. The stations have mean barometric pressures of 766 mb, and 883 mb., respectively. The barometric coefficients used to correct the data are 0.7665%/mb and 0.7718%/mb, respectively. *Hourly mean data from both installations are routinely distributed to the scientific community and the World Data Center A for Solar-Terrestrial Physics, Boulder, Colorado.* The data began March 1963 for Sulphur Mountain and January 1964 for Calgary, and are available at the World Data Center. The stations were set up by B. G. Wilson (now at Simon Fraser University, Burnaby, British Columbia).

The Thule nucleonic intensity detector, of standard IQSY design, is located at the Geopole Station Greenland: latitude $76^\circ 36' N$, longitude $68^\circ 48' W$, altitude 260m, geomagnetic threshold rigidity essentially zero. The data are communicated by Martin A. Pomerantz, Bartol Research Foundation, Swarthmore, Pa. 19081. Any changes in either the atmospheric attenuation length or in the sensitivity arising from long term drifts are applied retrospectively before the final hourly mean data are routinely distributed to the World Data Centers and to the scientific community.

Two other monitors, at Kiel and Tokyo, have asymptotic cones of acceptance much different from those given above. Therefore, they can be used to distinguish between UT-dependent and LT-dependent time variations. Higher cutoff rigidities also aid further estimation of rigidity dependence. The publication of these data began with the December 1973 data.

The data from both 18-NM-64 neutron monitors are routinely submitted to World Data Center A, B, C1 and C2 for Cosmic Rays as well as to listed researchers. Kiel data has been available since September 1964 and Tokyo (or Tokyo-Itabashi) data since January 1970. The data are communicated to *Solar-Geophysical Data* by M. Wada after receiving the Kiel data from O. Binder.

Charts -- Variations of cosmic ray intensity are depicted in chart form for the above stations. The vertical scale lines marks the days of the month in Universal Time. The horizontal scale lines are in intervals of 5% deviation from an arbitrarily chosen 100% reference level for each station. The 100% reference levels are based upon (after barometric correction) 1.846×10^6 counts per hours for Deep River; 0.6678×10^6 for Alert; 0.8827×10^6 for Sulphur Mountain; and 1.1767×10^6 for Calgary. For Thule, Kiel, Climax, and Tokyo, the plots represent percentage deviation from the monthly mean intensity which is taken to be the 100% level.

G E O M A G N E T I C A C T I V I T Y (D.1)

Kp, Kn, Ks, Km, Cp, Ap, aa, and Selected Quiet and Disturbed Days -- The data in the table are: five quietest days (QQ), ten quietest days (QQ or Q), and five most disturbed days of the month (D); three-hourly indices Kp, Kn, Ks, Km; character figure, Cp; daily "equivalent amplitude", Ap; and aa indices with quiet day figures K and C.

The data are made available by the International Service of Geomagnetic Indices under the auspices of the International Association of Geomagnetism and Aeronomy through Division V: Observatories, Instruments, Indices and Data. The Meteorological Institute, De Bilt, The Netherlands, collects the data from magnetic observatories distributed throughout the world, and compiles the selected days data. The Institut für Geophysik, Göttingen University, computes the planetary and equivalent amplitude indices. The aa-indices and Kn, Ks, Km are provided by the Institut de Physique du Globe, Paris, France.

K_p is the mean standardized K-index from 13 observatories between geomagnetic latitudes 47 and 63 degrees. The scale is 0 (very quiet) to 9 (extremely disturbed), expressed in third of a unit, e.g., 5- is 4 and 2/3, 5o is 5 and 0/3, and 5+ is 5 and 1/3. This planetary index is designed to measure solar particle-radiation by its magnetic effects, specifically to meet the needs of research workers in the other geophysical fields.

A full description of the indices K_n , K_s , K_m is given in a monograph, *Indices K_n , K_s et K_m , 1964-1967*, edited in 1968 by the Centre National de la Recherche Scientifique, 15 quai Anatole, France, 75007 PARIS, which contains these indices for 1964-1967. Yearly compilations of these data are published in the series of *IAGA Bulletins No. 32*. Indices for 1959-1963 will be published in a special number of the IAGA Bulletin. All of them are available at the World Data Centers.

Briefly, the three-hourly indices K_n and K_s for the Northern and Southern hemispheres respectively are derived from the K indices of observatories approximately well distributed in latitude and in longitude. The indices are standardized according to the distances of the stations to the auroral zones. The stations are arranged in groups, each group representing a longitude sector in one of the hemispheres (5 in the Northern hemisphere, 3 in the Southern). The observatories currently in use are:

Magadan	Witteveen	Tucson	Hermanus
Petropavlovsk	Hartland	Amberley	Port Alfred
Memambetsu	Ottawa	Toolangi	Argentine Island
Sverdlovsk	Fredericksburg	Gnangara	South Georgia
Tunguska	Victoria	Kerguelen	Trelew
Niemegk	Newport		

The mean standardized K of each sector is converted into an equivalent amplitude and the weighted (in longitude) averages an and as of these amplitudes are converted back into K_n and K_s . K_m is derived in the same way from am, the average of an and as. Indices an, as, and am are expressed in gammas (one gamma equals one nano-tesla) and correspond to the magnetic activity level (as it can be inferred from K indices) at an invariant magnetic latitude of 50°. Indices K_n , K_s , and K_m are expressed in the same units as K_p . Values published in these reports are only provisional because in some months all observatories used in each longitude sector have not sent K indices at the right time and because K indices of Antarctic stations have to be rescaled at the end of each wintering.

The C_p -figure is a standardized version of the C_i -figure formerly published and is derived from the indices K_p by converting the daily sum of ap into the range 0.0 to 2.5.

A_p is a daily index of magnetic activity on a linear scale rather than on the quasi-logarithmic scale of the K-indices. It is the average of the eight values of an intermediate 3-hourly index ap, defined as approximately one-half the average gamma range of the most disturbed of the three force components, in the three-hour interval at standard stations; in practice, ap is computed from the K_p for the 3-hour interval. The extreme range of the scale of A_p is 0 to 400. Values of A_p (like K_p and C_p) have been published for 1932 to 1961 in *IAGA Bulletin No. 18* by J. Bartels. Yearly compilations of these data, as well as the selected days, are published in the series of *IAGA-Bulletin No. 32 (the continuation of IAGA Bulletin No. 12)*. These Bulletins are available from the IUGG Publications Office 39, Rue Gay Lussac, Paris (V). These indices are also available at the World Data Centers.

The aa indices are the continuation of the series beginning in the year 1868. A full description of these indices is given in the *IAGA Bulletin 33*, which contains them for the years 1868-1967. Descriptions are also given (especially comparisons with am, ap, or C_i indices) in two short papers [*Ann. Geoph. 27*, 62-70, 1971, and *J. Geophys. Res.*, 77, 6870-6874, 1972]. aa values for 1968-1974 will soon be published in *IAGA Bulletin 32* series. A graph of these values through 1975 is published in the February issue of *Solar-Geophysical Data*. Briefly, such three-hourly indices, computed from K indices of two antipodal observatories (invariant magnetic latitude 50°), provide a quantitative characterization of the magnetic activity, which is homogeneous through the whole series. Half-daily and daily values give an estimation of the activity level very close to that obtained with am indices. Values are in gammas and correspond to the activity level at an invariant magnetic latitude of 50°. The aa indices are computed for:

- N = daily values for the Northern hemisphere,
- S = daily values for the Southern hemisphere,
- M = half-daily values of aa indices for the Greenwich day.

Letters C and K refer to a classification of the quiet days of the month (C = really quiet, K = quiet but with slightly disturbed three-hourly intervals). The letters on the left refer to the 24 hour Greenwich day, on the right to a period of 48 hours centered on the Greenwich noon.

The magnetically quiet and disturbed days (D & Q) are selected in accordance with the general outline in *Terr. Mag.* (Predecessor to *J. Geophys. Res.*) 48, 219-227, 1943. The method in current use calls for ranking the days of a month by their geomagnetic activity as determined from the following three criteria with equal weight: (1) the sum of the eight Kp's; (2) the sum of the squares of the eight Kp's; and (3) the greatest Kp.

Chart of Kp by Solar Rotations -- Monthly a graph of Kp is given for several solar rotations, furnished through the courtesy of the Geophysikalisches Institut of the University of Göttingen. Annually a graph of the whole year by solar rotations is included. From time to time another 27-day rotation chart depicting the daily geomagnetic character figure, C9, is presented. C9 is obtained from Cp by reducing the Cp-values to integers between 0 and 9 according to the key given in the charts.

Chart of Dst by Solar Rotations -- A plot of Dst values which has been given regularly following the table of Dst, described below, will also be presented on a Bartels Rotation basis corresponding to the Kp presentation. The purpose in making this presentation is to enable conformity with recommendations concerning scale lengths made for the years of International Magnetospheric Study (IMS). Since the vertical scale varies with each month the 100γ interval is illustrated at the end of each month.

The activity indices are described by J. Bartels in *Annals of the IGY, Vol IV*, 227-236, London, Pergamon Press, 1957. A table of Ap indices for the last 12 months is presented so that trends in magnetic activity can be easily followed.

Provisional Hourly Values of the Equatorial Dst Index -- The equatorial Dst index at given UT represents magnetic field variations at the dipole equator on the earth's surface, averaged over local time, that are caused mainly by the magnetospheric equatorial currents including the cross-tail current. The reference level of Dst is such that Dst is statistically zero on the days internationally designated as quiet days.

Provisional hourly Dst data are based on hourly values of the horizontal component from four magnetic observatories: San Juan, Honolulu, Kakioka, and Hermanus. These provisional hourly values are replaced by a more definitive annual set of the Dst index at the end of each year. The provisional hourly values are calculated and forwarded for publication by M. Sugiura, NASA-Goddard Space Flight Center, Greenbelt, Maryland 20771 and D. J. Poros, Computer Sciences Corporation, Silver Spring, Maryland 20910.

Principal Magnetic Storms -- Finally a table presents the principal magnetic storms for the month as reported by several observatories through cooperation with the International Association of Geomagnetism and Aeronomy. These are the data formerly published in the *Journal of Geophysical Research*. They are now, however, grouped by the storm rather than by station. The geomagnetic latitude of the station is indicated. The beginning time is given to the hour and minute in UT. The ending time is given only to the nearest hour. This is the time of cessation of reasonably marked disturbance movements in the trace. More specifically, it is the time when the K-index measure has diminished to 2 or less for a reasonable period.

The type of sudden commencement, if any, together with its magnitude in each element D, H, or Z is next in the table: sc = sudden commencement; sc* = small initial impulse followed by main impulse (in this case the amplitude is that of the main pulse only, neglecting the initial brief pulse); dots in these columns represent a storm with gradual commencement; dashes indicate no data entries. Signs of amplitudes of D and Z are taken algebraically; D reckoned positive if toward the east and Z reckoned positive if vertically downward. In the next columns the day and the three-hour periods on that day when the K index reached its maximum are given. Finally, in the last three columns the maximum ranges in D, H and Z during the storm are given. For each date the data are listed in north-to-south geomagnetic latitude order. The table below gives the abbreviation used for the observatory names.

GEOMAGNETIC OBSERVATORIES

<u>Code</u>	<u>Station</u>	<u>Geomag. Latitude</u>	<u>Code</u>	<u>Station</u>	<u>Geomag. Latitude</u>
AA	Addis Ababa	5.3N	HU	Huancayo	0.6S
AL	Alibag	9.5N	HD	Hyderabad	7.6N
AM	Amberley	47.7S	IR	Irkutsk	41.0N
AN	Annamalainagar	1.5N	KG	Kerguelen	56.5S
AP	Apia	16.0S	MB	M'Bour	21.3N
BD	Boulder	48.9N	NE	Newport	55.1N
CO	College	64.6N	PM	Port Moresby	18.7S
EB	Ebro	43.9N	SJ	San Juan	29.9N
FR	Fredericksburg	49.6N	SI	Sitka	60.0N
GN	Gnangara	43.2S	TO	Toolangi	46.7S
GU	Guam	4.0N	TV	Trivandrum	1.1S
HR	Hermanus	33.7S	TU	Tucson	40.4N
HO	Honolulu	21.1N	WI	Witteveen	54.2N

Sudden Commencements and Solar Flare Effects -- These reports are provided by A. Romãna for the International Service of Geomagnetic Indices, International Association of Geomagnetism and Aeronomy, Division V: Observatories, Instruments, Indices and Data. The sudden commencements (s.s.c.) and solar flare effects (s.f.e.) are from magnetograms of the world-wide network of magnetic observatories. The stations, together with their abbreviations, are given in *IAGA Bulletin No. 20* of the International Union of Geodesy and Geophysics as well as the series *IAGA Bulletin No. 32* which contain the yearly compilations of these data. These reports have been published quarterly in *Solar-Geophysical Data* beginning with data for January 1966. Previous to that time they were published periodically in the *Journal of Geophysical Research*.

Beginning with December 1970 these data are published monthly and, thus, are based on fewer reports and differ slightly in detail from the similar data published previously. The decision to publish this less complete report was made in order to make the data available more rapidly. The table gives date and UT time of event with stations by two letter abbreviations grouped by quality A, B, or C.

RADIO PROPAGATION QUALITY INDICES (B.51)

One can take as the definition of a radio propagation quality index: the measure of the efficiency of a medium-powered radio circuit operated under ideal conditions in all respects, except for the variable effect of the ionosphere on the propagation of the transmitted signal. The indices given here are derived from monitoring and circuit performance reports, and are the nearest practical approximation to the ideal index of propagation quality.

Quality indices are expressed on a scale that ranges from one to nine. Indices of four or less are generally taken to represent a significant disturbance. (Note that for geomagnetic K-indices, disturbance is represented by high numbers.) The adjectival equivalents of the integral quality indices, known as the CRPL quality figure scale, are as follows:

1 = useless	4 = poor-to-fair	7 = good
2 = very poor	5 = fair	8 = very good
3 = poor	6 = fair-to-good	9 = excellent

The forecasts are expressed on the same scale.

The quality figures represent a consensus of experience with radio propagation conditions. Since they are based entirely on monitoring or traffic reports, the reasons for low quality are not necessarily known and may not be limited to ionospheric storminess. For instance, low quality may result from improper frequency usage for the path and time of day. Although, wherever it is reported, frequency usage is included in the rating of reports, it must often be an assumption that the reports refer to optimum working frequencies. It is more difficult to eliminate from the indices conditions of low quality for reasons such as multipath or interference. These considerations should be taken into account in interpreting research correlations between the Q-figures and solar, auroral, geomagnetic or similar indices.

North Atlantic Radio Path -- The quality figures are compiled by the Telecommunication Services Center, Office of Telecommunications, at Boulder, Colorado from radio traffic data for North Atlantic transmission paths closely approximating New York-to-London. These are reported by the Canadian Broadcasting Corporation, International Telephone and Telegraph, Radio Corporation of America, U. S. Coast Guard, and Federal Communications Commission.

The original reports are submitted on various time intervals. The observations for each 6-hour interval are averaged on the original scale. These 6-hour indices are then adjusted to the 1 to 9 quality-figure scale by a conversion table prepared by comparing the distribution of these indices for at least four months, usually a year, with a master distribution determined from analysis of the reports originally made on the 1 to 9 quality-figure scale. A report whose distribution is the same as the master is thereby converted linearly to the Q-figure scale. The 6-hourly quality figure is the mean of the reports available for that period.

The 6-hourly quality figures are given in this table to the nearest one-third of a unit, e.g. 5.0 is 5 and 0/3; 5.5 is 4 and 2/3; 5.8 is 5 and 1/3. Other data included are:

- (a) Whole-day radio quality indices, which are averages of the four 6-hourly indices.
- (b) Short-term forecast, issued every six hours by the Telecommunication Services Center. These are issued one hour before 02^h, 08^h, 14^h, and 20^h UT and are applicable to the period 1 to 7 hours ahead.

- (c) Weekly Radio Telecommunication Forecasts (WF) are issued once a week and are applicable to 1 to 7 days ahead for HF radio propagation conditions on typical high latitude paths passing through or near the auroral zone. They are scored against the average of the whole day North Atlantic quality figures. They are modified as necessary by a supplemental forecast.
- (d) Half-day averages of the geomagnetic K indices measured by the Fredericksburg Magnetic Observatory of the U.S. Geological Survey, K_{Fr} .
- (e) Daily A indices calculated from the 3-hourly K indices measured at Fredericksburg.

North Pacific Radio Area -- A local tape-recorded service, telephone (area code 907) 753-9228 is operated at the Anchorage NOAA station giving a statement of current magnetic conditions, a forecast of geomagnetic conditions for the coming day, current ionospheric conditions, HF radio propagation conditions for the past 24 hours and predicted conditions for the next 24 hours.

Transmission Frequency Ranges -- The North Atlantic path (Lüchow (53.0°N, 11.2°E) - Halifax) is represented by five frequencies, 6.425, 8.542, 12.813, 17.084 and 22.378 MHz, recorded continuously. They are shown in a series of diagrams one for each day. The heavy solid lines represent field strength ≥ -12 dB above 1 μ V/m (transmitter power reduced to 1 kW). Observed field strengths between -12 dB and -40 dB above 1 μ V/m are shown by the fine line. These diagrams are based on data reported by the German Post Office through the Fernmeldetechnisches Zentralamt, Darmstadt, Federal Republic of Germany.

Radio Propagation Quality Indices are calculated from the records on five circuits received at Lüchow, Federal Republic of Germany, with highly directive rhombic antennas (except the short-haul path Bracknell-Lüchow, which is received with a non-directional vertical antenna). The quality figures are calculated for a twenty-four hour period (0600 - 0600 UT) using transmissions from Tokyo, Japan; Halifax, Canada; Moscow, USSR; Canberra, Australia; and Bracknell, England. The following frequencies are currently in use:

Tokyo	Halifax	Moscow	Canberra	Bracknell
22.770 MHz	22.378 MHz	15.9 MHz	19.690 MHz	18.261 MHz
18.220	17.084	11.0	13.920	14.436
13.597	12.813	7.7	11.030	9.203
9.970	8.542	5.4	5.100	4.782
3.622	6.425	3.9		

The index 0.0 corresponds to a median field strength of -30 dB above 1 μ V/m (converted to 1 kW and referred to an omnidirectional antenna). The figures are in steps of 5 dB (index 10.0 = +20 dB above 1 μ V/m). The field strength of the frequency with the highest value for each hour is used in place of a mean of all recorded frequencies. This is done on the assumption that the optimum frequency would be used for communication.

DATA FOR SIX MONTHS BEFORE MONTH OF PUBLICATION

TABLE OF CONTENTS

	<u>Page</u>
<u>Solar Flares</u>	
C.1ba Standardized Data and Individual Reports	43
C.1e Flare Index	45
C.1d No-Flare-Patrol Graph	46
<u>Solar Radio Waves</u>	
C.3 Outstanding Occurrences at Fixed Frequencies	46
<u>Energetic Solar Particles and Plasma (A.12e and A.13e)</u>	52
<u>Magnetograms of Geomagnetic Storms (D.1e)</u>	56

H α SOLAR FLARES
(C.1ba, C.1e, C.1d)

From January 1968 the flare reports published six months after observation were divided into two tables labeled "confirmed" and "unconfirmed". This separation was felt desirable in 1968 to present the most homogeneous and reliable flare data for use by the scientific community. However, it has become apparent that for small events, which currently constitute the majority of reports, such discrimination is questionable. Therefore, beginning with the January 1975 data, all reported H α flares are published in one chronological list.

The listing is prepared in cooperation with DASOP (Department d'Astronomie Solaire et Planetaire), Observatoire de Paris, 92190 Meudon, France. For each event there is a "group report" line more closely resembling the presentation of the flares as they will be published in the *IAU Quarterly Bulletin on Solar Activity (QBSA)*. In *Solar-Geophysical Data* the flares as reported by the individual observatories follow the "group report" line. In *QBSA* only the summary of the observatory contributions is included.

The "group report" line is intended as a summary of all individual reports. The principal criteria for grouping reports together are flare position and times. The following new rules have been adopted to determine times, areas and importances of grouped events:

- The beginning time is the time of first observation of an event by an observatory. If there is uncertainty in the beginning time, it is indicated by a "+" sign followed by the difference in minutes between the time of the first observation and the time of the latest observed beginning. More than 9 minutes difference appears as >9. The same applies for times of maximum. When two or more maxima are identified, their times are reported with the same group line.
- With near agreement among observatories an average of the areas is used in determining importance.
- With widely varying area measurements reported by several observatories the average area is not computed. The importance is estimated from the reported importances. An importance 1 or more is assigned only when reported by several observers or when only a single observatory is operating at the time of observing such a flare.
- If only one or two observers report a flare of importance 1 or more with considerable disagreement in importance, no importance is assigned and a "?" is inserted in the importance column.
- Queries are sent to observatories who have reported cinematographic observation at a time when only one or two observatories have reported an event of importance 1 or greater. Any new information thus obtained is included in the flare listing.
- When only one observatory has reported a flare the measured and corrected areas must be considered somewhat questionable. There is no way to confirm their accuracy and it has been noted that measurements vary considerably from one observatory to another.
- Bright surges at limb (BSL) are sometimes reported in the flare lists and may be retained in these reports.

The columns in the table are as follows:

- Group Number and Reporting Observatories using IAU abbreviation (see p. 45).
- The Universal date.
- Beginning time in UT.
- Time of maximum phase in UT. (more than one maxima may be listed)
- Ending time in UT.
- The heliographic coordinates in degrees for the "center of gravity" of the emission region, corresponding to the time of maximum intensity.
- The distance from the center of disk in units of disk radius.
- McMath serial number of the associated plage region.
- The time of central meridian passage of the position of the flare in tenths of the Universal date.
- Duration in minutes.
- The flare importance on the IAU scale of Sf* to 4b. (In the summary line for the group a "?" will be used when there has been too much discrepancy among individual reports to determine accurately the probable importance of the event).

* For easier visual selection of the more important flares a minus sign, "-", is used to indicate subflares instead of "S".

- Observing conditons where 1 means poor, 2 fair, and 3 good. (Observatories at Ramey, Palehua, Athenes and Tehran use a scale of 1-5).
- Nature and completeness of available observations where
 - C = a complete, or quasi-complete sequence of photographs was obtained,
 - P = one or a few photographs of the event were obtained resulting in incomplete time coverage,
 - V = all (or most of) the development of the flare was visually observed, or
 - S = flare was seen visually for a small part of its probable duration.

- Time of measurement for tabulated areas.
- Apparent (i.e., projected) area at time of maximum brightness in millionths of solar disk -- this is not necessarily the maximum area. (Prior to January 1975 this measured area in millionths was divided by 97 and was indicated as heliographic square degrees, hence the tabular heading was incorrect and should have been millionths/97.)
- Corrected area in square degrees.
- Remarks in the IAU system of notes where

- | | |
|---|--|
| <ul style="list-style-type: none"> A = Eruptive prominence whose base is less than 90° from central meridian. B = Probably the end of a more important flare. C = Invisible 10 minutes before. D = Brilliant point. E = Two or more brilliant points. F = Several eruptive centers. G = No visible spots in the neighborhood. H = Flare accompanied by a high speed dark filament. I = Active region very extended. J = Distinct variations of plage intensity before or after the flare. K = Several intensity maxima. L = Existing filaments show signs of sudden activity. M = White-light flare. | <ul style="list-style-type: none"> N = Continuous spectrum shows effects of polarization. O = Observations have been made in the calcium II lines H or K. P = Flare shows helium D₃ in emission. Q = Flare shows the Balmer continuum in emission. R = Marked asymmetry in Hα line suggests ejection of high velocity material. S = Brightness follows disappearance of filament (same position). T = Region active all day. U = Two bright branches, parallel () or converging (Y). V = Occurrence of an explosive phase: important and abrupt expansion in about a minute with or without important intensity increase. W = Great increase in area after time of maximum intensity. X = Unusually wide Hα line. Y = System of loop-type prominences. Z = Major sunspot umbra covered by flare. |
|---|--|

When importance is questionable the list of observatories reporting cinematographic patrol but not reporting flare follows the group report. The abbreviated observatory name is followed by "2" when a second look by the observer still did not identify a flaring event at that time. Observatories not observing the event and not making a second evaluation are followed by "1".

Intervals when no observatory reported times of patrol observation are listed chronologically in the table.

The dual importance scheme used which was adopted January 1, 1966 at IAU Commission 10, is summarized in the following table:

"Corrected" area in square degrees	Relative Intensity Evaluation		
	Faint (f)	Normal (n)	Brilliant (b)
≤ 2.0	Sf	Sn	Sb
2.1 - 5.1	1f	1n	1b
5.2 - 12.4	2f	2n	2b
12.5 - 24.7	3f	3n	3b
>24.7	4f	4n	4b

The area to be used in assigning the first figure of the dual importance is the area of the flaring region at the time of maximum brightness. The observatory measures apparent area in millionths of the solar disk. For flares less than 65° from the center of the solar disk, the formula relating apparent and corrected area is

$$\text{"corrected" area} = \frac{\text{apparent area}}{97} \times \sec \theta$$

where apparent area is in millionths of the disk and corrected area is in heliographic square degrees. For flares more than 65° from the center, the "sec θ law" becomes unsatisfactory. The first importance figure can be estimated from the table below where areas are given in millionths of the disk.

Angle	0°	-----	65°	70°	80°	90°
Limit S-1	200	sec θ law	90	75	50	45
Limit 1-2	500	sec θ law	280	240	180	170
Limit 2-3	1200	sec θ law	600	500	350	300

The intensity scale shown as the second importance figure is only a qualitative one where each observatory uses its experience to decide if a flare is rather faint (f), normal (n), or rather bright (b).

SOLAR FLARE OBSERVATORIES

COMPUTER CODE NO.	OBS. TYPE	I.A.U. ABBREV.	NAME, PLACE AND COUNTRY
824	C	ABST	ABASTUMANI, GEORGIAN SSR
512	VP	ARCE	ARCETRI, FLORENCE, ITALY
521	VP	AROS	AROSA, SWITZERLAND
508	VC	ATHN	NATL OBS., ATHENS, GREECE (USAF)
647	VC	BOUL	BOULDER, COLORADO, USA
560	VC	BUCA	NATL OBS., BUCHAREST, ROMANIA
570	VC	CATA	CATANIA, ITALY
826	C	CRIM	SIMEIS, CRIMEA, USSR
402	C	CULG	CULGOORA, AUSTRALIA
478	C	HALE	HALEAKALA, MAUI, HAWAII, USA
537	VP	HERS	R. GREENWICH OBS., HERSTMONCEUX, ENGLAND
563	C	HTPR	HAUTE-PROVENCE, FRANCE
718	C	HUAN	GEOPHYSICAL INST., HUANCAYO, PERU
517	V	HURB	HURBANOVO, CZECHOSLOVAKIA
358	V	ISTA	UNIV. OBS., ISTANBUL, TURKEY
827	VP	KHAR	KHARKOV, UKRANIAN SSR
828	C	KIEV	KIEV, GA0, UKRANIAN SSR
309	V	KODA	KODAIKANAL, INDIA
522	VP	LOCA	LOCARNO, SWITZERLAND
876	C	LVOV	LVOV, UKRANIAN SSR
468	VC	MANI	MANILA, PHILIPPINES
642	C	MCMA	MCMATH-HULBERT, PONTIAC, MICHIGAN, USA
505	C	MEUD	MEUDON, FRANCE
314	C	MITK	MITAKA, TOKYO, JAPAN
555	C	MONT	MONTE MARIO OBS., ROME, ITALY
504	V	ONDR	ONDREJOV, PRAGUE, CZECHOSLOVAKIA
476	VC	PALE	PALFHUA, HAWAII, USA
648	VC	RAMY	RAMEY SOLAR OBSERVATORY, RAMEY AFB, PUERTO RICO
862	VP	SIBE	SIBERIE (SIBERIAN IZMIR), IRKUTSK, USSR
823	VC	TACH	TACHKENT, UZBECK SSR
341	VP	TEHR	TEHRAN, IRAN
514	C	UPIC	UPICE, CZECHOSLOVAKIA
834	VC	VORO	VOROSHILOV, USSR
546	VP	WEND	WENDELSTEIN, GFR
523	PC	ZURI	EIDGENOSSISCHE STERNWARTE, ZURICH, SWITZERLAND

The above table gives the solar flare observatories presently cooperating in international data interchange through the World Data Centers as originally established during the International Geophysical Year. For each observatory are given the code numbers used on the punched cards at NOAA; the four letter IAU abbreviations; name, place and country; and type of patrol where C, V and P have the meanings explained above.

Note: All the flare data are recorded on punched cards. Copies of the cards, tabulations from them or magnetic tapes of the data are available at cost through the World Data Center A for Solar-Terrestrial Physics, NOAA, Boulder, Colorado U.S.A. 80302.

Flare Index -- The daily flare index is defined as

$$I_f = \frac{.76}{T^*} \sum A_d^2$$

where individual flare areas A_d are measured in millionths of solar disk and T^* is the effective observing time in minutes. I_f corresponds closely to the flare index developed at the High Altitude Observatory to measure the integrated intensity of flare radiation. The flare areas are not corrected for geometric foreshortening, so the definition of I_f places great weight on large flares, located near the center of the sun's disk. Characteristics of the index I_f are discussed in more detail in the paper by C. Sawyer "Daily Index of Solar Flare Activity" [*J. Geophys. Res.*, 72, 385, 1967].

The table lists the date, index and actual hours of observation included in the calculation and follows the table of Solar Flares. Beginning with the January 1975 data, this index is calculated using all flares. Previously it had been calculated using only those confirmed flares of greater than 1 square degree in area, as then included in the *IAU Quarterly Bulletin on Solar Activity*.

A regional flare index is described in the text for the data for seven months before month of publication on page 60.

Patrols -- Following the tables a graph of the intervals of no flare patrol observation for all the observatories included in the total patrol is given. The graph is divided into visual and cinematographic patrols. (See page 10 for more detail.)

S O L A R R A D I O W A V E S (C.3)

Outstanding Occurrences -- Solar radio emission bursts at fixed frequencies are reported by the worldwide network of observing stations. By the sixth month following observation, it is expected that all reports have been received and the data are published in table form in *Solar-Geophysical Data*. From time to time selected solar bursts are illustrated.

The code name used in this publication to identify the station, its alternate station names if appropriate, the geographic coordinates, and frequencies in MHz on which the station reports are presented in the table on page 52.

In the data presentation, bursts reported from different observing stations are joined by brackets when they occur near the same time. Each set of brackets may not always include all of the solar event. The frequency in MHz precedes the abbreviated station name. Following the name is given the type of event. The Type consists of two columns. The first column is the morphological *SGD* numerical code which has been used in *Solar-Geophysical Data*, and the second column is the letter symbol for easier recognition of type. The use of the letter symbol began with the January 1975 data. In the case of OTTA and PENT observations, letters are sometimes appended to the *SGD* numerical code. See page 47 for explanations. For each event start and maximum phase in UT, duration in minutes, and peak and mean flux densities in $10^{-22} \text{Wm}^{-2} \text{Hz}^{-1}$ are listed. Information on polarization, positions and other remarks are included in the final column.

Both the tables and illustrations prepared by H. Tanaka, as a part of the *Instruction Manual for Monthly Report*, and a table of definitions with a page of illustrations prepared by A. Covington are included here. It is felt that though the meanings are essentially the same, the two viewpoints may aid experimenters in interpreting how the symbols are assigned to bursts by the various observatories. Two possibly confusing items seem to remain. Covington feels those GRF bursts with obvious flat tops are a new type of burst best listed under 27(RF) rather than with the GRF symbol since it is also defined as more or less regular rise and fall of continuum with long duration. The illustration of the 10 cm wavelength "Group" with the letter code "SER" may also prove confusing as Covington feels it should rightfully be listed with the *SGD* number code 41 rather than 42(SER).

The modifications appended to the *SGD* numerical code for Ottawa and Penticton observations are given here as explained by A.E. Covington, National Research Council, Canada. These are illustrated by the figure on page 51. Records observed simultaneously at these widely separated stations have led to the recognition of other unique variations representing new types of events at cm wavelengths. These are the relatively small intensity, rise only event (which appears as a discontinuity in the daily level), the absorption only event, the GRF events of great duration, isolated events of very short duration or spikes, and the single cycle of a sinusoid. These basic profiles and all the others are shown in idealized form in the figure described above, identified by *SGD* numerical code and appended letters. Clarification of some of the profiles follow. To identify rise only encode as 240, and to identify the postrise enhanced level following the rise encode as either 24P or 25P. Through the types, the letter A can be added to indicate the basic or longest enduring part of a compound event or apparent compound event. The use of "A" enables a marginal line to be placed against the entry for the start and extended to include the superimposed events. The presence of unlisted fluctuations or variations which slightly modify the basic elementary form are denoted by the letter F added to the *SGD* numerical code for the event so modified. The table on page 50 defines these additions.

At Sagamore Hill an automated data correction and handling system was integrated into the patrol operation in June 1974. After being subjected to an extended period of evaluation, it is currently functioning as a regular part of the patrol operation. This automated data system provides real time burst integrated flux densities, a quantity which has been found to be of great value in predicting the occurrence and magnitude of PCA phenomena.

Event Types According to the *Instruction Manual for Monthly Report*
(prepared by H. Tanaka for ICSU-STP-IAU)

The key for identifying types of event by numerical SGD code and letter symbol.

SGD Code	New Letter Symbol	Morphological Classification	URANO Code	Remarks
1	S	Simple 1	1	
2	S/F	Simple 1F	1	S + F
3	S	Simple 2	1	
4	S/F	Simple 2F	1	S + F
5	S	Simple	1	
6	S	Minor	0	Defined as simple rise and fall of minor burst with duration 1 or 2 min.
7	C	Minor+	0	Defined as minor burst with second part.
8	S	Spike	1	Self-evident by duration.
20	GRF	Simple 3	1	
21	GRF	Simple 3A	1	A means underlying. Clearly superposed burst is to be listed separately, but separation is sometimes difficult and arbitrary. In such cases list as C.
22	GRF	Simple 3F		Fluctuations of short periods be listed separately.
23	GRF	Simple 3AF	1	
24	R	Rise	8	
25	R	Rise A	8	
26	FAL	Fall		
27	RF			
28	PRE	Precursor		
29	PBI	Post Burst Increase	2	
30	PBI	Post Burst Increase A	2	
31	ABS	Post Burst Decrease		
32	ABS	Absorption		
40	F	Fluctuations	4	
41	F	Group of Bursts	4	A group of minor bursts close to each other.
42	SER	Series of Bursts	4	A series of bursts occur intermittently from base level with considerable time intervals between bursts.
43	NS	Onset of Noise Storm	7	To be listed with starting time, and duration with symbol D.
44	NS	Noise Storm in Progress	7	Starting time with symbol E, and duration with symbol D.
45	C	Complex	3	
46	C	Complex F	3	
47	GB	Great Burst	3	
48	C	Major	5	Defined as complex variation of intensity with large amplitude
49	GB	Major+	6	Major increase of flux with duration greater than 10 min.

Explanation of letter symbols.

Basically, microwave bursts can be classified into the following types:

S	= Simple	:	Mostly nonthermal 'microwave impulsive burst' or 'decimetric burst' (see p. 32).
C	= Complex	:	Combination of a few or many simple bursts.
F	= Fluctuation	:	Minor C sometimes superposed on the main burst.
GB	= Great Burst	:	Major C of special importance.
PRE	= Precursor	:	Preburst activity connected to the main burst.
PBI	= Post Burst Increase	:	Tail of the main burst which may be regarded as enhancement of S-component.
GRF	= Gradual Rise and Fall	:	Temporal enhancement of S-component or similar activation in the flaring region. It may sometimes start with relatively sharp rise like a simple burst. If this sharp rise can be clearly recognized as simple burst, GRF becomes PBI. Note that both have similar characteristics.
ABS	= Absorption	:	Absorption due to surge-like material mainly appears after the burst and is sometimes called postburst decrease. This phenomenon may occur frequently, but it can only be recognized when the flux comes down to preburst level. Temporal fall of flux which is sometimes called negative burst may be listed as ABS, but it may simply be the temporal fall of emission.

The following three symbols are simply morphological, which may be necessary due to limited observation time, or for the simplicity of tabulation:

R	= Rise	:	This may also occur as the onset of long-enduring enhancement of S-component associated with other solar events.
FAL	= Fall		
SER	= Series of Bursts		

On dm-m-Dm wavelength range, most of the events may be C with F, GB, and PRE as more specific descriptions. The following two symbols were prepared for this range:

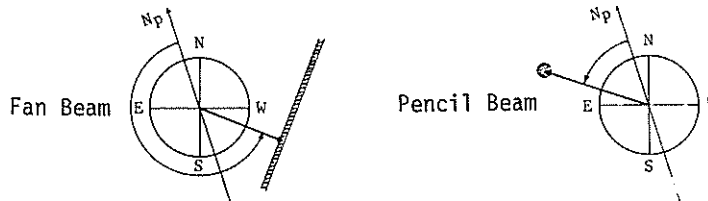
NS	= Noise Storm		
RF	= Rise and Fall	:	Defined as more or less irregular rise and fall of continuum with duration of the order of minutes to an hour.

S, FAL and SER may also be used.

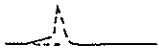
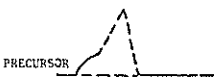
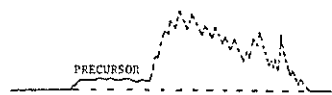
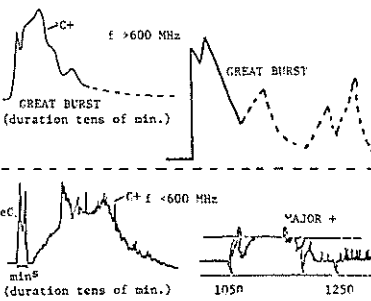
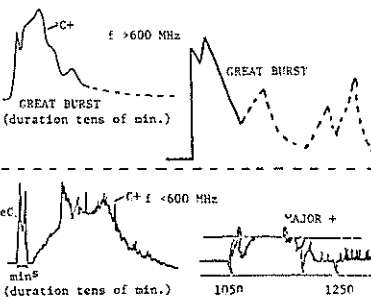
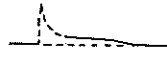
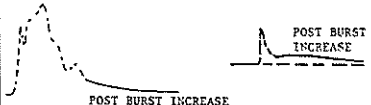

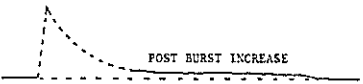
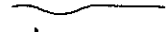



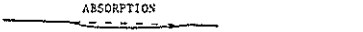
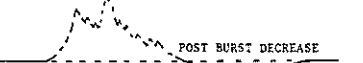
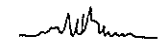
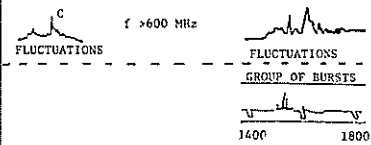
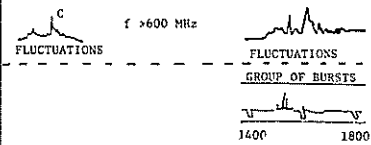

These types are illustrated in tables beginning on the following page in which samples from different sources are compared.

Polarization information is denoted by the letters R (right-handed) or L (left-handed). The degree of polarization in percent is shown in two digits. When precise values are not available, the degree of polarization is expressed in symbols, W = weak, M = moderate or S = strong. For example, 83R means -- 83% right-hand polarization, and SL means -- strong left-hand polarization.

Positional information is indicated by the letters F (fan-beam) or P (pencil-beam). Position angle is shown in the first three digits, and radial distance is shown by the following three digits. For example, 135120F means -- position angle = 135°, radial distance = 120% of solar radius observed by fan beam.



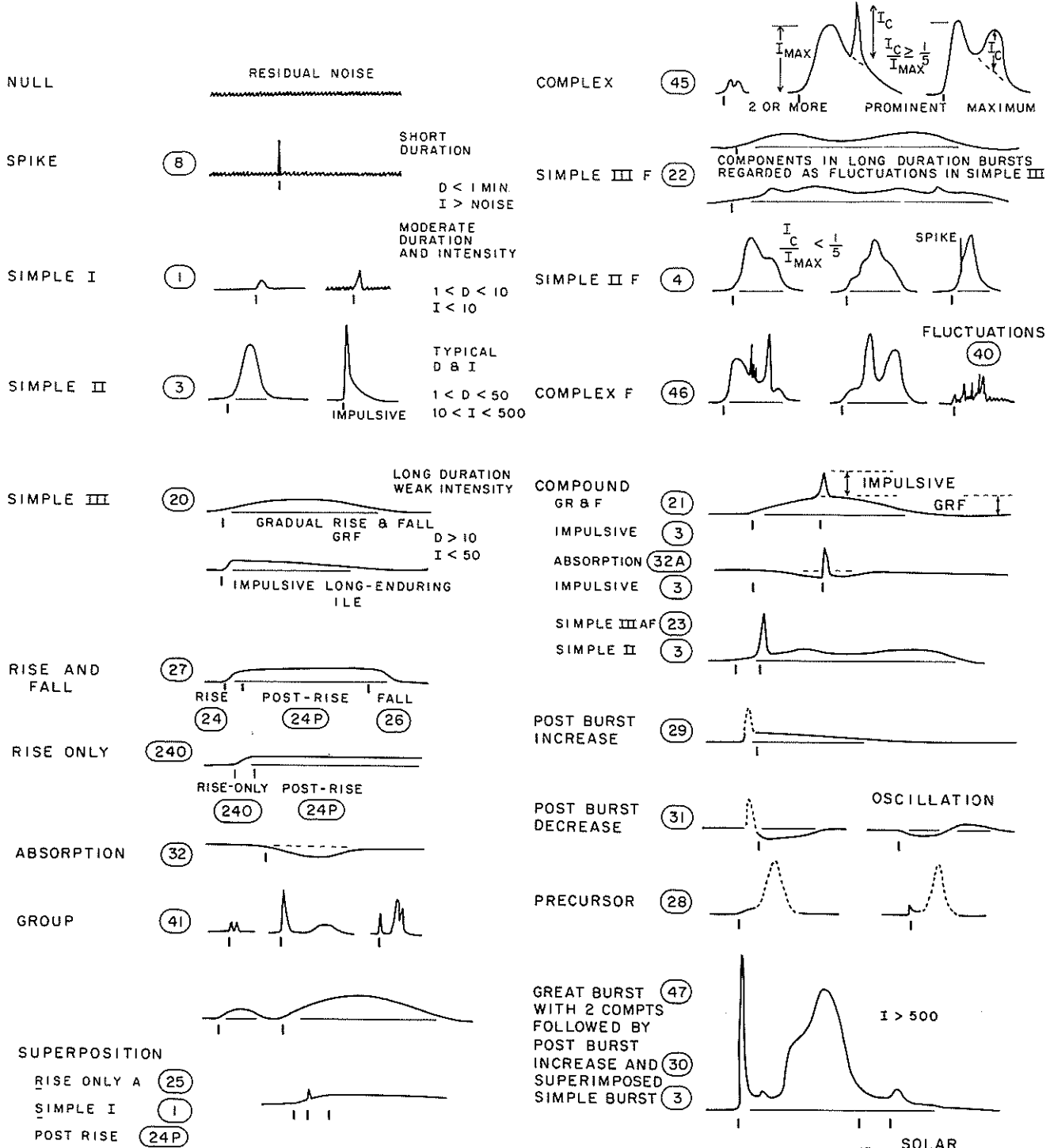
Letter Symbol	Covington's Classification	IQSY instruction	WDC-B Classification	Pennsylvania Classification
S	SIMPLE 1			SIMPLE
	SIMPLE 1F		(duration min.) SIMPLE 2	
	SIMPLE 2			SIMPLE 1
	SIMPLE 2F			SIMPLE 2
	SIMPLE 2F			MINOR
SIMPLE 2F		(duration sec. to min.)	1800 1830	SPIKE
SIMPLE 2F				PECULIAR
GRF	SIMPLE 3			PECULIAR
	SIMPLE 3 2 COMPONENTS		(duration hour) SIMPLE 3	
	SIMPLE 3A			
	SIMPLE 3		(duration hour)	
	SIMPLE 3A			
RISE AND FALL				(GRF+S)
C	COMPLEX 2 COMPONENTS			COMPLEX
			(duration min.)	
			MAJOR	
			2000 2100	
			MINOR+	PECULIAR
			1500 1600	SIMPLE
RF			RISE AND FALL	
		(duration tens of min.)	f < 600 MHz	1700 1750
NS			ONSET STORM	
			f < 600 MHz	
			NOISE STORM BEGINS	1600 1700 1800 1900
R	RISE ONLY		RISE	
			f > 600 MHz	RISE
SER	GROUP (3)			GROUP (4)
			f < 600 MHz	
			SERIES OF BURSTS	
FAL	FALL ONLY		FALL	
				FALL
	<p>Covington</p> <p>Peak Flux</p> <p>500</p> <p>10</p> <p>1 10 60 Min</p> <p>Duration</p> <p>1 2 3</p> <p>GREAT BURST</p> <p>Simple burst types</p>	<p>WDC-B</p> <p>Intensity</p> <p>0.150</p> <p>7.5 Min.</p> <p>Duration</p> <p>1 2 3</p>		

Letter Symbol	Covington's Classification	IQSY instruction	WDC-B Classification	Pennsylvania Classification
PRE	PRECURSOR 	PRECURSOR 		
GB	ANY BURST OF INTENSITY >500 UNITS			
PBI	POST BURST INCREASE 			
ABS	ABSORPTION  POST BURST DECREASE 			 
F	FLUCTUATIONS 			

Covington Additions to Tanaka's Proposed IAU Key

SGD Code	New Letter Symbol	Morphological Classification	Remarks
1A	S	Simple 1A	Single simple burst any duration and intensity. Event separable from other superimposed bursts.
3A	S	Simple 2A	
21A	GRF	Simple 3A GRF	
2A	S/F	Simple 1AF	Single simple burst any duration and intensity. Event separable from other superimposed bursts. Unlisted minor departures and fluctuations.
4A	S/F	Simple 2AF	
23A	GRF	Simple 3AF GRF	
240	R	Rise only	Discontinuity in daily level without observed restoration, any cause.
240F	R	Rise only F	With unlisted fluctuations.
24P	R	Post Rise	Post Rise enhanced level.
24PF	R	Post Rise F	Post Rise enhanced level with unlisted fluctuations.
26A	FAL	Fall A	Fall with listed superimposed event.
260	FAL	Fall Only	Fall only as discontinuity in daily level.
26F	FAL	Fall F	Fall with unlisted minor fluctuations.
27F	RF	Rise and Fall F	Rise and Fall with unlisted minor variations and fluctuations.
27AF	RF	Rise and Fall AF	Rise and Fall with listed superimposed events and unlisted minor variations and fluctuations.
31A	ABS	P.B. Decrease A	Post Burst Decrease with listed superimposed event.
32A	ABS	Absorption A	Absorption with listed superimposed emissive event.
46F	C	Complex F	Complex event with fluctuations.

2800-2700 MHz SOLAR BURST PROFILES



(2) - SIMPLE IF-EVENT DIFFICULT TO OBSERVE - NOT ILLUSTRATED
 (40) - FLUCTUATIONS-ORIGINALLY PERIOD OF IRREGULAR ACTIVITY

(XX) SOLAR GEOPHYSICAL DATA CODE
 (XXQ) MODIFIED CODE
 I START

AEC
1974-75

Solar Radio Observatories
(Fixed Frequency Observations)

CODE NAME	STATION	ALTERNATE NAME	GEOGRAPHIC		FREQUENCIES REPORTED (MHz)
			LAT	LONG	
ABST	Abastumani		42N	43E	221
ARCE	Arcetri		44N	11E	9240, 2830, 1420
ATHN	Athens		38N	24E	8800, 4995, 2695, 1415
BERL	Berlin-Adlershof		52N	13E	9500, 3000, 1470
BERN	Berne		47N	07E	10500
BORD	Bordeaux	Floriac	44N	01W	930
BOUL	Boulder		40N	105W	4995, 2695, 1420
CRIM	Simferopol	Crimea	44N	34E	3100
DWIN	Dwingeloo		53N	06E	315, 283
GORK	Gorky	Zimenki	56N	44E	9100, 2950, 950, 650, 200, 100
HARS	Harestua	Blindern	60N	10E	228
HIRA	Hiraiso		36N	140E	500, 200, 100
HUAN	Huancayo		12S	75W	9400
IRKU	Irkutsk	Siberian IZMIR	52N	104E	9300
IZMI	Moscow IZMIRAN	Krasnaja Pakhra	55N	37E	207
KIEL	Kiel		54N	10E	1420, 1000, 800, 600, 400, 240
KIEV	Kiev		50N	30E	550, 188
KISV	Kislovodsk		43N	42E	15000, 6100
MANI	Manila		14N	121E	8800, 4995, 2695, 1415, 606, 245
MCMA	McMath-Hulbert		42N	83W	18
ONDR	Ondrejov		49N	14E	808, 536, 260
OTTA	Ottawa ARO	Algonquin	45N	78W	2800
PALE	Palehua		21N	156W	8800, 1415
PENN	Penn. State Univ.		41N	78W	10700, 2700, 960
PENT	Penticton		49N	119W	2695
POTS	Potsdam	Tremsdorf	52N	13E	510, 234, 113
SAOP	Sao Paulo		22S	46W	7000
SGMR	Sagamore Hill		52N	72W	35000, 15400, 8800, 4995, 2695, 1415, 606, 410, 245
SLOU	Slough		51N	00E	71000, 37000, 19000, 9400, 2800
SYDN	Sydney		34S	151E	1420, 720
TORN	Torun		53N	19E	127
TRST	Trieste		46N	14E	408, 237
TYKW	Toyokawa		34N	137E	9400, 3750, 2000, 1000
UCCL	Uccle	Humain	50N	04E	600
UPIC	Upice		50N	16E	30
VORO	Voroshilov	Ussurisk	43N	132E	2930, 202

E N E R G E T I C S O L A R P A R T I C L E S A N D P L A S M A
(A.12e, A.13e)

A series of data plots are presented using data obtained on the NASA spacecraft IMP 7 and IMP 8. The purpose of the plots is to convey on as near continuous a basis as possible the state of the interplanetary particle environment. The plots consist of hourly averaged solar wind plasma parameters and representative fluxes of energetic electrons, protons, and alpha particles.

Plasma plots are generated at MIT. Energetic particle flux plots are generated at the National Space Science Data Center (Code 601, Goddard Space Flight Center, Greenbelt, Maryland 20771) from machine sensible hourly averaged fluxes ($(\text{cm}^2 \text{ ster sec MeV/n})^{-1}$) provided by several experimental groups. Updated composite magnetic tapes are available at NSSDC, as are 35 mm microfilm flux plots with standard International Magnetospheric Study scalings.

IMP 7 (Explorer 47, IMP H) was launched into a near-circular geocentric, ~ 12 day orbit at 30-40 R_E on September 23, 1972. IMP 8 (Explorer 50, IMP J) was launched on October 26, 1973 into a similar orbit. The two spacecraft were instrumented to measure the plasmas, fields, and energetic particle fluxes found in the interplanetary medium and in the distant magnetosheath and magnetotail. The relative orbital phase of the two spacecraft evolved such that the percent of each 12-day period during which at least one spacecraft was in the interplanetary medium was 100% until mid-1975, decreased to a minimum of about 65% near January 1976, and will return to 100% in late 1976.

Due to the relatively large number of flux plots, multiple traces are graphed on individual frames. Accordingly, the statistical error bar associated with each data point is omitted in order to maximize cleanliness of plot. To compensate for this, only data points with statistical uncertainties of about 20% or less are plotted. As this corresponds to 25 counts ($1/\sqrt{25} = 20\%$), averages of hourly fluxes are taken over a sufficient number of hours to assure that the longer term averaged flux corresponds to at least 25 incident particles. In this process it is assumed that during each hour for which a flux is given, the instrument was counting for a full 60 minutes. This assumption is rarely significantly in error, and, after the first two months of data submission, only data for hours during which at least 30 minutes of counting occurred were provided to NSSDC. Such >1 -hour - averaged fluxes are plotted as a series of apparent hourly fluxes of the common value. The reader is cautioned against interpreting such a series of apparently constant flux values as representing a physically real time-independence in the flux level.

In order to preserve particle event onset-time information low flux averages are terminated whenever the flux for a single hour exceeds that associated with 50 counts.

Data gaps in the data are distinguished by the lack of connecting lines between data points.

The purpose of the IMP data plots is to convey on as near continuous a basis as possible the state of the interplanetary particle environment. As such, for most of the data channels, IMP 7 and IMP 8 data are interspersed to maximize interplanetary coverage. Exceptions to this are the GSFC and University of Chicago contributions, for which particle fluxes measured while within the geomagnetic tail are expected to be insignificantly different than interplanetary fluxes. These two contributions contain time-continuous IMP 8 data.

Plasma plots contain data only for hours during which the appropriate spacecraft was beyond the earth's bow shock. These interplanetary identifications are made by a visual inspection of preliminary data plots at MIT. On the two lowest energy proton plots, fluxes obtained in the magnetotail during hours when no interplanetary values are available are distinguishable. For only the 0.16 - 0.22 MeV protons is there a significant probability that the fluxes so plotted will be significantly different than the interplanetary fluxes. MIT plasma identifications of hours of non-interplanetary spacecraft residence are used if available early enough in each month's data processing cycle. Otherwise, predicted times of model bow shock crossings are used.

Plasma Data -- Hourly averaged plasma parameters (bulk speed, proton number density, most probable thermal speed), determined from the MIT plasma experiments on IMP's 7 and 8, are provided by H. Bridge, A. Lazarus and J. Sullivan of the Massachusetts Institute of Technology. The instrument is a split-collector, modulated-grid Faraday cup designed to measure the positive ion component of the solar wind. Particle fluxes in 24 contiguous energy channels and in 14 angular sectors are measured every 15 seconds (IMP 7) or 30 seconds (IMP 8). The hourly averages are based on preliminary plasma parameters computed by fitting the observations to a convected, isotropic Maxwellian distribution function. The error bars on each plotted data point indicate the standard deviation of the data contributing to the hourly average. Note that the thermal speed plot has scales for both thermal speed (left side) and temperature (right side).

Energetic Particle Data -- The sources and some characteristics of the energetic particle data are summarized in Table 1. The geometric factors are in some cases average values over the indicated energy ranges. Neglect of energy dependence in geometric factors leads to an error whose magnitude depends on sensor geometry and ambient particle spectrum. Thus for the highest energy proton mode which uses a non-curved, relatively thick sensor, a flux $\sim 5\%$ too high is found for an E^{-4} spectrum. Typically, smaller errors are made for other modes.

The "Multi-Parameter Analysis?" column indicates whether multi-parameter analysis (typically dE/dx vs. E) is used in flux determination. Such analysis permits unambiguous identification of particle species [see, for example, discussion in Garcia-Munoz et al., *Astrophys. J.*, 184, 967, 1973] but is generally not feasible for particles which have insufficient energy to penetrate one sensor and reach a second sensor. As discussed below, however, an attempt has been made to remove the non-proton component from the 0.97 - 1.85 MeV proton fluxes.

TABLE 1

SPECIES	ENERGY (Mev/n)	GEOMETRIC FACTOR (cm ² ster)	MULTI-PARAMETER ANALYSIS?	SOURCE
Electrons	1-5	0.07 to 1.6 (see text)	yes	Caltech.
Protons	0.16-0.22	0.03	no	U. of Md.
Protons	0.97-1.85	1.51	no	JHU/APL
Protons	4.0-12.5	0.07 or 0.23 (see text)	yes	Caltech.
Protons	13.7-25.2	0.32	yes	JHU/APL
Protons	19.8-40.1	3.13	yes	GSFC
Protons	40.1-81.8	2.68	yes	GSFC
Alphas	11-20	2.05	yes	U. Chicago
Alphas	20-25	2.05	yes	U. Chicago
Alphas	25-90	2.05	yes	U. Chicago

Fluxes in units of (cm² ster sec)⁻¹ have been obtained by folding together count rates, geometric factors, and, where appropriate, pulse height analysis data. These fluxes are then divided by the width of the energy window to yield the differential fluxes plotted. The ratio of these average differential fluxes, to the "true" differential flux at the midpoint of the energy range E₁ to E₂, is indicated in Table 2 for Eⁿ spectra and for R = E₂/E₁. Alternatively, one can ask at what energy within the E₁ to E₂ interval is the true differential flux equal to the average differential flux. The ratio of this energy [(n-1) (E₂-E₁)/(E₁¹⁻ⁿ - E₂¹⁻ⁿ)] to the midpoint energy (½ (E₁ + E₂)) is given in Table 3. It is clear from these tables that great care must be used when obtaining spectral parameters from fluxes resulting from wide energy windows at times of steep spectra.

TABLE 2

RATIO OF AVERAGE TO TRUE DIFFERENTIAL FLUX AT MIDPOINT OF ENERGY INTERVAL

n \ R	1.3	1.6	2	3
0.5	1.0021	1.0068	1.0146	1.0353
2	1.0173	1.0563	1.1250	1.3333
5	1.0893	1.3110	1.7798	3.9506

TABLE 3

RATIO OF ENERGY AT WHICH TRUE FLUX = AVERAGE FLUX TO MIDPOINT ENERGY

n \ R	1.3	1.6	2	3
0.5	.9957	.9865	.9714	.9330
2	.9914	.9730	.9428	.8660
5	.9830	.9473	.8912	.7598

The 1-5 MeV electron data and 4.0-12.5 MeV proton data are obtained from telescopes consisting of eleven fully depleted silicon detectors surrounded by a plastic scintillator anti-coincidence cup. These data are provided by E. C. Stone, R. E. Vogt, R. A. Mewaldt, and co-workers at the California Institute of Technology. During most times, the electron fluxes result from a "wide geometry" mode (effective geometric factor = 1.6 cm² ster for IMP 7, 1.5 cm² ster for IMP 8), although for times of large solar particle fluxes, a "narrow geometry" mode is used (effective geometric factor = 0.07 cm² ster for IMP 7, 0.23 cm² ster for IMP 8). Electron fluxes have been

corrected for secondary electrons produced by the interaction of gamma rays in the detector stack. (This background flux is separately monitored by the instrument.) Periods during which magnetospheric electrons seriously contaminate the observed 1-5 MeV electron fluxes have been identified and eliminated by analysis of 0.2-1.0 MeV electron fluxes and by a comparison of the IMP 7 and IMP 8 counting rates. Plotted proton fluxes result from a mode having geometric factors of 0.07 cm² ster on IMP 7 and 0.23 cm² ster on IMP 8. Illustrations and further descriptions of the instruments can be found in Hurford et al., [*Ap. J.*, 192, 541, 1974], and in Mewaldt et al., [*Ap. J.*, 205, (May 1), 1976, in press].

The 0.16-0.22 MeV proton fluxes are provided from a University of Maryland experiment. They are obtained from an electrostatic analyzer in which incident particles are deflected by an applied electric field by an amount dependent on their energy/charge ratio. The deflected particles are then counted by a series of lithium-drifted (IMP 7) or surface-barrier (IMP 8) detectors positioned to measure particles having experienced various amounts of deflection. The flux as plotted results from the counting rate of one of these sensors and consists of:

- (1) 0.16-0.22 MeV ambient protons,
- (2) ambient Helium and heavier ions which generally do not exceed 10% of the proton component,
- (3) a background flux level of ≈ 90 particles/cm² ster sec MeV caused by interactions of galactic cosmic rays in the spacecraft, and
- (4) during times of intense fluxes of high energy particles, a complicated time-variable background.

This last component may be particularly important in the onset phase of solar flare particle events. For further details on the instrument, see Tums, et al., [*IEEE Trans. Nuc. Sci.*, NS-21, 1, 210, 1974].

The University of Maryland data are provided by G. Gloeckler, C. Y. Fan (University of Arizona), D. Hovestadt (Max-Planck Institute), F. Ipavich and co-workers.

The 0.97-1.85 MeV and 13.7-25.2 MeV proton fluxes are provided from an experiment of the Johns Hopkins University/Applied Physics Laboratory. They are obtained from a telescope consisting of three colinear sensors (two surface-barrier totally depleted detectors followed by a lithium-drifted detector) surrounded by a plastic scintillator anti-coincidence cup. The 0.97-1.85 MeV proton fluxes correspond to particles stopping in the first sensor; hence standard $dE/dx - E$ analysis is not possible. However, ratios of proton to alpha particle fluxes and alpha particle to medium nuclei fluxes measured at slightly higher energies have been used to estimate the magnitude of, and to eliminate, the non-proton component of this 0.97-1.85 MeV proton mode. These data are provided by S. M. Krimigis and T. P. Armstrong (University of Kansas). Further details on the instrument and on data analysis techniques may be found in Sarris et al., [*Observations of Magnetospheric Bursts of High Energy Protons and Electrons at $\approx 35 R_E$ with IMP 7*"], *J. Geophys. Res.*, 81, 1976, in press].

The 19.8 - 40.1 MeV and 40.1 - 81.8 MeV proton fluxes are obtained from a telescope consisting of two CsI (Na) scintillators viewed by phototubes and surrounded by an active anti-coincidence detector. These fluxes are obtained on IMP 8 only and are provided by F. B. McDonald and T. T. von Rosenvinge of NASA, Goddard Space Flight Center. The dE/dx element is 1 mm x 5 cm diameter whereas the E element is 2.01 cm x 5 cm diameter. The finite thickness of the E element yields a geometric factor which decreases nearly linearly with increasing energy, being 3.25 cm² ster at 19.8 MeV and 2.35 cm² ster at 81.8 MeV. In computing fluxes, the average geometric factors in each of the two energy intervals is used. No correction is made for the resultant error which ranges from zero for a flat spectrum to 5% (computed flux too high) for an E^{-4} spectrum. Corrections for slow gain shifts in the scintillator/phototube output are made.

The three alpha particle fluxes are provided by J. A. Simpson and G. M. Mason of the University of Chicago. They are obtained from a telescope consisting of three lithium-drifted silicon detectors, a CsI (Tl) scintillator viewed by four photodiodes and a sapphire scintillator/Cerenkov radiator, all surrounded by a plastic anti-coincidence scintillator. The three fluxes correspond to alpha particles stopping in the second, third, and fourth sensors of the telescope. Background contamination of these fluxes is less than 10%. Care should be taken when proton and electron fluxes above 0.5 MeV are $\geq 3 \times 10^3$ particles/cm² ster sec, since these high rates may interfere with the proper operation of the instrument logic and analysis. The quoted fluxes include He³ and He⁴. During quiet periods, He³ may contribute up to 10% of the total 25-90 MeV/n flux, and considerably less for the two lower energy fluxes. The instrument is further described in Garcia-Munoz et al., [*Astrophys. J. Lett.*, 201, 145, 1975].

MAGNETOGRAMS OF GEOMAGNETIC STORMS (D.1e)

In the past the Kp and other indices have provided some information on geomagnetic disturbances. However, during the last few years there has been an increasing demand for more quantitative indices with finer time resolution and based upon records from a more suitable distribution of observatories. The indices Kn, Ks, and Km have been developed and continue to satisfy the requirement for 3-hourly indices of activity as observed at mid-latitude locations. Both the Dst and AE indices have been devised to fulfill the need for quantitative indices having finer time resolution. Dst provides an estimate of the field of the ring current although ignoring its asymmetry. AE provides an estimate of the field of the auroral electrojets.

Recent progress in magnetospheric physics has made it clear that a comprehensive study of the asymmetric growth of the ring current belt is essential in understanding the mechanism of its formation and the generating mechanism of magnetospheric storms as well. For this purpose, Dst is not necessarily the most suitable index. Auroral electrojets have a lifetime of order one to three hours and the increasing availability of 2.5-min AE(11)* provides indices having excellent time resolution for the study of these high-latitude magnetic variations. However, the delay inherent in acquisition and processing of all magnetograms used in deriving AE(11) and the desirability of including a record of magnetic variations at mid-latitude and equatorial locations suggest that no combination of indices is completely self-sufficient.

Table of Observatories

	Geog. Coord.		Geomag. Coord.			Geog. Coord.		Geomag. Coord.	
	Lat.	Long.	Lat.	Long.		Lat.	Long.	Lat.	Long.
Narssarssuaq	61.20	314.60E	71.14	37.42E	Dixon Island	73.55	80.57E	63.01	161.84E
Leirvogur	64.18	338.30	70.12	71.51	Tixie Bay	71.58	129.00	60.48	191.72
Fort Churchill	58.80	265.90	68.74	323.46	Tashkent	41.33	69.62	32.30	144.43
Barrow	71.30	203.25	68.64	241.55	San Juan	18.12	293.85	29.57	3.63
Great Whale River	55.27	282.22	66.57	348.05	Kakioka	36.23	140.18	26.09	106.38
Cape Chelyuskin	77.72	104.28	66.28	176.70	Honolulu	21.32	202.00	21.17	266.99
Abisko	68.36	18.82	65.94	115.28	Davao	07.08	125.58	-4.00	194.97
College	64.87	212.17	64.73	256.99	Tangerang	-06.17	106.63	-17.62	175.93

- * UAG-37 "Auroral Electrojet Magnetic Activity Indices AE(10) for 1966", by Joe Haskell Allen, Carl C. Abston and Leslie D. Morris, National Geophysical and Solar-Terrestrial Data Center, Environmental Data Service, December 1974, 142 pages, price 75 cents.
- UAG-33 "Auroral Electrojet Magnetic Activity Indices AE(10) for 1967", by Joe Haskell Allen, Carl C. Abston and Leslie D. Morris, National Geophysical and Solar-Terrestrial Data Center, Environmental Data Service, May 1974, 142 pages, price 75 cents.
- UAG-29 "Auroral Electrojet Magnetic Activity Indices AE(11) for 1968", by Joe Haskell Allen, Carl C. Abston and Leslie D. Morris, National Geophysical and Solar-Terrestrial Data Center, Environmental Data Service, October 1973, 148 pages, price 75 cents.
- UAG-31 "Auroral Electrojet Magnetic Activity Indices AE(11) for 1969", by Joe Haskell Allen, Carl C. Abston and Leslie D. Morris, National Geophysical and Solar-Terrestrial Data Center, Environmental Data Service, February 1974, 142 pages, price 75 cents.
- UAG-22 "Auroral Electrojet Magnetic Activity Indices (AE) for 1970", by Joe Haskell Allen, National Geophysical and Solar-Terrestrial Data Center, Environmental Data Service, November 1972, 146 pages, price 75 cents.
- UAG-39 "Auroral Electrojet Magnetic Activity Indices AE(11) for 1971", by Joe Haskell Allen, Carl C. Abston and Leslie D. Morris, National Geophysical and Solar-Terrestrial Data Center, Environmental Data Service, February 1975, 144 pages, price \$2.05.
- UAG-45 "Auroral Electrojet Magnetic Activity Indices AE(11) for 1972", by Joe Haskell Allen, Carl C. Abston and Leslie D. Morris, National Geophysical and Solar-Terrestrial Data Center, Environmental Data Service, May 1975, 144 pages, price \$2.10.
- UAG-47 "Auroral Electrojet Magnetic Activity Indices AE(11) for 1973", by Joe Haskell Allen, Carl C. Abston and Leslie D. Morris, National Geophysical and Solar-Terrestrial Data Center, Environmental Data Service, June 1975, 144 pages, price \$2.10.

For these reasons, actual records of magnetic variations at a number of observatories are still very useful. In this publication, one or two interesting geomagnetic events may be chosen for each month and are illustrated by reconstructed H-component magnetograms. The magnetograms are reduced from the original records to display the same amplitude scale and time base. Reduced magnetograms are included from about 10 of the 16 observatories listed in the table although delays in receipt of some magnetograms may necessitate using records from substitute stations. If an adequate coverage of auroral zone observatories is available, preliminary AU and AL graphs are also prepared for each event. No reduced magnetograms are prepared for months having activity of only minimal interest.

These reduced magnetograms and index graphs are now produced under the direction of J. H. Allen and W. Paulishak of the National Geophysical and Solar-Terrestrial Data Center from magnetograms furnished by the World Data Center A for Solar-Terrestrial Physics. For the interval January 1967 through September 1973, reduced magnetograms were provided by Dr. S.-I. Akasofu.

DATA FOR SEVEN MONTHS BEFORE MONTH OF PUBLICATION

TABLE OF CONTENTS

	<u>Page</u>
H.62 <u>Abbreviated Calendar Record</u>	59
C.1f <u>Flare Index (by Region)</u>	60

ABBREVIATED CALENDAR RECORD (H.62)

The Abbreviated Calendar Record is a monthly summary chronological account of solar and geophysical activity and events published in the seventh month after observation. It is intended to give a background for the early interpretation of solar-geophysical results. It continues the series published in *IQSY NOTES* beginning with data for January 1964 in No. 7, through data for December 1966 in No. 21, and for January 1967 through November 1968 in *STP Notes* No. 1-3, 5, and 7. (A Condensed Calendar Record has continued in *STP NOTES*. Data for December 1968 through March 1975 are published in Nos. 7-14.) It is similar to the Calendar Record compiled for the IGY and IGC-1959 [*Annals of the IGY*, Vol. 16] and compiled for 1960-1965 [*Annals of the IQSY*, Vol. 2]. It is prepared from data reports available at the World Data Center A for Solar-Terrestrial Physics. However, it is compiled rapidly, including some provisional data, and should not be relied on for details of solar and geophysical events in preference to standard publications.

The format is as follows:

The period covered on each date is 0000 to 2400 UT (Universal Time). At the beginning of each month a chart of the sun for the month locates the calcium plages, as reported by the McMath-Hulbert Observatory, at the latitude and longitude of their Central Meridian passage by the last two digits of the plage serial number. The general activity of the region is approximately evaluated, mainly from area and intensity of plage and associated sunspots, by use of the symbols: G = great activity, M = moderate activity and S = small activity. This chart is superimposed on the most recent revision of the H α synoptic chart for the same month which was originally published at the beginning of the second section of Part I (Prompt Reports).

For each date a series of time lines are presented. In the first block the duration of flares of importance $\geq 1f$ is shown by a horizontal line, followed by the importance with a slant line separating the last two digits of the serial number of the calcium plage region in which the flare occurred. These are selected from the grouped flare reports as published in these *Solar-Geophysical Data* reports. Fixed frequency solar noise bursts are indicated by vertical tick marks by wavelength range at the time of beginning of the burst. The ranges are defined as dekameter = ~ 40 MHz, meter = 40-400 MHz, decimeter = 400-1500 MHz, and centimeter = >1500 MHz. Spectral events of types II and IV are shown at the time of beginning by the appropriate Roman numeral. Noise storms at meter wavelength are indicated by horizontal lines. On the next two lines are vertical tick marks at the time of beginning to show sudden ionospheric disturbances and solar x-ray bursts from SMS/GOES (.5-4Å; 1-8Å).

The Ap for the day is given in the left-hand portion of the next two lines which give the eight Kp centered in the appropriate three-hour time blocks, and the time of storm sudden commencements, if any, by a triangle. The daily planetary Ap index is derived from the 3-hourly Kp indices, which are based on reports from a selected standard group of geomagnetic observatories. The Ap index increases with increasing magnetic activity to a maximum of 400. The data are provided by the International Service of Geomagnetic Indices (Göttingen of IAGA. [*Annals of the IGY*, Vol. 4, pp. 227-236]. Beside the Ap value will appear, when appropriate, "D" for one of the five most disturbed days, "Q" for one of the 10 most quiet days and "QQ" for one of the five most quiet days. Adjacent to the sc triangle the exact time of the sc is given with the number of observatories reporting it in the parentheses.

Auroral displays are usually mentioned only if the southern limit reached ϕ (geomagnetic latitude) less than 60°. The ϕ given is that of overhead occurrence in the USSR. The time and type of aurora follows this. N. V. Pushkov provides descriptions of aurora summarizing reports from a network of about 130 stations between 30° and 140° E longitude. After December 1975 the Western Europe sector data are no longer available.

The following Codes to describe the aurora, as defined by F. Jacka and J. Paton in the *IQSY Instruction Manual No. 3 Aurora*, are used:

1. Auroral Forms: A (arc); B (band); P (patch); V (veil); R (rays); G (glow); N (not identifiable).
2. Structure: H (homogeneous); S (striated); R (rayed); ₁ - short rays; ₂ - medium length rays; ₃ - long rays.
3. Qualifying Symbols: m (multiple); f (fragmentary); c (coronal).
4. Condition: q (quiet); a (active); p (pulsing); p₂ (flaming); p₃ (flickering); p₄ (streaming).
5. Brightness:
 1. weak, comparable with the Milky Way.
 2. comparable with moonlit cirrus clouds.
 3. comparable with moonlit cumulus clouds.
 4. much brighter than 3 if extensive aurora may cast discernible shadows.

On the next line is given the Forbush cosmic ray decreases from the Deep River or Sulphur Mountain charts limited to those of 3% or greater.

Outstanding green corona as published in *Solar-Geophysical Data* Part I are mentioned by limb quadrant on date the peak would be at CMP.

The indices on the next line are as follows:

-- The provisional daily Zürich relative sunspot number, R_z , as communicated by Prof. M. Waldmeier of the Swiss Federal Observatory. It is based on observations at Zürich, Arosa and Locarno only. Final values of R_z , issued after the end of each calendar year, usually differ slightly from the provisional ones. If available at time of publication these final values are used.

-- The 10 cm solar radio flux at 2800 MHz is observed at the Algonquin Radio Observatory by the National Research Council, Canada, at about 1700 UT daily. It is expressed in unit of $10^{-22} \text{Wm}^{-2} \text{Hz}^{-1}$. The observed flux should be used for most solar-terrestrial studies. The values adjusted for the varying Sun-Earth distance are published elsewhere in *Solar-Geophysical Data*.

-- The flare index gives the daily flare index with the hours of flare patrol on which the index was based (see p. 45 of this text).

-- The daily Ca plage index is given next (see p. 28 of this text).

-- The ionospheric indices, I_p and I_a , are computed by the method of Y. Hakura, Y. Takenoshita, and K. Matsuoka in "Influence of solar activity on the ionosphere blackout index", [*J. Radio Res. Labs., Japan*, 14, No. 73, 1967]. If "-" is entered, it signifies less than 12 hours of data, so no value has been computed. The index I_p is for polar cap blackout, and the index I_a is for auroral zone blackout. The indices are on a scale from "0" representing 0.4 hours or less of blackout per day increasing to "9" representing 20.1 to 24 hours of blackout per day. Ionospheric f-min data from selected stations are used. The indices differ from Hakura et al. in that Kiruna and Fort Churchill data have been substituted for Point Barrow for I_a , and only Resolute Bay and Thule data are available for I_p .

Next are given the McMath calcium plage region numbers on their date of CMP together with their latitude and number of rotations, if more than one, in the parentheses. The Mt. Wilson sunspot region numbers, together with their latitude, magnetic classification by α , β , γ or δ and largest spot (preceding "p" or following "f") and a digit encoding field strength are listed under the calcium plage region in which they appeared.

The digits used to encode field strength are as follows:

1 = 100 - 500 gauss	6 = 2600 - 3000 gauss
2 = 600 - 1000	7 = 3100 - 3500
3 = 1100 - 1500	8 = 3600 - 4000
4 = 1600 - 2000	9 = 4100 - 4500
5 = 2100 - 2500	10 = >4500

If the Mt. Wilson sunspot is at CMP on a different date than the calcium plage was, this date is given in parentheses following the sunspot information. If the calcium or sunspot region numbers are in parentheses, this signifies the regions were never actually at the Central Meridian; these had either died while on the Eastern Hemisphere or were born on the Western Hemisphere.

When necessary, written remarks may appear at the end of the day.

FLARE INDEX BY REGION (C.1f)

An index that characterizes the flare productivity of McMath calcium plage regions integrated over a disk passage has been developed by Constance Sawyer and Catherine Candelaria. The scale is consistent with the HAO flare index, and with the NOAA whole-disk index which is briefly described on page 45. The same formula,

$$I_f = \frac{.76}{T^*} \sum A_d^2$$

is used where A_d is the measured (apparent) area in millionths of solar disk, but the sum is taken for each region separately over all the days of its disk passage.

The total number of flares is also given and the dates on which the first and last flares were observed in the region. The "flare-index mean" is the flare-index sum divided by the interval in days from the first flare to the last flare.

DATA FOR
MISCELLANEOUS TIME PERIODS
RETROSPECTIVE WORLD INTERVALS (H.63)

Retrospective World Intervals selected by the Monitoring of Sun Earth Environment (MONSEE) program of the ICSU Special Committee on Solar-Terrestrial Physics will be presented as appropriate.

OTHER DATA

Information available either annually or on a non-routine publication basis will be given. The descriptive material necessary to understand the data will be included in the issue presenting the data. Data received too late for publication in the normal section may also appear here.

PARTIAL LIST OF CONTRIBUTORS

These monthly reports would not be possible without the continuing support and cooperation of scientists throughout the world. Much of the data included have been obtained through either the International Ursigram and World Days Service program or the international exchange of geophysical observations between World Data Centers in accordance with the principles set forth in recommendations of relevant organizations of the International Council of Scientific Unions. (See *Guide to International Data Exchange*, issued in 1972 by the ICSU Panel on World Data Centers).

Special thanks are due to many individuals including the following:

<u>Name</u>	<u>Organization</u>	<u>Data Type</u>
C. H. Hossfield	American Association of Variable Star Observers Solar Division 540 N. Central Avenue Ramsey, New Jersey 07446	Sunspots
P. S. McIntosh	Space Environment Laboratory NOAA Boulder, Colorado 80302	Sunspots, H α photographs, H α synoptic charts
M. Waldmeier	Eidgen, Sternwarte Schmelzbergstrasse 25 8006 Zürich, Switzerland	Sunspots
Helen W. Dodson	McMath-Hulbert Observatory University of Michigan 895 Lake Angeles Rd. North Pontiac, Michigan 48055	Calcium plages, flares, SID
G. Godoli	Osservatorio Astrofisico Citta Universitaria Viale A. Doria 95123 Catania, Italy	Calcium plages, flares
R. Howard J. M. Adkins	Mount Wilson Observatory 813 Santa Barbara Street Pasadena, California 91101	Magnetic classifications of sunspots, solar magnetograms
J. W. Harvey W. Livingstone	Kitt Peak National Observatory P.O. Box 26732 Tucson, Arizona 85726	Solar magnetograms
A. A. Giesecke M. Ishitsuka	Observatorio de Huancayo Instituto Geofisico del Peru Apartado 46 Huancayo, Peru	SID, solar radio emission flares
V. Badillo F. J. Heyden	Manila Observatory P.O. Box 1231 Manila, Philippines	Flares, SID, solar radio emission, sunspots
M. Bernot P. Simon	Observatoire de Meudon 92190 Meudon, France	Flares
H. Tanaka	Toyokawa Observatory The Research Institute of Atmospheric Nagoya University Toyokawa, 442 Japan	Solar radio emission
J. P. Castelli Wm. R. Barron	USAF Geophysics Laboratories L. G. Hanscom Field Code LIR Bedford, Massachusetts 01730	Solar radio emission
W. N. Christiansen Arthur Watkinson	School of Electrical Engineering University of Sydney Sydney, N.S.W. 2006, Australia	Solar radio emission

<u>Name</u>	<u>Organization</u>	<u>Data Type</u>
A. E. Covington M. B. Bell	Astrophysics Branch National Research Council Ottawa 27 Ontario, Canada	Solar radio emission
A. Maxwell	Harvard Radio Astronomy Station Fort Davis, Texas 79734	Solar radio emission
H. Urbarz	Aussenstelle Astronomy Institut der Universitat Tübingen 7981 Weissenau Federal Republic of Germany	Solar radio emission
A. O. Benz G. L. Tarnstrom H. K. Asper	Microwave Laboratory Gloriastrasse 35 CH-8006 Zürich, Switzerland	Solar radio emission
C. Slottje	Solar Radio Observatory Netherlands Foundation for Radio Astronomy Dwingeloo, Netherlands	Solar radio emission
M. Pick	Observatoire de Meudon 92190 Meudon, France	Solar radio emission
J. W. Warwick	Dept. of Astro-geophysics University of Colorado Boulder, Colorado 80302	Solar radio emission
J. P. Wild S. F. a Smerd	CSIRO Division of Radio Physics P.O. Box 76 Epping N.S.W. 2121 Australia	Solar radio emission
M. P. Bleiweiss F. L. Wefer	NELC La Posta Rt. 1, Box 591 Campo, California 92006	Solar radio maps
H. Zirin K. A. Marsh	Big Bear Solar Observatory California Institute of Technology North Shore Drive Big Bear City, California 92314	Coronal holes
B. J. Rickett	University of California, San Diego Dept. of Applied Physics and Information Science La Jolla, California 92037	Solar wind
J. H. Wolfe	NASA Mail Code 245-11 Electrodynamics Branch Ames Research Center Moffett Field, California 94035	Solar wind
D. S. Colburn C. P. Sonett	NASA/ARC Moffett Field, California 94035	IP Electric Field
F. L. Scarf	Space Science Department TRW Systems One Space Park Bldg. R-5, Rm. 1280 Redondo Beach, California 90278	IP Electric Field
N. F. Ness	Laboratory for Extraterrestrial Physics NASA/GSFC, Code 690 Greenbelt, Maryland 20771	IP Magnetic Field
F. Mariani	Instituto Fisica Universita Piazza Annunziata 67100 L'Aquila, Italy	IP Magnetic Field

<u>Name</u>	<u>Organization</u>	<u>Data Type</u>
J. H. King	NASA/GSFC Code 601 Greenbelt, MD 20771	Solar particles, plasmas
W. R. Webber J. A. Lezniak	Physics Department University of New Hampshire Demerritt Hall Durham, New Hampshire 03824	Solar cosmic ray protons
A. Frosolone	Space Weather Consultants P.O. Box 213 Moffett Field, California 94035	Pioneer spacecraft
R. B. Doeker G. Heckman	Space Environment Services Center NOAA Boulder, Colorado 80302	Solar proton events Inferred IP Magnetic Fields
S. Mansurov	IZMIRAN P.O. Akademgorodok Moscow Region, USSR	Inferred IP Magnetic Fields
R. B. Ammons (AAVSO)	P.O. Box 1441 Missoula, Montana 59801	SES, SWF
C. Hornback	Table Mountain Geophysical Monitoring Station Space Environment Laboratory NOAA Boulder, Colorado 80302	SID, Solar radio emission
S. Katahara	Ionospheric Sounding Station P.O. Box 578 Puunene, Maui, Hawaii 96784	SPA
A. P. Mitra	Radio Research Committee National Physical Laboratory of India Hillside Road New Delhi 12, India	SID
P. C. Yuen	Department of Electrical Engineering University of Hawaii Honolulu, Hawaii 96822	SFD
R. F. Donnelly	Space Environment Laboratory NOAA Boulder, Colorado 80302	Solar x-rays
L. W. Acton C. J. Wolfson	Lockheed Research Laboratory Div. 52/10, Bldg. 202 3251 Hanover Street Palo Alto, California 94304	X-ray maps
M. Bercovitch Margaret D. Wilson	National Research Council of Canada Division of Physics Ottawa, Ontario, Canada K1A 0R6	Cosmic rays
D. Venkatesan M. Tjoei	Department of Physics University of Calgary Calgary, Alberta, Canada T2N, 1N4	Cosmic rays
J. A. Simpson G. Lentz	LASR Enrico Fermi Institute University of Chicago 933 E. 56th Street Chicago, Illinois 60637	Cosmic rays, Solar cosmic ray protons
M. A. Pomerantz	Bartol Research Foundation Swarthmore, Pennsylvania 19081	Cosmic rays

<u>Name</u>	<u>Organization</u>	<u>Data Type</u>
M. Wada	Institute of Physical and Chemical Research 7-13 Kaga-1, Itabashi Tokyo, Japan 173	Cosmic rays
O. Binder	Institut für Reine und Angewandte Kernphysik Olshausenstr 40/60, Gebäude N20a 23 Kiel, German Federal Republic	Cosmic rays
M. Siebert	Geophysikalisches Institut Herzberger Landstrasse 180 34 Göttingen, G.F.R.	Magnetic indices
D. Van Sabben	Kon. Nederlands Meteorologisch Instituut DeBilt, The Netherlands	Magnetic indices
M. Sugiura	Magnetic and Electric Fields Branch NASA/GSFC, Code 625 Greenbelt, Maryland 20771	Magnetic indices
D. J. Poros	Computer Sciences Corporation Silver Spring, Maryland 20910	Magnetic indices
P. N. Mayaud	Institut de Physique du Globe 4, Place Jussieu - Tour 14 75230 Paris, France	Magnetic indices
A. Romaña	Observatorio del Ebro Roqueta (Tarragona) Spain	ssc, sfe
J. H. Allen H. Kroehl	NGSDC/EDS/NOAA Boulder, Colorado 80302	Magnetograms
T. Damboldt	Forschungsinstitut der Deutschen Bundespost 61 Darmstadt, Postfach 800 G.F.R.	Radio quality figures
K. D. Boggs	Institute for Telecommunication Sciences Office of Telecommunications Boulder, Colorado 80302	Radio quality figures

I N D E X F O R
S O L A R - G E O P H Y S I C A L D A T A

An index to *Solar-Geophysical Data* beginning with the data for the year 1957 can be found on pages 67-83. The serial number of the report in which data for a given year and month were published is listed in the index according to type of data. The types are keyed according to ICSU recommendations; and this key, expanded for the data published in *Solar-Geophysical Data*, precedes the index. Listed with the kinds of data received are the periods during which they were available for publication.

Beginning with 1969, when *Solar-Geophysical Data* was divided into Part I and Part II, the index gives pages on which the data appear in addition to the serial number. A "B" appears between the serial number and the page number when the data were published in Part II.

S T O N Y H U R S T D I S K S

Two transparencies provide Stonyhurst disks in degrees from CMP in the size of most of the maps or drawings presented in the second section of these monthly reports. A second set of transparencies with meridians calibrated in days from CMP are included to fit the Mount Wilson and Kitt Peak magnetograms. The two sizes as calibrated in degrees or days from CMP are reversed from those published in the last Explanatory Text which may also be used with these maps.

The dates shown were for 1969 but are within 1 day of appropriate date for 1976. See any Ephemeris.

KEY TO INDEX OF SOLAR GEOPHYSICAL DATA

		<u>Mo/Yr</u>	<u>Mo/Yr</u>
<u>A. Solar and Interplanetary Phenomena</u>			
A.1	Sunspot Drawings	1/67	- present
A.1a	Sunspot Data (see A.5a)	7/57	- present
A.2a	Zürich Provisional Relative Sunspot numbers, R _Z	7/57	- present
A.2b	Zürich Final Sunspot numbers, R _Z	7/57	- present
A.2c	American Relative Sunspot numbers, R _A '	7/57	- present
A.2d	27-day Plot of Relative Sunspot numbers (see D.1c)	7/57	- present
A.2e	Sunspot Cycle (Smoothed numbers) Graphs - in each issue	7/57	- present
A.2f	Table of Observed and Predicted Smoothed Sunspot numbers	10/64	- present
A.3a	Mt. Wilson Magnetograms	9/66	- present
A.3b	Mt. Wilson Sunspot Magnetic Field Classifications	1/62	- present
A.3c	Kitt Peak Magnetograms	7/74	- present
A.4	H α Spectroheliograms	1/67	- present
A.5	Calcium Plage Drawings - McMath (or Catania)	1/67	- present
A.5a	Calcium Plage (McMath) and Sunspot Regions	7/57	- present
A.5b	Daily Calcium Plage Index	12/70	- present
A.6	H α Synotic Charts	6/73	- present
A.7a	Coronal Line Emission Indices (Provisional)	7/57	- 5/66
A.7b	Coronal Line Emission Indices (Final)	1/60	- present
A.7c	White-Light Corona (NRL OSO-7, 1971-083A)	2/72	- 6/74
A.7d	Solar EUV Spectroheliograms FeXV 284 Å (GSFC OSO-7, 1971-083A)	5/72	- 3/74
A.7e	Solar XUV Coronagrams (NRL OSO-7, 1971-083A)	10/72	- 12/73
A.7f	Coronal Holes (Helium D3)	1/76	- present
A.8aa	2800 MHz (ARO-Ottawa) Daily Observed Values of Solar Flux	7/57	- present
A.8ab	2800 MHz (Ottawa) Final - Daily Observed Values of Solar Flux	1/62	- 12/66
A.8ac	2800 MHz (ARO-Ottawa) Daily Values Solar Flux Adjusted to 1 A.U.	1/64	- present
A.8ad	2800 MHz (Ottawa) Final - Daily Values of Solar Flux Adjusted to A.U.	1/64	- 12/66
A.8b	470 MHz (Boulder) Daily 3-hourly Averages	7/57	- 3/58
A.8c	167 MHz (Boulder) Daily 3-hourly Averages	7/57	- 12/58
A.8d	200 MHz (Cornell) Daily 3-hourly Averages	7/57	- 12/58
A.8e	9530 MHz (USNRL) Daily Averages	2/58	- 4/59
A.8f	3200 MHz (USNRL) Daily Averages	2/58	- 4/59
A.8g	15400, 8800, 4995, 2695, 1415, 606, 410, 245 MHz (AFCL) Solar Flux Adjusted to 1 A.U. (15400 MHz began 6/69 and 245 MHz began 1/70)	1/67	- present
A.9a	9.1 cm (Stanford) Radio Maps of the Sun	4/60	- 8/73
A.9aa	9.1 cm Spectroheliogram Data	1/69	- 8/73
A.9b	21 cm (Fleurs) Radio Maps of the Sun	12/64	- 12/73
A.9c	8.6 mm (Prospect Hill) Radio Maps of the Sun	4/70	- 2/74
A.9cb	8.6 mm (NELC) Radio Maps of the Sun	11/74	- present
A.9d	2 cm (NELC) Radio Maps of the Sun	6/74	- present
A.10a	169 MHz (Nancay) Interferometric Observations	7/57	- present
A.10b	408 MHz (Nancay) Interferometric Observations	11/65	- 8/71
A.10c	21 cm (Fleurs) East-West Solar Scans	10/65	- present
A.10d	43 cm (Fleurs) East-West Solar Scans	4/66	- present
A.10e	10.7 cm (Ottawa-ARO) East-West Solar Scans	6/68	- present
A.11aa	Solar X-ray Background Levels (NRL) satellites, see below	1/64	- 4/74
A.11ab	Solar X-ray Background Levels (NRL Graphs) " " "	3/65	- 4/74
A.11ac	Solar X-ray Background Levels (Boulder) " " "	12/65	- 11/68
A.11ad	Solar X-ray Background Levels (France) " " "	4/66	- 5/66
A.11ae	Solar X-ray Background Levels (Aberdeen, S. D.) " "	1/66	- 11/68
	Popular Name		
	Satellite Designation		
	SOLRAD 7A	1964-1D	1/64 - 10/64
	SOLRAD 7B	1965-16D	3/65 - 12/65
	SOLRAD 8	1965-93A	
	(Explorer 30)		1/66 - 12/67
	OGO-4	1967-73A	
	OSO-4	1967-100A	1/68 - 3/68
	SOLRAD 9	1968-17A	
	(Explorer 37)		3/68 - 7/72
	(Beginning 12/68 daily/hourly averages presented)		6/73 - 4/74
	SOLRAD-10	1971-58A	
	(Explorer 44)		8/72 - 6/73

A. Solar and Interplanetary Phenomena (continued)

A.11b	Solar X-ray Background Levels, 0-20Å Injun 1/SOLRAD-3, 1961-02	6/61 - 12/61
A.11c	Solar X-ray Background Levels (Vela 1,2; 1963-39A,C)	(10/63)
A.11d	Solar X-ray Background Levels (McMath) (OSO-3; 1967-20A), 8-12Å	3/67 - 8/67
A.11e	Solar X-ray (OSO-5; 1969-6A) Spectroheliograms (University College London, Leicester Univ.)	7/69 - 11/72 7/74 - 6/75
A.11f	Solar X-ray (GSFC OSO-7, 1971-083A) Spectroheliograms	12/72 - 7/74
A.11g	Solar X-ray Background Levels (SMS-1/GOES, 1974-033A; SMS-2/GOES, 1975-011A)	1/74 - present
A.11h	Solar X-ray (OSO-8, 1975-057A) 2-14 keV (Lockheed)	8/75 - present
A.12aa	Solar Protons, Daily-hourly Values, JPL/GSFC (satellites, see below)	5/67 - 5/73
A.12ab	Solar Protons, Graphs, JPL/GSFC	5/67 - 5/73
	<u>Popular Name</u>	<u>Satellite Designation</u>
	Explorer 34	1967-51A, Ep >10, >30, >60 Mev
	Explorer 41	1969-53A, Ep >10, >30, >60 Mev
	Explorer 43	1971-19A, Ep >10, >30, >60 Mev
A.12ba	Cosmic Ray Protons, Ep 0.6-13, 13-175, >175 Mev, Univ. of Chicago (Pioneer 6; 1965-105A and Pioneer 7; 1966-75A)	3/69 - present
A.12bb	Cosmic Ray Protons, Ep >13.9, >64 or >40 Mev, Univ. of New Hampshire (Pioneer 8; 1967-123A and Pioneer 9; 1968-100A)	12/69 - present
A.12c	Cosmic Ray Protons, Ep 5-21, 21-70 Mev, Aerospace (ATS-1; 1966-110A)	1/70 - 8/72
A.12d	Low Energy Protons (NOAA satellites 1972-082A, 1973-086A, 1974-089A)	7/74 - present
A.12e	Energetic Solar Particles (IMP H, 1972-073A and IMP J, 1973-078A)	8/75 - present
A.13a	Solar Wind (Pioneer 6, 1965-105A; and Pioneer 7, 1966-75A) NASA Ames	12/65 - present
A.13b	Solar Wind, M.I.T. Pioneer 6, 1965-105A	3/69 - 2/70 12/73 - present
	Pioneer 7, 1966-75A	6/69 - 12/69
A.13c	Solar Wind (Vela 3, 1964-40A; Vela 5, 1965-58A)	1/69 - 6/72
A.13d	Solar Wind from IPS Measurements (UCSD)	1/75 - present
A.13e	Solar Plasma Data (IMP H, 1972-073A and IMP J, 1973-078A)	8/75 - present
A.17	Interplanetary Magnetic Field Pioneer 8, 1967-123A	10/72 - present
	Pioneer 9, 1968-100A	4/72 - present
A.17c	Inferred Interplanetary Magnetic Field	12/71 - present
A.18	Interplanetary Electric Field Pioneer 8, 1967-123A	5/72 - present
	Pioneer 9, 1968-100A	4/72 - present

B. Ionospheric (and Radio Wave Propagation) Phenomena

B.10	Radar Meteor Indices, perpetual, based upon 1958-1962 data for N45 latitude -- see issues 246, 251	
B.51aa	NARWS Quality Figures and Forecasts (NBS/ESSA)	7/57 - 12/65
B.51ab	NARWS Comparison Graphs (NBS/ESSA)	7/57 - 12/65
B.51ba	NPRWS Quality Figures and Forecasts (NBS)	7/57 - 12/65
B.51bb	NPRWS Comparison Graphs (NBS)	7/57 - 10/64
B.51ca	High Latitude Quality Figures and Forecasts (ESSA/OT)	11/64 - present
B.51cb	High Latitude Comparison Graphs (ESSA/OT)	11/64 - 11/73
B.52	North Atlantic Graphs of Useful Frequency Ranges (German PTT)	7/57 - present
B.53	Quality Figures Based Upon Frequency Ranges (German PTT)	1/70 - present

C. Flare-Associated Events

C.1a	H-α Solar Flares (Preliminary)	7/57 - present
C.1ba	H-α Solar Flares (including Standardized Data) (Divided into Confirmed and Unconfirmed Flares from 1/68-12/74)	9/66 - present
C.1c	H-α Subflares (included in C.1a and C.1b after 1/62)	7/57 - present
C.1d	H-α Flare Patrol (The most recent issue listed for a month contains the comprehensive flare patrol.)	7/57 - present
C.1e	H-α Flare Index (Daily)	9/69 - present
C.1f	H-α Flare Index (by Region)	9/70 - present
C.1g	Frequency of Occurrence of Confirmed Solar Flares	1/68 - 6/68

C. Flare-Associated Events (continued)

C.3a	2800 MHz (Ottawa) Outstanding Occurrences	7/57 - present
C.3aa	2800 MHz (Ottawa) Hours of Observation	7/57 - 12/65
C.3b	470 MHz (Boulder) Outstanding Occurrences	7/57 - 3/58
C.3c	167 MHz (Boulder) Outstanding Occurrences	7/57 - 10/60
C.3ca	167 MHz (Boulder) Hours of Observation	1/59 - 12/59
C.3d	200 MHz (Cornell) Outstanding Occurrences	7/57 - 12/58
C.3e	9530 MHz (USNRL) Outstanding Occurrences	2/58 - 4/59
C.3f	3200 MHz (USNRL) Outstanding Occurrences	2/58 - 4/59
C.3g	200 MHz (Hawaii) Outstanding Occurrences	6/59 - 8/59
C.3h	108 MHz (Boulder) Outstanding Occurrences	1/60 - 6/66
C.3ha	108 MHz (Boulder) Hours of Observation	1/60 - 12/65
C.3i	221 MHz (Boeing-Seattle) Outstanding Occurrences (Interferometric) - Changed to 223 MHz in May 1963	4/62 - 7/63 5/65 - 11/65 6/65 - 3/66
C.3j	107 MHz (Haleakala) Outstanding Occurrences	7/64 - 5/75
C.3k	10700, 2700, 960 MHz (Pennsylvania State Univ.) Outstanding Occurrences	7/66 - 4/69
C.3l	486 MHz (Washington State Univ.) Outstanding Occurrences	7/66 - 4/69
C.3m	18 MHz Bursts (Boulder) (reported with C.6 1/63 - 11/66, C.6ab prior to 1/63)	11/67 - present
C.3n	35000, 15400, 8800, 4995, 2695, 1415, 606, 410, 245 MHz (AFCRL - Sagamore Hill) Outstanding Occurrences (15400 MHz began 11/67, 35000 and 245 MHz began early 1969, 410 MHz began 1971)	1/66 - present
C.3p	184 MHz (Boulder) Outstanding Occurrences	3/67 - 7/72
C.3q	7000 MHz (Sao Paulo) Outstanding Occurrences	11/67 - present
C.3r	408 MHz (San Miquel) Outstanding Occurrences	10/67 - 4/72
C.3s	18 MHz (McMath-Hulbert) Bursts	1/68 - present
C.3t	43.25, 80 and 160 MHz (Culgoora) Selected Bursts	12/72 - present

Note: Beginning with the data for April 1966, in CRPL-FB-261, the C.3 entries on Solar Radio Outstanding Occurrences for the western hemisphere observatories and frequencies were combined into a single table "Solar Radio Emission Outstanding Occurrences, C.3." Beginning with June 1969 data, the table was expanded to worldwide coverage, and the various observatories are no longer indexed separately.

C.4aa	Solar Radio Spectrograms of Events (Fort Davis)	7/57 - 12/58
	100 - 580 MHz	7/57 - 12/58
	25 - 580 MHz	1/59 - 12/62
	50 - 320 MHz	1/63 - 3/65
	25 - 320 MHz	4/65 - 12/66
	10 - 580 MHz	1/67 - 2/70
	10 - 1000 MHz	3/70 - 4/70
	10 - 2000 MHz	5/70 - 5/73
	20 - 4000 MHz	5/73 - 3/74
	25 - 320 MHz	4/74 - present
C.4ab	2100-3900 MHz Solar Radio Spectrograms of Events (Fort Davis)	1/60 - 12/61
C.4b	Solar Radio Spectrograms of Events (Boulder)	
	7.6 - 41 MHz	3/61 - 8/68
	7.6 - 80 MHz	9/68 - present
C.4c	450-1000 MHz Solar Radio Spectrograms of Events (Owens Valley)	11/60 - 10/61
C.4d	Solar Radio Spectrograms of Events (Culgoora)	
	10 - 210 MHz	1/67 - 7/69
	8 - 2000 MHz	8/69 - 2/70
	8 - 4000 MHz	3/70 - 10/70
	8 - 8000 MHz	11/70 - present
C.4e	30-1000 MHz Solar Radio Spectrograms of Events (Weissenau, GFR)	3/68 - present
C.4f	Solar Radio Spectrograms of Events (AFCRL - Sagamore Hill)	
	19 - 41 MHz	1/68 - 7/70
	24 - 48 MHz	7/70 - 7/75
	25 - 75 MHz	8/75 - present
C.4g	20-60 MHz Solar Radio Spectrograms of Events (Clark Lake)	4/70 - 9/70
C.4h	160-320 MHz Solar Radio Spectrograms of Events (Dwingeloo)	1/74 - present
C.4i	100-1000 MHz Solar Radio Spectrograms of Events (Dürnten)	1/74 - present
C.4j	24-48 MHz Solar Radio Spectrogram of Events (Manila)	4/74 - present

C. Flare-Associated Events (continued)

C.5a	Solar X-ray Events (Vela 1,2; 1963-39A,C)	(10/63)
C.5b	Solar X-ray Events (Univ. of Iowa)	
	Explorer 33; 1966-58A (2-12Å)	7/66 - 10/71
	Explorer 35; 1967-70A (2-12Å)	12/67 - 7/72
C.5c	Solar X-ray Events (NRL Tabulation)	1/64 - 10/64
	(See A.11ab for NRL Graphs and list of Satellites)	and 3/65 - present
C.5d	Solar X-ray Events (McMath-Hulbert) OSO-3; 1967-20A (8-12Å)	3/67 - 8/67
C.5e	Solar X-ray Events (SMS-1/GOES, 1974-033A; SMS-2/GOES, 1975-011A)	11/74 - present
C.6	Sudden Ionospheric Disturbances (SID)	1/63 - present
C.6aa	Sudden Ionospheric Disturbances (SWF) (included with C.6 after 12/62)	7/57 - present
C.6ab	Sudden Ionospheric Disturbances (SCNA, SEA, bursts)	" 1/58 - present
C.6ac	Sudden Ionospheric Disturbances (SPA)	" 6/61 - present
C.7	Solar Proton Events - Direct Measurement - same as A.12	5/67 - present
C.8	Solar Proton Events - Riometer	1/67 - 6/67
	Confirmed Polar Cap Absorption Events (ESSA)	
C.8ba	Solar Protons, 26 MHz Riometer Events (South Pole) Provisional	9/63 - 11/67
C.8bc	Solar Protons, 30 MHz Riometer Events (Frobisher Bay)	1/65 - 5/65
C.8be	Solar Protons, 30 MHz Riometer Events (Great Whale River)	6/65 - 2/67

D. Geomagnetic and Magnetospheric Phenomena

D.1a	Geomagnetic Indices Ci, Ks, Kn, Km, Cp, Kp, Ap, aa, Selected Days (aa first published 1/74; Ks, Kn, Km first published 12/75; Ci discontinued 8/75)	7/57 - present
D.1b	27-day Chart of Kp for Year	7/57 - present
D.1ba	27-day Chart of Kp Indices	7/57 - present
D.1c	27-day Chart of C9 for Year	7/57 - present
D.1d	Principal Magnetic Storms	7/66 - present
D.1e	Reduced Magnetograms	1/67 - present
D.1f	Sudden Commencements and Solar Flare Effects	1/66 - present
D.1g	Equatorial Indices Dst	5/73 - present

F. Cosmic Rays

F.1a	Cosmic Ray Daily Averages Neutron Monitors (Deep River - graph of hourly values, daily averages begin 11/65)	1/59 - present
F.1b	Cosmic Ray Daily Averages Neutron Monitors (Climax) Daily Averages and Graph of hourly values	9/60 - 3/72 12/74 - present
F.1c	Cosmic Ray Daily Averages Neutron Monitors (Dallas)	1/64 - 3/74
F.1d	Cosmic Ray Daily Averages Neutron Monitors (Churchill)	5/64 - 6/72
F.1e	Cosmic Ray Daily Averages Neutron Monitors (Alert) Graph of hourly values (Alert)	3/74 - present 7/66 - present
F.1f	Cosmic Ray Daily Averages Neutron Monitors (Calgary - also graph of hourly values)	1/71 - present
F.1g	Cosmic Ray Daily Averages Neutron Monitors (Sulphur Mountain - also graph of hourly values)	1/71 - present
F.1h	Cosmic Ray Daily Averages Neutron Monitors (Thule - also graph of hourly values)	4/73 - present
F.1i	Cosmic Ray Daily Averages Neutron Monitors (Tokyo - also graph of hourly values)	12/73 - present
F.1j	Cosmic Ray Daily Averages Neutron Monitors (Kiel - also graph of hourly values)	12/73 - present

H. Miscellaneous

H.60	Alert and Special World Interval Decisions (IUWDS Geophysical Alerts)	7/57 - present
H.61	International Geophysical Calendar	1/62 - 12/62
H.62	Abbreviated Calendar Record	12/68 - present
H.63	Retrospective World Intervals	1/66 - 12/67

INDEX TO "SOLAR-GEOPHYSICAL DATA"

Key *	1957						1958											
	Jul	Aug	Sep	Oct	Nov	Dec	Jan	Feb	Mar	Apr	May	Jun	Jul	Aug	Sep	Oct	Nov	Dec
A.2a	156	157	158	159	160	161	162	163	164	165	166	167	168	169	170	171	172	173
A.2b	166	166	166	166	166	166	175	175	175	175	175	175	175	175	175	175	175	175
A.2c	157	158	159	160	161	162	163	164	165	166	167	168	169	170	171	172	173	174
A.5a	156	157	158	159	160	161	162	163	164	165	166	167	168	169	170	171	172	173
A.7	156	157	158	159	160	161	162	163	164	166	166	167	168	169	170	171	172	173
			165	165	165	165	165	171	171	171	171	171	171					
A.8aa	156	157	158	159	160	161	162	163	164	164	165	166	167	168	169	170	171	172
A.8b	156	157	158	159	161	162	163	164	165									
A.8c	156	157	158	159	162	162	163	164	165	167	168	169	170	172	173	174	175	176
A.8d	156	157	158	159	160	161	163	163	164	165	167	167	168	169	170	171	172	173
A.8e								176	175	174	172	170	170	170	170	171	172	173
A.8f								176	175	174	172	170	170	170	170	171	172	173
A.10a	171	171	171	171	171	171	171	171	171	171	171	171	171	171	171	171	172	173
B.51aa	157	158	159	160	161	162	163	164	165	166	167	168	169	170	171	172	173	174
B.51ab	157	158	159	160	161	162	163	164	165	166	167	168	169	170	171	172	173	174
B.51ba	157	158	159	160	161	162	163	164	165	166	167	168	169	170	171	172	173	174
B.51bb	157	158	159	160	161	162	163	164	165	166	167	168	169	170	171	172	173	174
B.52	157	159	159	160	161	162	163	164	165	166	167	168	169	170	171	172	173	174
C.1a	156	157	158	159	160	161	162	163	164	165	166	167	168	169	170	171	172	173
	166	167	168	168	169	169	170	170	171	171	172	172	173	173	174	174	175	175
	169	174	174	174	161	174	174		174	174	174							
	174		175		174											176		
C.1c	156	157	158	160	161	162	163	164	165	166	167	168	169	170	171	172	173	174
C.1d	158	158	158	159	160	161	162	163	164	165	166	167	168	169	170	171	172	173
	166	167	168	168	169	169	170	170	171	171	172	172	173	173	174	174	175	175
	176	176	176	176	176	176	176	176	176	176								
C.3a	156	157	158	159	160	161	162	163	164	165	166	167	168	169	170	171	172	173
C.3aa	158	158	158	161	161	161	164	164	164	167	167	167	170	170	170	173	173	173
C.3b	156	157	159	159	161	162	163	164	165									
C.3c	156	157	159	159	162	162	163	164	165	168	169	169	170	172	173	174	175	176
C.3d	156	157	158	159	160	161	163	163	164	165	167	167	168	169	170	171	172	173
C.3e								176	175	174	172	170	170	170	170	171	172	173
C.3f								176	175	174	172	170	170	170	170	171	172	173
C.4aa												174	168	169	170	171	172	174
C.6aa	157	158	159	160	161	162	163	164	165	166	167	168	169	170	171	172	173	174
C.6ab									171	172	173	174	175	176	177	178	178	179
D.1a	157	158	159	160	161	162	163	164	165	166	167	168	169	170	171	172	173	174
D.1b	174	174	174	174	174	174	174	174	174	174	174	174	174	174	174	174	174	174
D.1c	190	190	190	190	190	190	190	190	190	190	190	190	190	190	190	190	190	190
H.60	158	158	158	159	160	161	162	163	164	165	165	167	168	168	170	171	172	173
										166	166			169				

* See "Key" on pages 67 and following.

INDEX TO "SOLAR-GEOPHYSICAL DATA"

Key *	1959												1960											
	Jan	Feb	Mar	Apr	May	Jun	Jul	Aug	Sep	Oct	Nov	Dec	Jan	Feb	Mar	Apr	May	Jun	Jul	Aug	Sep	Oct	Nov	Dec
A. 2a	174	175	176	177	178	179	180	181	182	183	184	185	186	187	188	189	190	191	192	193	194	195	196	197
A. 2b	187	187	187	187	187	187	187	187	187	187	187	187	187	187	188	189	190	191	192	193	194	195	196	197
A. 2c	175	176	177	178	179	180	181	182	183	184	185	186	187	188	189	190	191	192	193	194	195	196	197	198
A. 5a	174	175	176	177	178	179	180	181	182	183	184	185	186	187	188	189	190	191	192	193	194	195	196	197
A. 7a	174	175	176	177	178	179	180	181	183	183	184	185	186	187	188	189	190	191	192	193	195	196	196	197
A. 7b													185	185										
A. 8aa	174	175	176	177	178	179	180	181	182	183	184	185	186	187	188	189	190	191	192	193	194	195	196	197
A. 8e	174	175	176	177																				
A. 8f	174	175	176	177																				
A. 9a																196	197	199	210	211	212	212	212	
A. 10a	174	175	176	177	178	179	180	181	182	183	184	185	186	187	188	189	190	191	192	193	194	195	196	197
B. 51aa	175	176	177	178	179	180	181	182	183	184	185	186	187	188	189	190	191	192	193	194	195	196	197	198
B. 51ab	175	176	177	178	179	180	181	182	183	184	185	186	187	188	189	190	191	192	193	194	195	196	197	198
B. 51ba	175	176	177	178	179	180	181	182	183	184	185	186	187	188	189	190	191	192	193	194	195	196	197	198
B. 51bb	175	176	177	178	179	180	181	182	183	184	185	186	187	188	190	190	191	192	193	194	195	196	197	198
B. 52	175	176	177	178	179	180	181	182	183	184	185	186	187	188	190	190	191	192	193	194	195	196	197	198
C. 1a	174	175	176	177	178	179	180	181	182	183	184	185	186	187	188	189	190	191	192	193	194	195	196	197
	176	178	179	180	181	182	183	184	185	186	187	188	189	190	191	192	193	194	195	196	197	198	199	200
	178	185	185	185	185	185	185	185					191	189	194	194	201	195	201	201	201	201	201	201
	185												191	194	194			201						
C. 1c	175	176	177	178	179	180	181	182	183	184	185	186	187	188	189	190	191	192	193	194	195	196	197	198
C. 1d	174	175	176	177	178	179	180	181	182	183	184	185	186	187	188	189	190	191	192	193	194	195	196	197
	176	178	179	180	181	182	183	184	185	186	187	188	189	190	191	192	193	194	195	196	197	198	199	200
	178	185	185	185	185	185	185	185					191	191			202	202	202	202	202	202	202	202
	185					200																		
C. 3a	174	175	176	177	178	179	180	181	182	183	184	185	186	187	188	189	190	191	192	193	194	195	196	197
C. 3aa	176	176	176	179	179	179	182	182	182	185	185	185	188	188	188	191	191	191	194	194	194	197	197	197
C. 3c	176	177	178	178	179	180	180	181	182	183	184	185	195	195	195	195	195	195	195	195	195	195	195	195
C. 3ca	182	182	182	182	182	182	182	182	182	183	184	185												
C. 3e	174	175	176	177																				
C. 3f	174	175	176	177																				
C. 3g						180	182	185																
C. 3h																								
C. 4aa	182	182	182	184	184	184	188	188	188	192	192	192	186	187	188	189	190	191	192	193	194	195	196	197
C. 4ab													197	197	197	198	198	198	199	199	199	200	200	200
C. 4c																								
C. 6aa	175	176	177	178	179	180	181	182	183	184	185	186	187	188	189	190	191	192	193	194	195	196	197	198
C. 6ab	180	181	182	183	184	184	184	185	186	187	187	188	188	189	189	190	191	192	193	194	195	196	197	198
D. 1a	175	176	177	178	179	180	181	182	183	184	185	186	187	188	189	190+	191	192	193	194	195	196	197	198
D. 1b	186	186	186	186	186	186	186	186	186	186	186	186	198	198	198	198	198	198	198	198	198	198	198	198
D. 1c	190	190	190	190	190	190	190	190	190	190	190	190	190	190	190	226	226	226	226	226	226	226	226	226
F. 1a	195	195	195	195	195	195	195	195	195	195	195	195	195	195	195	195	195	195	195	195	195	196	197	198
F. 1b																								
H. 60	174	175	176	177	178	179	180	181	182	183	184	185	186	187	188	189	190	191	192	193	194	195	196	197

* See "Key" on pages 67 and following.

INDEX TO "SOLAR-GEOPHYSICAL DATA"

Key *	1961												1962											
	Jan	Feb	Mar	Apr	May	Jun	Jul	Aug	Sep	Oct	Nov	Dec	Jan	Feb	Mar	Apr	May	Jun	Jul	Aug	Sep	Oct	Nov	Dec
A.2a	198	199	200	201	202	203	204	205	206	207	208	209	210	211	212	213	214	215	216	217	218	219	220	221
A.2b	211	211	211	211	211	211	211	211	211	211	211	211	223	223	223	223	223	223	223	223	223	223	223	223
A.2c	199	200	201	202	203	204	205	206	207	208	209	210	211	212	213	214	215	216	217	218	219	220	221	222
A.3b													210	211	212	213	214	215	216	217	218	219	220	221
A.5a	198	199	200	201	202	203	204	205	206	207	208	209	210	211	212	213	214	215	216	217	218	219	220	221
A.7a	198	199	200	201	202	203	205	205	207	207	208	209	210	211	212	213	214	215	216	217	218	219	220	221
A.7b	204	204	204	205	205	205	208	208	208	212	212	212	213	213	213	216	216	216	220	220	220	226	226	226
A.8aa	198	199	200	201	202	203	204	205	206	207	208	209	210	211	212	213	214	215	216	217	218	219	220	221
A.8ab													223	223	223	223	223	223	223	223	223	223	223	223
A.9a			213	213												213	214	215	216	217	218	219	220	221
A.10a	198	200	201	201	202	203	204	205	206	207	208	209	210	211	212	213	214	215	216	217	218	219	220	221
A.11b						249	249	249	249	249	249	249												
B.51aa	199	200	201	202	203	204	205	206	207	208	209	210	222	212	213	214	215	216	217	218	219	220	221	222
B.51ab	199	200	201	202	203	204	205	206	207	208	209	210	211	212	213	214	215	216	217	218	219	220	221	222
B.51ba	199	200	201	202	203	204	205	206	207	208	209	210	211	212	213	214	215	216	217	218	219	220	221	222
B.51bb	199	200	201	202	203	204	205	206	207	208	209	210	211	212	213	214	215	216	217	218	219	220	221	222
B.52	199	200	201	202	203	204	205	206	207	208	209	210	211	212	213	214	215	216	217	218	219	220	221	222
C.1a	198	199	200	201	202	203	204	205	206	207	208	209	210	211	212	213	214	215	216	217	218	219	220	221
	208	208	208	208	208	208	208	208	210-	210	211	212	213	214	215	216	217	218	219	220	221	222	223	224
C.1c	199	200	201	202	203	204	205	206	207	208	209	210	211 included in C.1a after Jan. 1962											
C.1d	198	199	200	201	202	203	204	205	206	207	208	209	210	211	212	213	214	215	216	217	218	219	220	221
	201	202	203	204	205	206	207	208	210	210	211	212	213	214	215	216	217	218	219	220	221	222	223	224
C.3a	198	199	200	201	202	203	204	205	206	207	208	209	210	211	212	213	214	215	216	217	218	219	220	221
							206		209		209													
C.3aa	200	200	200	203	203	203	206	206	206	209	209	209	212	212	212	215	215	215	218	218	218	221	221	221
C.3b	198	199	200	201	202	203	204	205	206	207	208	209	210	211	212	213	214	215	216	217	218	219	220	221
C.3ha													210	211	212	213	214	215	216	217	218	219	220	221
C.3i													-	-	-	221	221	221	221	221	221	221	221	221
C.4aa	203	203	203	204	204	204	208	208	208	209	209	209	213	213	213	216	216	216	219	219	219	222	222	222
C.4ab	203	203	203	204	204	204	208	208	208	209	209	209												
C.4b				207	207	207	207	207	207	207	208	209	210	211	212	213	214	215	216	217	218	219	220	221
C.6aa	199	200	201	202	203	204	207	206	207	208	209	210	211	212	213	214	215	216	219	219	219	220	221	222
C.6ab	199	200	201	202	203	204	205	206	207	208	209	210	211	212	213	214	215	216	219	219	219	220	221	222
C.6ac						204	205	206	207	208	209	210	211	212	213	214	215	216	219	219	219	220	221	222
D.1a	199	200	201	202	203	204	205	206	207	208	209	210	211	212	213	214	215	216	217	218	219	220	221	222
D.1b	208	208	208	208	208	208	208	208	208	208	208	208	221	221	221	221	221	221	221	221	221	221	221	221
D.1c	226	226	226	226	226	226	226	226	226	226	226	226	226	233	233	233	233	233	233	233	233	233	233	233
F.1a	199	200	201	202	203	204	204	206	207	208	209	210	211	212	213	214	223	223	223	223	223	223	233	222
							205																	
F.1b	199	200	201	202	203	204	205	206	207	208	210	210	211	212	213	214	215	216	217	218	219	220	221	222
H.60	198	199	200	201	202	203	204	205	206	207	208	209	210	211	212	213	214	215	216	217	218	219	220	221
H.61													207	207	207	207	207	207	207	207	207	207	207	207

* See "Key" on pages 67 and following.

INDEX TO "SOLAR-GEOPHYSICAL DATA"

Key*	1974																								
	Jan	Feb	Mar	Apr	May	June	July	Aug	Sep	Oct	Nov	Dec													
A.																									
A.1	355	24	356	24	357	26	358	30	359	22	360	42	361	30	362	32	363	28	364	32	365	26	366	24	
A.2a	354	7	355	7	356	7	357	7	358	7	359	7	360	7	361	7	362	7	363	7	364	7	365	7	
A.2b	367A	6	367A	6	367A	6	367A	6	367A	6	367A	6	367A	6	367A	6	367A	6	367A	6	367A	6	367A	6	
A.2c	354	7	355	7	356	7	357	7	358	7	359	7	360	7	361	7	362	7	363	7	364	7	365	7	
A.3a	355	24	356	24	357	26	358	30	359	22	360	42	361	30	362	32	363	28	364	32	365	26	366	24	
A.3b	355	86	356	80	357	88	358	90	359	84	360	102	361	92	362	94	363	88	364	94	365	86	366	86	
A.3c	---	---	---	---	---	---	---	---	---	---	---	---	361	27	362	32	363	28	364	32	365	26	366	24	
A.4	355	24	356	24	357	26	358	30	359	22	360	42	361	30	362	32	363	28	364	32	365	26	366	24	
A.5	355	24	356	24	357	26	358	30	359	22	360	42	361	30	362	32	363	28	364	32	365	26	366	24	
A.5a	355	86	356	80	357	88	358	90	359	84	360	102	361	92	362	94	363	88	364	94	365	86	366	86	
A.5b	355	92	356	86	357	96	358	97	359	94	360	110	361	102	362	102	363	97	364	101	365	92	366	92	
A.6	355	23	356	23	357	25	358	29	359	21	360	40	361	26	362	31	363	27	364	31	365	24	366	23	
A.7b	355	24	356	24	357	26	358	30	359	22	360	42	361	30	362	32	363	28	364	32	365	26	366	24	
A.7c	355	24	356	24	357	26	358	30	359	22	360	42	---	---	---	---	---	---	---	---	---	---	---	---	
A.7d	355	24	356	24	357	26	---	---	---	---	---	---	---	---	---	---	---	---	---	---	---	---	---	---	
A.8a	354	7	355	7	356	7	357	7	358	7	359	7	360	7	361	7	362	7	363	7	364	7	365	7	
A.8ac	354	7	355	7	356	7	357	7	358	7	359	7	360	7	361	7	362	7	363	7	364	7	365	7	
A.8g	354	7	355	7	356	7	357	7	358	7	359	7	360	7	361	7	362	7	363	7	364	7	365	7	
A.9c	356B	56	356	24	---	---	---	---	---	---	---	---	---	---	---	---	---	---	---	---	---	---	---	---	
A.9cb	---	---	---	---	---	---	---	---	---	---	---	---	---	---	---	---	---	---	---	---	---	365	26	366	24
A.9d	---	---	---	---	---	---	---	---	---	---	---	360	42	361	30	362	32	363	28	364	32	365	26	366	24
A.10a	354	13	355	13	356	12	357	14	358	14	359	13	360	16	361	13	362	14	364	110	364	13	365	12	
A.10c	354	15	355	15	356	14	357	16	358	16	360B	32	360	18	361	15	362	16	363	15	364	15	365	14	
A.10d	354	16	355	16	356	15	357	17	358	17	360B	33	360	19	361	16	362	17	363	16	364	16	365	15	
A.10e	354	14	355	14	356	13	357	15	358	15	359	14	360	17	361	14	362	15	363	14	364	14	365	13	
A.11aa	355	93	356	87	364B	57	364B	59	---	---	---	---	---	---	---	---	---	---	---	---	---	---	---	---	
A.11ab	359B	18	364B	44	365B	84	365B	92	---	---	---	---	---	---	---	---	---	---	---	---	---	---	---	---	
A.11e	---	---	---	---	---	---	---	---	---	---	---	---	---	---	---	---	---	---	---	---	---	---	---	---	
A.11f	355	24	356	24	357	26	358	30	359	22	360	42	361	30	---	---	---	---	---	---	---	---	---	---	
A.11g	---	---	---	---	---	---	---	---	---	---	---	---	---	---	---	---	---	---	---	---	---	364	21	365	18
A.12ba	---	---	---	356	17	---	---	---	---	---	---	---	---	---	361	18	---	---	---	---	---	---	---	365	17
A.12bb	354	19	355	19	356	18	---	358	23	---	---	360	31	361	19	362	22	---	---	364	19	---	---	---	
A.12d	---	---	---	---	---	---	---	---	---	---	---	360	33	361	20	362	23	363	22	364	24	---	---	---	
A.13a	---	---	---	356	17	---	---	---	---	---	---	---	---	361	18	---	---	---	---	---	---	---	---	365	17
A.17	354	19	---	---	---	---	---	---	---	---	---	360	31	361	19	362	22	---	---	---	---	---	---	---	---
A.17	354	19	355	19	356	18	---	358	23	---	---	360	31	361	19	---	---	363	21	364	19	---	---	---	
A.17c	354	20	355	20	356	19	357	22	358	25	359	18	360	32	361	23	362	26	363	24	364	27	365	21	
A.18	354	19	---	---	---	---	---	---	---	---	---	---	360	31	361	19	362	22	---	---	---	---	---	---	---
A.18	354	19	355	19	356	18	---	358	23	---	---	360	31	361	19	---	---	363	21	364	19	---	---	---	
B.																									
B.51ca	355	111	356	107	357	111	358	117	359	119	360	131	361	131	362	119	363	123	364	119	365	109	366	111	
B.52	355	112	356	108	357	112	358	118	359	120	360	132	361	132	362	120	363	124	364	120	365	110	366	112	
B.53	355	114	356	110	357	114	358	120	359	122	360	134	361	134	362	122	363	126	364	122	365	112	366	114	
C.																									
C.1a	354	10	355	10	356	10	357	10	358	10	359	10	360	10	361	10	362	10	363	10	364	10	365	10	
C.1ba	359B	4	360B	4	361B	4	362B	4	363B	4	364B	4	365B	4	366B	4	367B	4	368B	4	369B	4	370B	4	
C.1d	359B	12	360B	12	361B	10	362B	23	363B	18	364B	17	365B	26	366B	14	367B	20	368B	24	369B	14	370B	11	
C.1e	359B	9	360B	10	361B	8	362B	18	363B	14	364B	13	365B	20	366B	13	367B	16	368B	20	369B	11	370B	8	
C.1f	360B	29	361B	22	362B	47	363B	41	364B	39	365B	81	366B	29	367B	52	368B	56	369B	34	370B	26	371B	22	
C.3	359B	13	360B	13	361B	11	362B	24	363B	19	364B	18	365B	27	366B	15	367B	21	368B	25	369B	15	370B	12	
C.3	354	17	355	17	356	16	357	18	358	18	359	15	360	20	361	17	362	18	363	17	364	17	365	16	
C.3t	355	103	356	98	357	103	359B	51	359	110	360	122	361	122	362	111	363	115	365B106	365	101	366	100	---	
C.4aa	355	98	356	91	357	99	358	102	359	98	361B	24	361	106	362	104	363	101	364	104	365	94	366	94	
C.4b	355	98	356	91	357	99	358	102	359	98	360	113	361	106	362	104	363	101	364	104	365	94	366	94	
C.4d	355	98	356	91	357	99	359B	48	359	98	360	113	361	106	362	104	363	101	365B103	365	94	366	94	---	
C.4e	355	98	356	91	357	99	358	102	359	98	360	113	361	106	362	104	363	101	364	104	365	94	366	94	
C.4f	355	98	356	91	357	99	358	102	359	98	360	113	361	106	362	104	363	101	364	104	365	94	366	94	
C.4h	---	---	356	91	357	99	358	102	---	---	360	113	361	106	362	104	---	---	---	---	365	94	366	94	
C.4i	---	---	---	---	357	99	---	---	359	98	360	113	361	106	362	104	363	101	364	104	365	94	366	94	
C.4j	---	---	---	---	---	358	102	359	98	360	113	261	106	362	104	363	101	364	104	265	94	365	94	---	
C.5c	355	95	356	89	---	364B	61	---	---	---	---	---	---	---	---	---	---	---	---	---	---	---	---	---	
C.5e	---	---	---	---	---	---	---	---	---	---	---	---	---	---	---	---	---	---	---	---	---	364	23	365	18
C.6	355	96	356	90	357	97	358	98	359	95	360	111	361	103	362	103	363	99	364	102	365	93	366	93	
D.																									
D.1a	355	106	356	102	357	106	358	112	359	114	360	126	361	126	362	114	363	118	364	113	365	104	366	103	
D.1ba	355	107	356	103	357	107	358	113	359	115	360	127	361	127	362	115	363	119	364	114	365	104	366	105	
D.1c	366	107	366	107	366	107	366	107	366	107	366	107	366	107	366	107	366	107	366	107	366	107	366	107	---
D.1d	355	109	356	105	357	109	358	115	359	117	360	129</													

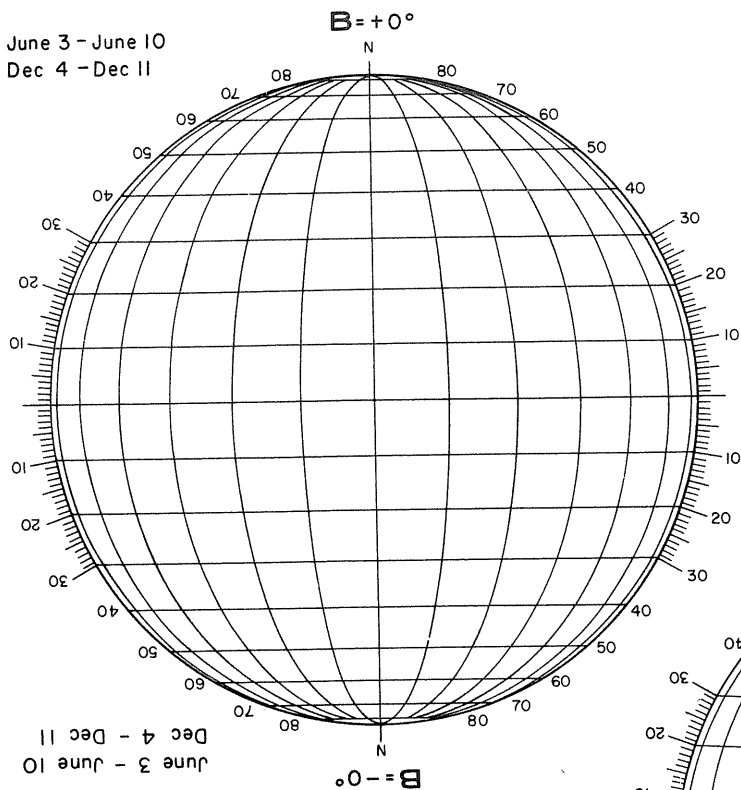
INDEX TO "SOLAR-GEOPHYSICAL DATA"

Key*	1975											
	Jan	Feb	Mar	Apr	May	Jun	Jul	Aug	Sep	Oct	Nov	Dec
A.												
A.1	367A 24	368A 26	369A 26	370A 24	371A 24	372A 28	373A 34	374A 28	375A 24	376A 28	377A 26	378A 28
A.2a	366A 7	367A 7	368A 7	369A 7	370A 7	371A 7	372A 7	373A 7	374A 7	375A 7	376A 7	377A 7
A.2b	378A 6	378A 6	378A 6	378A 6	378A 6	378A 6	378A 6	378A 6	378A 6	378A 6	378A 6	378A 6
A.2c	366A 7	367A 7	368A 7	369A 7	370A 7	371A 7	372A 7	373A 7	374A 7	375A 7	376A 7	377A 7
A.3a	367A 24	368A 26	369A 26	370A 24	371A 24	372A 28	374A 34	374A 28	375A 24	376A 28	377A 26	378A 28
A.3b	367A 86	368A 82	369A 88	370A 84	371A 86	372A 88	373A 96	374A 90	375A 84	376A 90	377A 86	378A 90
A.3c	367A 24	368A 26	369A 26	370A 24	371A 24	372A 28	373A 34	374A 28	375A 24	376A 28	377A 26	378A 28
A.4	367A 24	368A 26	369A 26	370A 24	371A 24	372A 28	373A 34	374A 28	375A 24	376A 28	377A 26	378A 28
A.5	367A 24	368A 26	369A 26	370A 24	371A 24	372A 28	373A 34	374A 28	375A 24	376A 28	377A 26	378A 28
A.5a	367A 86	368A 82	369A 88	370A 84	371A 86	372A 88	373A 96	374A 90	375A 84	376A 90	377A 86	378A 90
A.5b	367A 93	368A 89	369A 93	370A 91	371A 92	372A 93	373A101	374A 95	375A 90	376A 96	377A 92	378A 94
A.6	367A 23	368A 25	369A 25	370A 23	371A 23	372A 27	373A 33	374A 26	375A 23	376A 27	377A 25	378A 27
A.7b	367A 24	368A 26	369A 26	370A 24	371A 24	372A 28	373A 34	374A 28	375A 24	376A 28	377A 26	378A 28
A.8aa	366A 7	367A 7	368A 7	369A 7	370A 7	371A 7	372A 7	373A 7	374A 7	375A 7	376A 7	377A 7
A.8ac	366A 7	367A 7	368A 7	369A 7	370A 7	371A 7	372A 7	373A 7	374A 7	375A 7	376A 7	377A 7
A.8g	366A 7	367A 7	368A 7	369A 7	370A 7	371A 7	372A 7	373A 7	374A 7	375A 7	376A 7	377A 7
A.9cb	367A 24	368A 26	369A 26	370A 24	371A 24	372A 28	373A 34	374A 28	375A 24	376A 28	377A 26	378A 28
A.9d	367A 24	368A 26	369A 26	370A 24	371A 24	372A 28	373A 34	374A 28	375A 24	376A 28	377A 26	378A 28
A.10a	366A 12	367A 12	369A101	369A 12	370A 12	371A 12	372A 15	373A 15	374A 12	375A 12	376A 14	377A 12
A.10c	366A 14	367A 14	368A 14	369A 14	371A100	371A 14	372A 17	373A 17	374A 14	375A 14	376A 16	378B 57
A.10d	366A 15	367A 15	368A 15	369A 15	371A101	371A 15	372A 18	373A 18	374A 15	375A 15	376A 17	378B 58
A.10e	366A 13	367A 13	368A 13	369A 13	370A 13	371A 13	372A 16	373A 16	374A 13	375A 13	376A 15	377A 13
A.11g	368B 58	369B 36	369A 26	371B 24	371A 24	373A 34	---	---	---	---	---	---
A.11h	366A 18	367A 18	368A 18	369A 20	370A 18	---	---	373A 25	374A 20	375A 18	376A 21	377A 19
A.12ba	---	---	---	---	---	---	---	374A 28	375A 24	376A 28	377A 26	378A 28
A.12bb	---	---	---	369A 18	370A 16	371A 18	---	---	374A 18	---	---	377A 18
A.12d	---	---	---	369A 19	370A 17	371A 19	---	---	374A 19	---	---	---
A.13a	---	---	---	369A 18	370A 16	371A 18	---	---	374A 18	---	---	377A 18
A.13d	366A 17	367A 17	368A 17	369A 17	370A 15	371A 17	372A 21	373A 24	374A 17	375A 17	376A 20	377A 17
A.17	---	---	---	369A 19	370A 17	371A 19	---	---	374A 19	---	---	---
A.17	---	---	---	369A 19	---	371A 19	372A 22	---	374A 19	---	---	---
A.17c	366A 20	367A 20	368A 21	369A 22	370A 20	371A 20	372A 24	373A 29	374A 23	375A 20	376A 24	377A 21
A.18	---	---	---	369A 19	370A 17	371A 19	---	---	374A 19	---	---	---
A.18	---	---	---	369A 19	---	371A 19	372A 24	---	374A 19	---	---	---
B.												
B.51ca	367A111	368A103	369A109	370A105	371A108	372A109	373A119	374A115	375A103	376A113	377A111	378A114
B.52	367A112	368A104	369A110	370A106	371A109	372A110	373A120	374A116	375A104	376A114	377A112	378A115
B.53	367A114	368A106	369A112	370A108	371A111	372A112	373A122	374A118	375A106	376A116	377A114	378A117
C.												
C.1a	366A 10	367A 10	368A 10	369A 10	370A 10	371A 10	372A 10	373A 10	374A 10	375A 10	376A 10	377A 10
C.1ba	375B 26	375B 30	375B 35	375B 39	375B 6	376B 4	377B 4	378B 4	---	---	---	---
C.1d	366A 11	367A 11	368A 11	369A 11	370A 11	371A 11	372A 14	373A 14	374A 11	375A 11	376A 13	377A 11
C.1d	371B 6	372B 6	373B 6	374B 5	375B 10	376B 9	377B 15	378B 25	---	---	---	---
C.1e	371B 5	372B 5	373B 4	374B 4	375B 9	376B 8	377B 14	378B 24	---	---	---	---
C.1f	372B 20	375B 41	375B 41	375B 24	376B 22	377B 32	378B 52	---	---	---	---	---
C.3	371B 7	372B 7	373B 7	374B 6	375B 11	376B 10	377B 16	378B 26	---	---	---	---
C.3	366A 16	367A 16	368A 16	369A 16	370A 14	371A 16	372A 19	373A 19	374A 16	375A 16	376A 18	377A 16
C.3t	367A103	368A 95	369A100	370A 97	371A 99	372A101	363A111	374A107	376B 26	376A105	377A102	378A101
C.4a	367A 96	368A 91	369A 95	370A 93	371A 94	372A 95	373A103	374A 99	375A 92	376A 98	377A 94	378A 96
C.4b	367A 96	368A 91	369A 95	370A 93	371A 94	372A 95	373A103	374A 99	375A 92	376A 98	377A 94	378A 96
C.4d	367A 96	368A 91	369A 95	370A 93	371A 94	372A 95	374B 19	378B 54	376B 24	376A 98	377A 94	378A 96
C.4e	367A 96	368A 91	369A 95	370A 93	371A 94	372A 95	373A103	374A 99	375A 92	376A 98	377A 94	378A 96
C.4f	367A 96	368A 91	369A 95	370A 93	371A 94	372A 95	373A103	374A 99	375A 92	376A 98	377A 94	378A 96
C.4h	367A 96	368A 91	369A 95	---	---	372A 95	373A103	---	---	376A 98	---	---
C.4i	367A 96	368A 91	369A 95	370A 93	371A 94	372A 95	373A103	374A 99	375A 92	376A 98	377A 94	378A 96
C.4j	367A 96	368A 91	369A 95	370A 93	371A 94	372A 95	373A103	374A 99	375A 92	376A 98	377A 94	378A 96
C.5e	366A 18	367A 18	368A 18	369A 20	370A 18	---	372A 23	373A 27	374A 22	375A 18	376A 23	377A 23
C.6	367A 95	368A 90	369A 94	370A 92	371A 93	372A 94	373A102	374A 96	375A 91	376A 97	377A 93	378A 95
D.												
D.1a	367A106	368A 98	369A104	370A100	371A104	372A104	373A114	374A110	374A 98	376A108	377A105	378A105
D.1ba	367A107	368A 99	369A105	370A101	371A105	372A105	373A115	374A111	374A 99	376A109	377A106	378A107
D.1c	378A108	378A108	378A108	378A108	378A108	378A108	378A108	378A108	378A108	378A108	378A108	378A108
D.1d	367A109	368A101	369A107	370A103	371A106	372A107	373A117	374A113	374A101	376A111	377A108	378A112
D.1e	---	---	373B 10	---	---	---	---	---	---	---	---	---
D.1f	367A110	368A102	369A108	370A104	371A107	372A108	373A118	374A114	374A102	376A112	377A110	378A113
D.1g	367A108	368A100	369A106	370A102	372B 24	372A106	373A116	374A112	374A100	376A110	377A107	378A111
F.												
F.1a	367A104	368A 96	369A102	370A 98	371A102	372A102	373A112	374A108	375A 96	377B 34	377A103	378A104
F.1b	367A104	368A 96	369A102	370A 98	371A102	372A102	373A112	374A108	375A 96	376A106	377A103	378A104
F.1e	367A104	368A 96	369A102	370A 98	371A102	372A102	373A112	374A108	375A 96	377B 34	377A103	378A104
F.1f	367A104	368A 96	369A102	370A 98	371A102	372A102	374B 22	374A108	375A 96	376A106	377A103	378A104
F.1g	367A104	368A 96	369A102	370A 98	371A102	372A102	374B 22	374A108	375A 96	376A106	377A103	378A104
F.1h	367A104	368A 96	369A102	370A 98	371A102	372A102	373A112	374A108	375A 96	376A106	377A103	378A104
F.1i	367A104	368A 96	370A102	370A 98	371A102	372A102	373A112	374A108	375A 96	376A106	377A103	378A104
F.1j	367A104	368A 96	369A102	370A 98	371A102	372A102	373A112	374A108	375A 96	376A106	377A103	378A104
H.												
H.60	366A 4	367A 5	368A 4	369A 5	370A 5	371A 5	372A 4	373A 4	374A 4	375A 5	376A 5	377A 5
H.62	372B 11	373B 15	374B 8	375B 16	376B 14	377B 24	378B 44	---	---	---	---	---

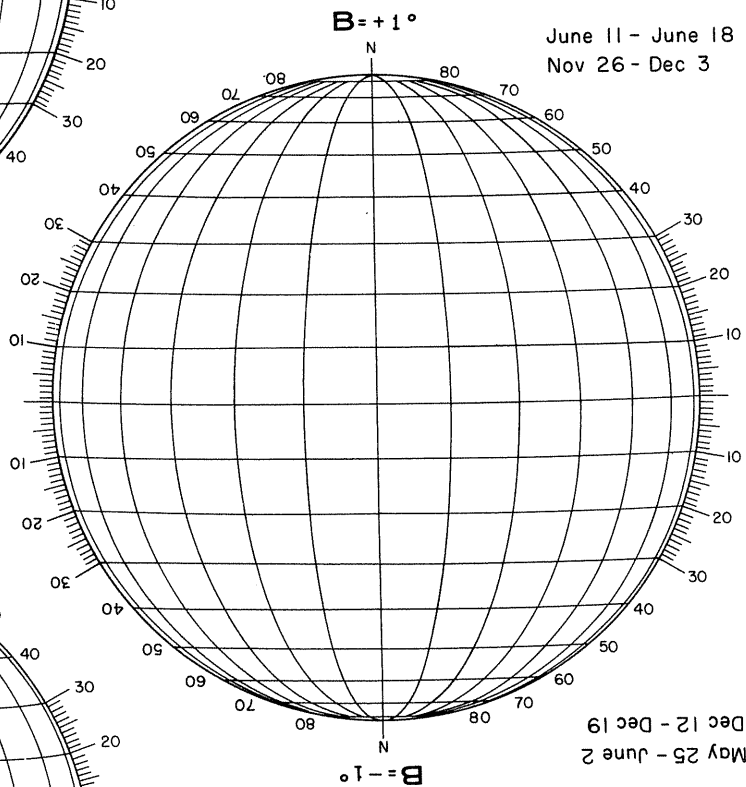
* See "Key" on pages 67 and following.

DAYS FROM CENTRAL MERIDIAN

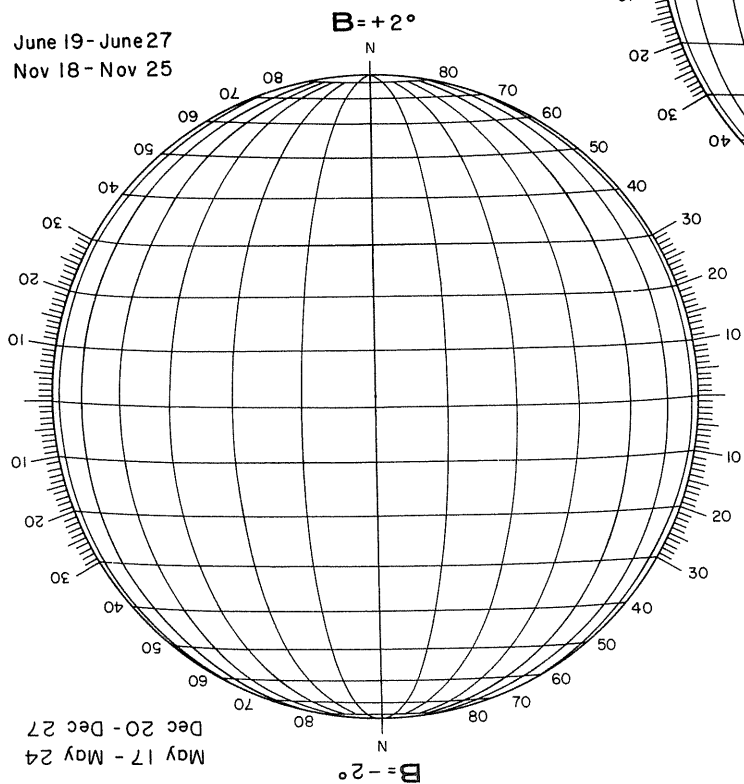
June 3 - June 10
Dec 4 - Dec 11



June 11 - June 18
Nov 26 - Dec 3

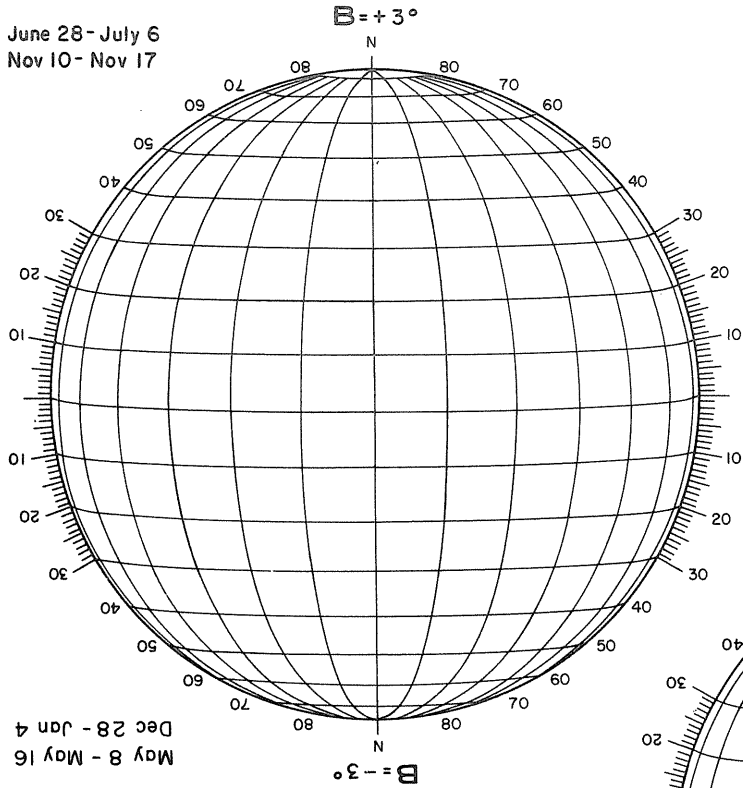


June 19 - June 27
Nov 18 - Nov 25



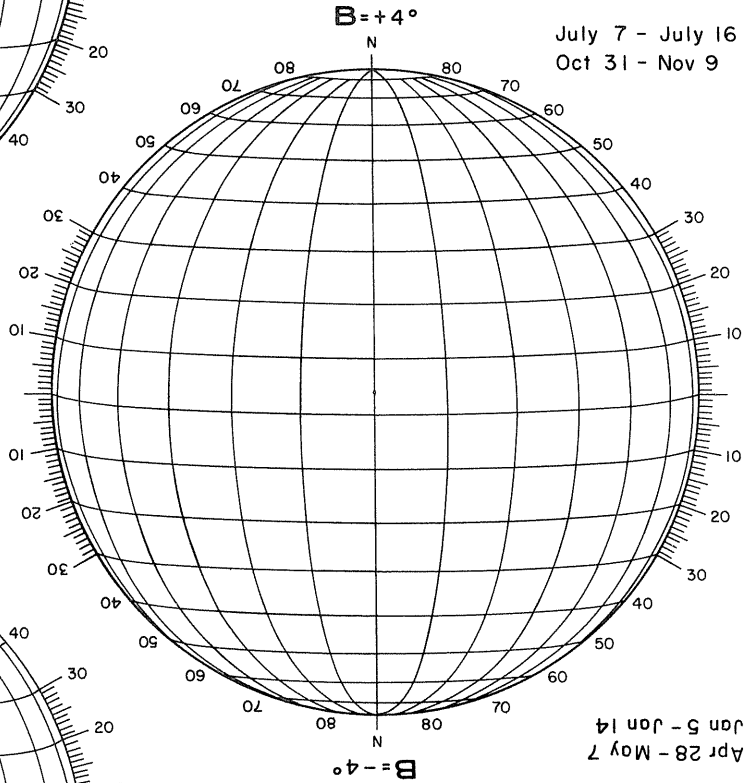
DAYS FROM CENTRAL MERIDIAN

June 28 - July 6
Nov 10 - Nov 17



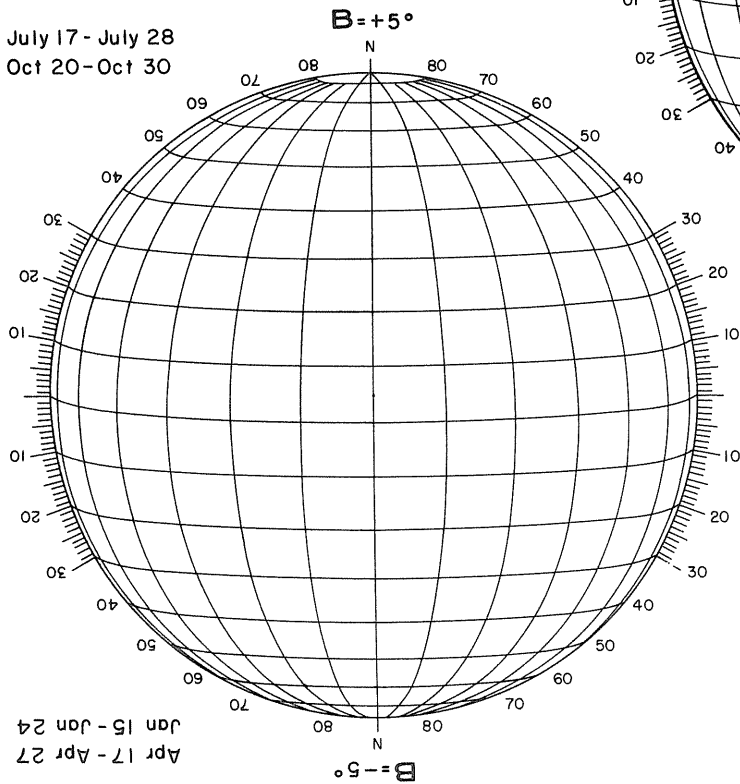
May 8 - May 16
Dec 28 - Jan 4

July 7 - July 16
Oct 31 - Nov 9



Apr 28 - May 7
Jan 5 - Jan 14

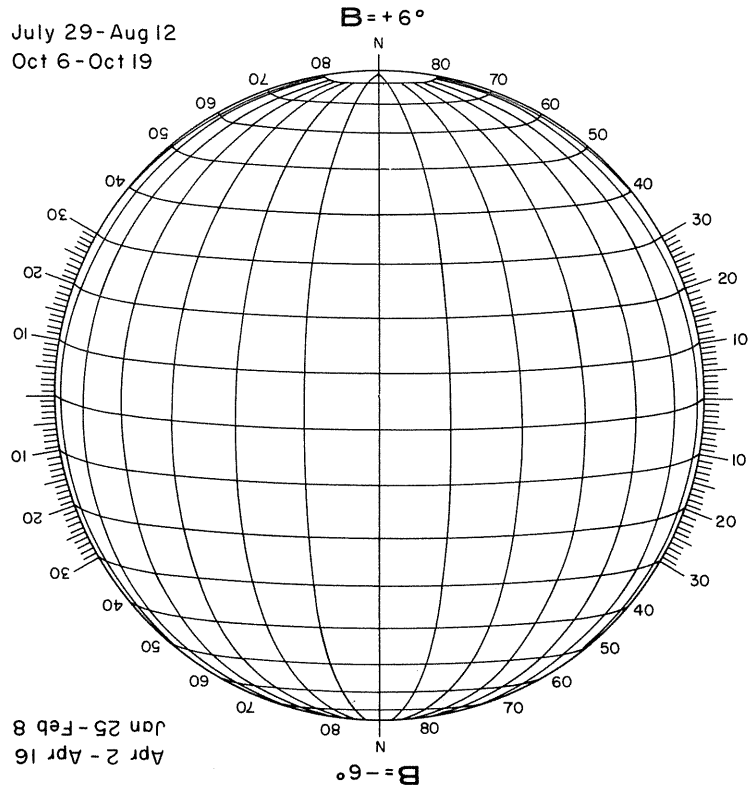
July 17 - July 28
Oct 20 - Oct 30



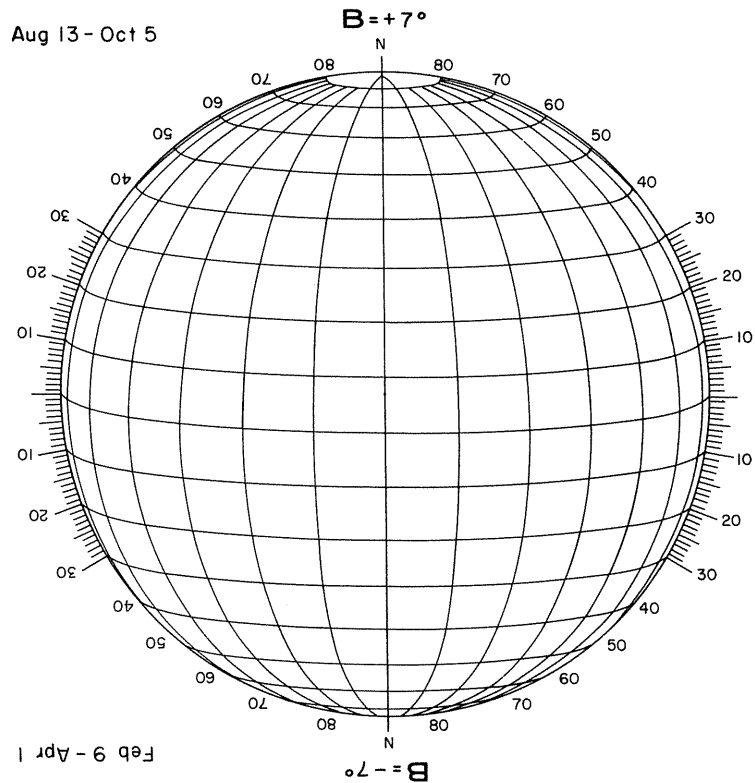
Apr 17 - Apr 27
Jan 15 - Jan 24

DAYS FROM CENTRAL MERIDIAN

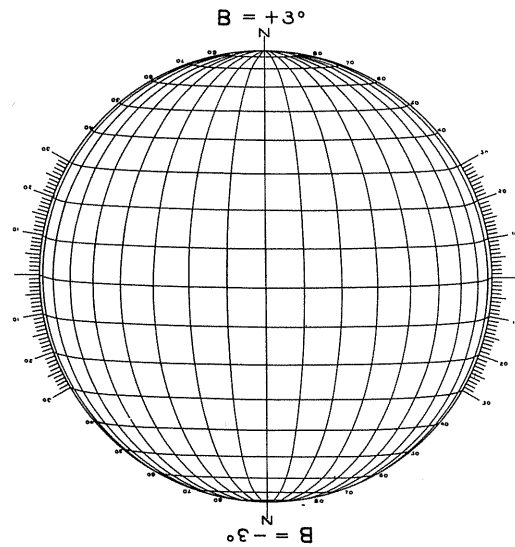
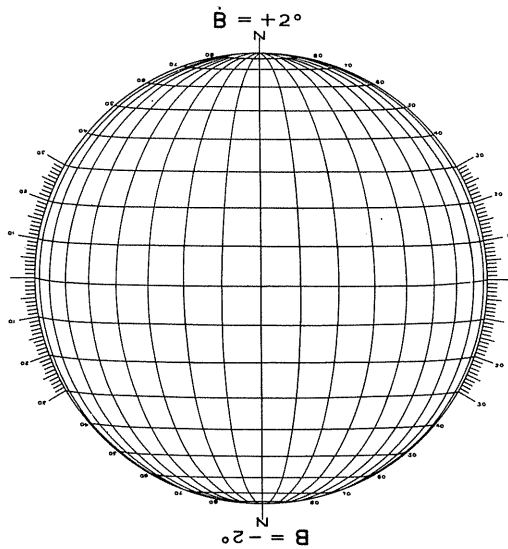
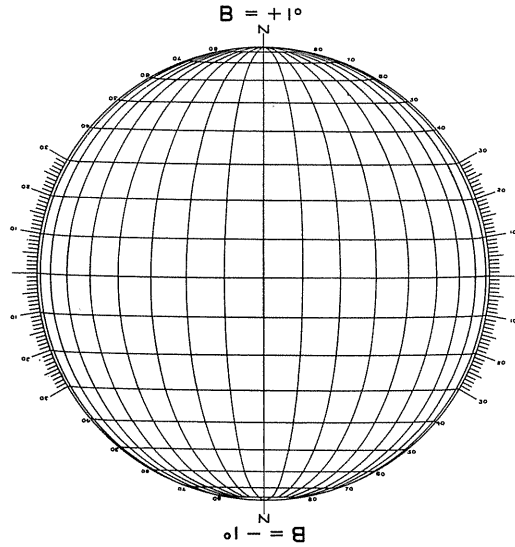
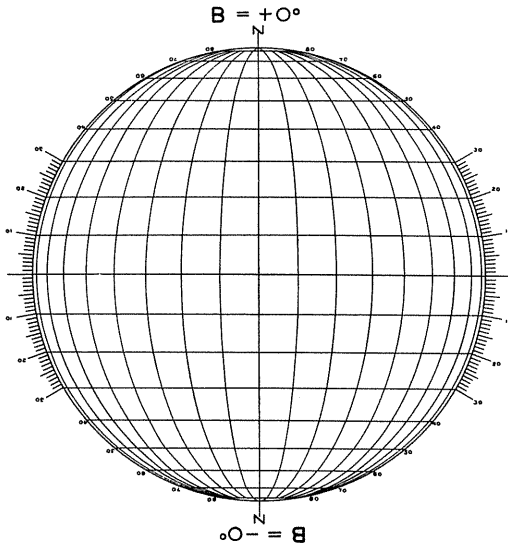
July 29 - Aug 12
Oct 6 - Oct 19

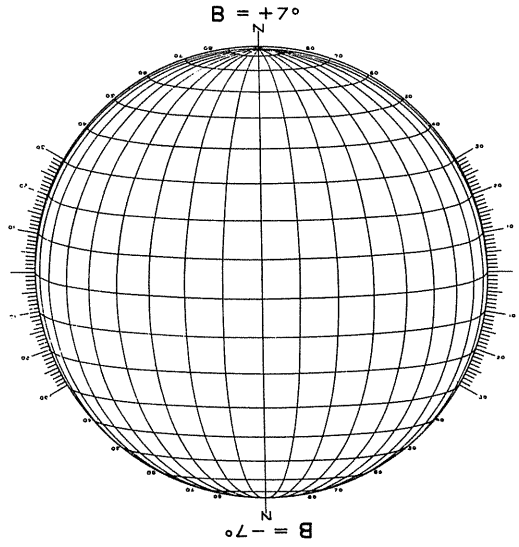
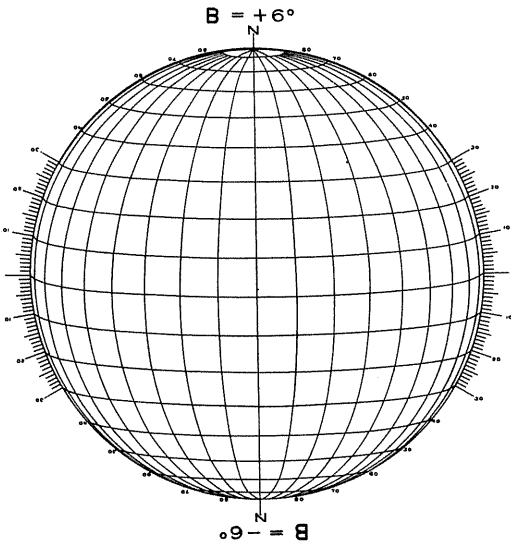
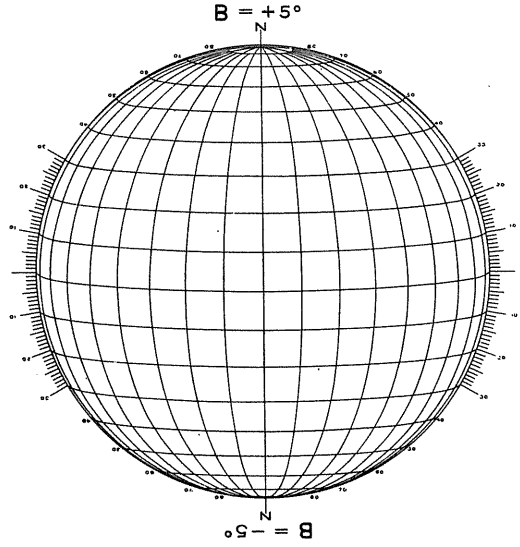
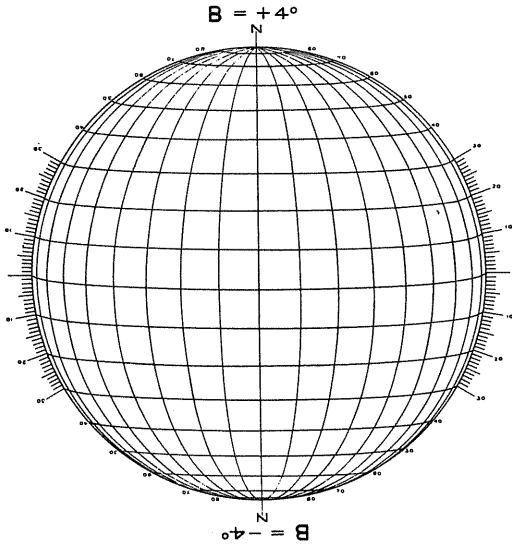


Aug 13 - Oct 5



DEGREES FROM CENTRAL MERIDIAN







WORLD DATA CENTER A
FOR
SOLAR-TERRESTRIAL PHYSICS



The ICSU Panel on WDCs has recommended that it would be appropriate courtesy to acknowledge in publications that data were obtained from the originating station or investigator through the intermediary of the WDCs. The following statement is suggested:

"Data used in this study were provided by WDC-A for Solar-Terrestrial Physics, NOAA E/GC2, 325 Broadway, Boulder Colorado 80303, USA."